

AD-A092 231

WOODS HOLE OCEANOGRAPHIC INSTITUTION MASS

F/G 8/10

COMPOSITION AND CHARACTERISTICS OF PARTICLES IN THE OCEAN: EVID-ETC(U)

NOV 80 M J RICHARDSON

N00014-79-C-0071

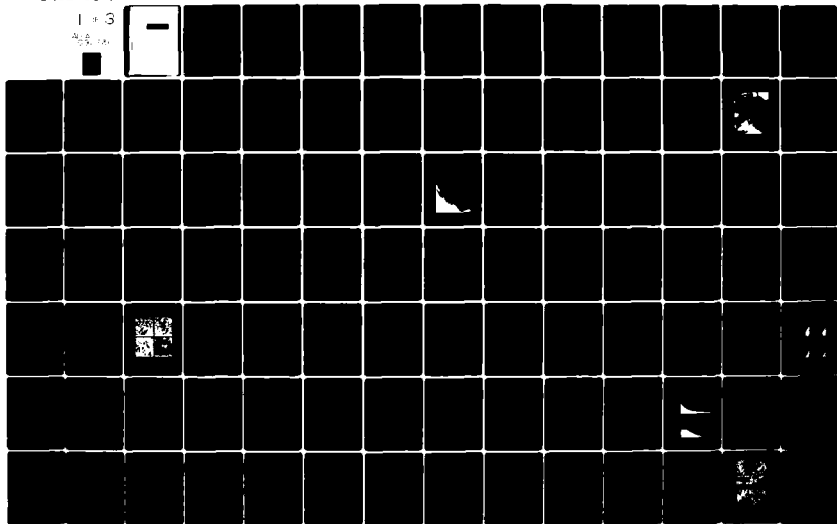
WHOI-80-52

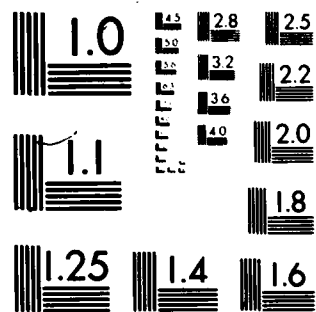
NL

UNCLASSIFIED

1 of 3

AD-A092 231





MICROCOPY RESOLUTION TEST CHART  
NATIONAL BUREAU OF STANDARDS 1963-A

AD A092231

UNCLASSIFIED 11/80

SECURITY CLASSIFICATION OF THIS PAGE (When Data Entered)

REPORT DOCUMENTATION PAGE		READ INSTRUCTIONS BEFORE COMPLETING FORM
1. REPORT NUMBER WHOI-80-52 ✓	2. GOVT ACCESSION NO. AD-A092	3. RECIPIENT'S CATALOG NUMBER 281
4. TITLE (and Subtitle) COMPOSITION AND CHARACTERISTICS OF PARTICLES IN THE OCEAN: EVIDENCE FOR PRESENT DAY RESUSPENSION.		5. TYPE OF REPORT & PERIOD COVERED Technical
6. PERFORMING ORG. REPORT NUMBER		
7. AUTHOR(s) 10 Mary Josephine Richardson	8. CONTRACT OR GRANT NUMBER(s) 15 N00014-79-C-0071, N00014-74-C-0262 N00014-75-C-0291	
9. PERFORMING ORGANIZATION NAME AND ADDRESS Woods Hole Oceanographic Institution Woods Hole, MA 02543		10. PROGRAM ELEMENT, PROJECT, TASK AREA & WORK UNIT NUMBERS NR 083-004
11. CONTROLLING OFFICE NAME AND ADDRESS NORDA National Space Technology Laboratory Bay St. Louis, MS 39529		12. REPORT DATE 11 November 1980
13. NUMBER OF PAGES 238		
14. MONITORING AGENCY NAME & ADDRESS (if different from Controlling Office) 12 240		15. SECURITY CLASS. (of this report) Unclassified
16. DISTRIBUTION STATEMENT (of this Report) Approved for public release; distribution unlimited. U L T		15a. DECLASSIFICATION/DOWNGRADING SCHEDULE
17. DISTRIBUTION STATEMENT (of the abstract entered in Block 20, if different from Report)		
18. SUPPLEMENTARY NOTES		
19. KEY WORDS (Continue on reverse side if necessary and identify by block number) 1. Suspended sediment 2. Resuspension processes 3. Abyssal sedimentation		
20. ABSTRACT (Continue on reverse side if necessary and identify by block number) See back		

DD FORM 1 JAN 73 1473

EDITION OF 1 NOV 68 IS OBSOLETE  
S/N 0102-014-6601UNCLASSIFIED 11/80  
SECURITY CLASSIFICATION OF THIS PAGE (When Data Entered)

381000

UNCLASSIFIED 11/80

SECURITY CLASSIFICATION OF THIS PAGE(When Data Entered)

This study of particulate matter in the water column and the underlying surface sediments verifies the occurrence of local, present-day resuspension in the deep sea. The location of the major portion of this work was the South Iceland Rise, a region influenced by the flow of Norwegian Sea Overflow Water. Measured current velocities exceeded 20 cm/sec in the axis of the bottom current for the duration of the deployments, approximately two weeks. Particulate matter was sampled with Niskin bottles, to obtain the standing crop of suspended matter and with sediment traps, to obtain the material in flux through the water column. Box cores were taken to obtain surface sediment samples for comparison with the trap samples.

Suspended particulate matter (SPM) and light-scattering studies demonstrate that in the Iceland Rise area the correlation of the L-DGO nephelometer to concentration of SPM differs between clear water and the nepheloid layer. Correlations of light scattering to SPM concentration also differ regionally, but for predicting concentration from light scattering, regression lines at two locations are indistinguishable. Particle size distributions have lower variance in the nepheloid layer than those in clear water which have roughly equal volumes of material in logarithmically increasing size grades from 1-20  $\mu\text{m}$ . Apparent density differences between SPM in clear water and the nepheloid layer are not distinguishable in the Iceland Rise study; apparent densities increase in the nepheloid layer in the western North Atlantic. An apparent density of 1.1 g/cm<sup>3</sup> adequately separates clear water from nepheloid layer samples in this region. Compositional variations seen between clear water and the nepheloid layer include a decrease in small coccoliths and an increase in clays and mineral matter. These compositional variations are more dramatic in the western North Atlantic region, due to dissolution of carbonate at the seafloor, later resuspended into the nepheloid layer.

A comparison of sediment-trap samples with box-core surface samples further supports present-day resuspension. Benthic foraminifera, iron-oxide coated planktonic foraminifera and the glacial, subpolar planktonic foraminifera (*Neogloboquadrina pachyderma* (sinistral)) in traps at 10, 100 and a few specimens at 500 mab, provide conclusive evidence for local resuspension. The coarse fraction (<125  $\mu\text{m}$ ) of the sediment trap material collected at 10 mab comprises 21-34% of the samples. Calculations indicate that this material is locally derived (few kilometers) resuspended material.

Accession	✓
NTIS	
DTIC TAB	
Unannounced	
Justification	
By	
Participating	
Availability	
Notes	

**A**

UNCLASSIFIED 11/80

SECURITY CLASSIFICATION OF THIS PAGE(When Data Entered)

WHOI-80-52

COMPOSITION AND CHARACTERISTICS OF  
PARTICLES IN THE OCEAN:  
EVIDENCE FOR THE PRESENT DAY RESUSPENSION

by

Mary Josephine Richardson

WOODS HOLE OCEANOGRAPHIC INSTITUTION  
Woods Hole, Massachusetts 02543

November 1980

DOCTORAL DISSERTATION

*Prepared for the Office of Naval Research under Contracts  
N00014-79-C-0071, NR 083-004, N00014-74-C-0262; NR 083-004,  
N00014-75-C-0291 and Sandia Laboratories through Contracts  
13-7923 and 13-2559.*

*Reproduction in whole or in part is permitted for any pur-  
pose of the United States Government. This thesis should  
be cited as: Mary Josephine Richardson, 1980. Composition  
and Characteristics of Particles in the Ocean: Evidence for  
the Present Day Resuspension. Ph.D Thesis. Massachusetts  
Institute of Technology/Woods Hole Oceanographic Institution  
WHOI-80-52.*

*Approved for public release; distribution unlimited.*

Approved for Distribution:

*John I. Ewing*  
John I. Ewing, Chairman  
Department of Geology & Geophysics

*Charles D. Hollister*  
Charles D. Hollister  
Dean of Graduate Studies

COMPOSITION AND CHARACTERISTICS OF PARTICLES

IN THE OCEAN:

EVIDENCE FOR PRESENT DAY RESUSPENSION

by

MARY JOSEPHINE RICHARDSON

A.B., Smith College  
(1975)

SUBMITTED IN PARTIAL FULFILLMENT  
OF THE REQUIREMENTS FOR THE  
DEGREE OF

DOCTOR OF PHILOSOPHY

at the

MASSACHUSETTS INSTITUTE OF TECHNOLOGY

and the

WOODS HOLE OCEANOGRAPHIC INSTITUTION

May 1980

Signature of Author:

*Mary Jo Richardson*

Joint Program in Oceanography  
Massachusetts Institute of Technology - Woods  
Hole Oceanographic Institution, May 1980

Certified by:

*Charles D. Hollibaugh*

Thesis Supervisor

Accepted by:

*R. P. Von Herzen*

Chairman, Joint Oceanography Committee in the  
Earth Sciences, Massachusetts Institute of  
Technology - Woods Hole Oceanographic Institution

COMPOSITION AND CHARACTERISTICS OF PARTICLES IN THE OCEAN:  
EVIDENCE FOR PRESENT-DAY RESUSPENSION

by

MARY JOSEPHINE RICHARDSON

Submitted to the Massachusetts Institute of Technology - Woods  
Hole Oceanographic Institution Joint Program in Oceanography  
on May 2, 1980, in partial fulfillment of the requirements  
for the degree of Doctor of Philosophy

ABSTRACT

This study of particulate matter in the water column and the underlying surface sediments verifies the occurrence of local, present-day resuspension in the deep sea. The location of the major portion of this work was the South Iceland Rise, a region influenced by the flow of Norwegian Sea Overflow Water. Measured current velocities exceeded 20 cm/sec in the axis of the bottom current for the duration of the deployments, approximately two weeks. Particulate matter was sampled with Niskin bottles, to obtain the standing crop of suspended matter and with sediment traps, to obtain the material in flux through the water column. Box cores were taken to obtain surface sediment samples for comparison with the trap samples.

Suspended particulate matter (SPM) and light-scattering studies demonstrate that in the Iceland Rise area the correlation of the L-DGO nephelometer to concentration of SPM differs between clear water and the nepheloid layer. Correlations of light scattering to SPM concentration also differ regionally, but for predicting concentration from light scattering, regression lines at two locations are indistinguishable. Particle size distributions have lower variance in the nepheloid layer than those in clear water which have roughly equal volumes of material in logarithmically increasing size grades from 1-20  $\mu\text{m}$ . Apparent density differences between SPM in clear water and the nepheloid layer are not distinguishable in the Iceland Rise study; apparent densities increase in the nepheloid layer in the western North Atlantic. An apparent density of 1.1 g/cm<sup>3</sup> adequately separates clear water from nepheloid layer samples in this region. Compositional variations seen between clear water and the nepheloid layer include a decrease in small coccoliths and an increase in clays and mineral matter. These compositional variations are more dramatic in the western North Atlantic region, due to dissolution of carbonate at the seafloor, later resuspended into the nepheloid layer.



Sedimentological evidence of resuspension and redistribution of material are: 1) presence of sediment drifts throughout the Iceland Basin; 2) occurrence of coarse, glacial age sediments beneath the axis of the bottom current; and 3) differences in mineralogy, carbonate and organic carbon contents between surface sediments beneath the bottom current and those in a channel.

A comparison of the vertical flux of material measured by sediment traps at 500 meters above bottom (mab) with the accumulation rate in cores, shows that the present-day surface input is an order of magnitude smaller than the accumulation rate. This observation suggests transport of material into some sections of the region by bottom currents or by turbidity currents.

The horizontal flux of particulate matter into and out of the region by the bottom current is 100 kg/sec. This material may contribute to the formation of Gardar sediment drift downstream. The trends in %  $\text{CaCO}_3$  and % organic carbon through the water column and in the surface sediments suggest that dissolution of carbonate and decomposition and consumption of organic carbon occurs primarily at the seafloor. These data also suggest preferential preservation at channel stations and/or preferential erosion beneath the bottom current.

A comparison of sediment-trap samples with box-core surface samples further supports present-day resuspension. Benthic foraminifera, iron-oxide coated planktonic foraminifera and the glacial, subpolar planktonic foraminifera (*Neogloboquadrina pachyderma* (sinistral)) in traps at 10, 100 and a few specimens at 500 mab, provide conclusive evidence for local resuspension. The coarse fraction ( $>125 \mu\text{m}$ ) of the sediment trap material collected at 10 mab comprises 21-34% of the samples. Calculations indicate that this material is locally derived (few kilometers) resuspended material.

Thesis Supervisor: Dr. Charles D. Hollister

Title: Senior Scientist

-4-

TO MY PARENTS

#### ACKNOWLEDGEMENTS

Many people have contributed in helping me make this thesis a reality. To all, I am grateful, particularly to any whom I've forgotten to specifically mention.

Charley Hollister, my thesis advisor, has guided, encouraged and financially supported my research. I thank Charley for his tutelage through the years, and for many stimulating discussions on land and at sea. I am especially appreciative of his concern for me as a scientist and as a friend.

I thank Ed Laine, Wilf Gardner, Roger Flood and Sandy Shor, (Charley's other students when I began the Joint Program) for their part in our cooperative ventures and especially for being surrogate advisors in Charley's absence.

The crew and scientists aboard AII-96 made this study possible. In particular, I am grateful for the organization and assistance provided by Dave Johnson, the chief scientist, and Sandy Shor, (a fellow student whose thesis was also derived from that cruise). Al Driscoll, Rick Chandler and Rod Davies were extremely helpful in technical assistance at sea. Mary Lee Bremer and Kristin Rohr aided in collection of Coulter Counter data, without whose help I never would have slept. I also thank Ted Spencer and Bobby Weeks for teaching and encouraging me in the art of machining, for construction of the sediment traps.

This work was financially supported by the Woods Hole Oceanographic Institution, ONR through contracts N00014-79-C-00-71 NR 083-004, N00014-74-C0262 NR 083-004, and N00014-75-C-0291 and ERDA through contracts 13-7923 and 13-2559.

Data reduction was helped immeasurably by Brian Von Herzen. Lois Toner and Roy Smith kindly allowed use of their laboratories and balances. I am grateful to Chuck Denham and Derek Spencer for assistance with my statistical problems. I thank Bruce Corliss for help in identifying foraminifera, and for perpetual (and occasionally helpful) haranguing. The assistance of Kozo Takahashi with radiolaria and dinoflagellate identification, and that of Carol Parmenter and Margaret Goreau, who operated the SEM for this study, is gratefully acknowledged.

My thesis committee, C.D. Hollister, J.B. Southard and D.W. Spencer and other readers, W.D. Gardner, S. Shor, D.A. Johnson, I.N. McCave, P. Biscaye and S. Honjo, have been superb in reading my material promptly and commenting liberally. I am appreciative of their efforts which have improved this thesis substantially.

My thanks to Caki Herrity and Cindy Brown-Stanton who saved me infinite hours by typing the manuscript and tables on the Wang Word Processor. They transformed my arrows and inserts into a finished document. Rick Chandler also helped on the Word Processor. I thank Laurie, Mike, Chic and Dave at WHOI Graphic Arts for quickly and accurately drafting and photographing the figures.

My friends have provided the necessary moral support, encouragement and friendship through the years. Specifically I thank Alice, Jim, Jerry, Sally, Lin, Peter, Marti, Sharon and Nina.

Finally, I specially acknowledge and thank Wilf Gardner. Wilf has aided my intellectual, emotional, psychological, physical and spiritual well-being. I thank him for working with me, traveling with me, running with me, and for so many times driving from New York just to be with me.

# TABLE OF CONTENTS

	Page
ABSTRACT . . . . .	2
ACKNOWLEDGEMENTS . . . . .	4
LIST OF FIGURES. . . . .	11
LIST OF PLATES . . . . .	14
LIST OF TABLES . . . . .	15
CHAPTER I - INTRODUCTION. . . . .	16
CHAPTER II - REGIONAL SETTINGS, HYDROGRAPHY AND SAMPLING SCHEMES	19
A. REGIONAL SETTING: ICELAND RISE . . . . .	19
B. REGIONAL SETTING: WESTERN NORTH ATLANTIC. . . . .	28
C. HYDROGRAPHY. . . . .	31
D. SAMPLING SCHEMES AND APPROACHES . . . . .	36
Current Competence. . . . .	36
Suspended Matter . . . . .	37
CHAPTER III - CHARACTERISTICS OF SUSPENDED PARTICULATE MATTER FROM NISKIN BOTTLES. . . . .	40
A. INTRODUCTION . . . . .	40
Nepheloid Layers . . . . .	41
Historical Perspective . . . . .	42
B. OBJECTIVES . . . . .	46
C. OBSERVATIONAL TECHNIQUES . . . . .	46
Concentration of SPM . . . . .	47
Size Distributions. . . . .	48
Light Scattering . . . . .	49
Compositional Analyses . . . . .	50
D. RESULTS . . . . .	51
SPM Concentration . . . . .	51
Iceland Rise . . . . .	54
Western North Atlantic. . . . .	62
Light-scattering Observations . . . . .	62
Size Distribution Analyses . . . . .	77
Iceland Rise . . . . .	77
Western North Atlantic. . . . .	78
Composition of SPM. . . . .	83
Iceland Rise . . . . .	83
Western North Atlantic. . . . .	96
E. DISCUSSION . . . . .	96
Correlation of Light-Scattering Measurements with SPM Concentrations . . . . .	96
Size Distribution Variations . . . . .	106
Volumetric Histograms . . . . .	107
Differential Volume Distributions . . . . .	110

	Page
Apparent Density . . . . .	115
Iceland Rise . . . . .	119
Western North Atlantic. . . . .	119
Compositional Differences . . . . .	125
Iceland Rise . . . . .	125
Western North Atlantic. . . . .	128
F. CONCLUSIONS. . . . .	129

#### CHAPTER IV - COMPARISON OF SEDIMENT TRAP SAMPLES AND THE SURFACE

SEDIMENT: EVIDENCE FOR LOCAL RESUSPENSION . . . . .	132
A. INTRODUCTION . . . . .	132
B. OBJECTIVES . . . . .	134
C. METHODS . . . . .	134
Suspended Particulate Matter . . . . .	134
Surface Sediment Samples. . . . .	140
Size Distribution Analyses . . . . .	146
Optical Identification . . . . .	146
Mineralogy . . . . .	147
Carbonate Determinations. . . . .	147
Organic Carbon and Nitrogen Analyses. . . . .	147
D. RESULTS . . . . .	148
Mass Collected by the Sediment Traps. . . . .	148
Particle Size Distributions. . . . .	152
Sediment Traps . . . . .	152
Surface Sediments . . . . .	155
Optical Identification . . . . .	156
Sediment Traps . . . . .	156
Foraminifera . . . . .	156
Radiolaria . . . . .	163
Pteropods . . . . .	164
Diatoms . . . . .	164
Dinoflagellates . . . . .	167
Fecal Pellets . . . . .	167
Unidentified Biogenic Material . . . . .	170
Volcanic Glass. . . . .	170
Mineral Grains and Aggregates. . . . .	170
Surface Sediments . . . . .	171
Foraminifera . . . . .	171
Radiolaria . . . . .	175
Pteropods . . . . .	175
Diatoms . . . . .	176
Dinoflagellates, Fecal Pellets and	
Unidentified Biogenic Material. . . . .	176
Volcanic Glass. . . . .	176
Mineral Grains and Aggregates. . . . .	176

	Page
Mineralogy . . . . .	179
Sediment Traps . . . . .	179
Surface Sediments . . . . .	179
Carbonate Content . . . . .	182
Organic Carbon and Nitrogen Contents. . . . .	190
E. DISCUSSION . . . . .	197
Present Day Resuspension of Sediments . . . . .	197
Advective Transport by the Bottom Current . . . . .	200
Relationship of the Bottom Water to Suspended Particulate Matter . . . . .	201
Quantity and Variability of Advection Transport . . . . .	206
Horizontal Versus Vertical Fluxes. . . . .	207
Estimates of the Quantity of Resuspended Material . . . . .	209
Dissolution and Degradation at the Seafloor . . . . .	213
Regional Patterns of Surface Sediments . . . . .	214
Distance of Transport. . . . .	215
F. CONCLUSIONS. . . . .	220
CHAPTER V - SUMMARY AND CONCLUSIONS . . . . .	222
REFERENCES . . . . .	227
BIOGRAPHICAL NOTE . . . . .	237



LIST OF FIGURES

Figure	Page
CHAPTER II	
2.1 Generalized flow of bottom water in the North Atlantic with study area locations . . . . .	21
2.2 Bathymetry, station locations and current measurements in the Iceland Rise study area . . . . .	24
2.3 Bathymetry of the northeastern North Atlantic showing the major sediment drifts . . . . .	26
2.4 Station locations and current patterns in the western North Atlantic study area . . . . .	30
2.5 Stick diagrams of current meter velocities on the East Katla Ridge . . . . .	34
CHAPTER III	
3.1 Idealized nephelometer profile . . . . .	44
3.2 Cross-section of concentration of suspended matter for the western Atlantic Ocean. . . . .	56
3.3 Profiles of concentration of SPM for the northern and southern lines in the Iceland Rise region. . . . .	58
3.4 Profiles of concentration for stations 28-29, 40 and P5 in the Iceland Rise region. . . . .	61
3.5 Cross-sections of SPM for the northern and southern lines. . . . .	64
3.6 Cross-section of SPM for the western North Atlantic region . . . . .	66
3.7 Nephelometer profiles from the Iceland Rise region. .	69
3.8 Nephelometer profiles from stations 28, 40 and 84 . .	74
3.9 Cross-section of light-scattering for the Iceland Rise region. . . . .	76

Figure		Page
3.10	Particle size distributions at station 25 from clear water and nepheloid layer samples . . . . .	80
3.11	Particle size distributions at station 39 from clear water and nepheloid layer samples . . . . .	82
3.12	Particle size distributions at station 718 from clear water and nepheloid layer samples . . . . .	85
3.13	Compositional variability of suspended particulate matter -- Iceland Rise . . . . .	88
3.14	Compositional variability of suspended particulate matter -- western North Atlantic. . . . .	98
3.15	Correlation of light-scattering to concentration of SPM for Iceland Rise data . . . . .	102
3.16	Correlation of light-scattering to concentration of SPM from Biscaye and Eittrheim (1974; 1977) . . . . .	105
3.17	Particle size distributions from 700 and 1479 m for station 67 . . . . .	109
3.18	Particle size distributions and associated parameters . . . . .	112
3.19	Slopes from normalized differential volume distributions versus depth. . . . .	114
3.20	Individual profiles of normalized differential volume distributions. . . . .	117
3.21	Apparent density of samples from the Iceland Rise . . . . .	121
3.22	Apparent density of samples from the continental rise southeast of New York . . . . .	124
CHAPTER IV		
4.1	Box core and sediment trap mooring locations. . . . .	137
4.2	Mooring diagram of sediment traps for northern transect. . . . .	139

Figure		Page
4.3	Mooring diagram of sediment traps for the canyon station . . . . .	142
4.4	Schematic diagram of the sediment trap used . . . . .	144
4.5	Apparent vertical fluxes of material through the water column . . . . .	151
4.6	Particle size distributions for sediment trap samples.	154
4.7	Particle size distributions for surface sediment samples . . . . .	158
4.8	Energy dispersive X-ray spectroscopy of sediment trap material . . . . .	169
4.9	Energy dispersive X-ray spectroscopy of surface sediments . . . . .	178
4.10	X-ray diffractogram for a sediment trap sample . . . . .	181
4.11	X-ray diffractogram for a surface sediment sample . . . . .	185
4.12	Calcium carbonate percentages in sediment trap and box core samples. . . . .	187
4.13	Calcium carbonate percentages for box core surface samples . . . . .	189
4.14	Organic carbon percentages in sediment trap and box core samples . . . . .	192
4.15	Organic carbon percentages for box core surface samples . . . . .	194
4.16	Potential temperature and light-scattering plot. . . . .	203
4.17	Potential temperature versus salinity . . . . .	205

LIST OF PLATES

Plate		Page
CHAPTER III		
3.1	SEM photomicrographs of suspended particulate matter from the Iceland Rise and western North Atlantic . .	53
3.2	SEM photomicrographs of suspended particulate matter from clear water and nepheloid layer samples. . . .	91
CHAPTER IV		
4.1	SEM photomicrographs of components of the $>63 \mu\text{m}$ fraction of the sediment traps . . . . .	161
4.2	SEM photomicrographs of components of the $>63 \mu\text{m}$ fraction of the sediment traps and surface sediments .	166
4.3	SEM photomicrographs of components of the $>63 \mu\text{m}$ fraction of the surface sediments . . . . .	174

# LIST OF TABLES

Table	Page
CHAPTER II	
2.1 Current meter data summary from the Iceland Rise. . .	32
CHAPTER III	
3.1 Percentage of SPM by particle type from the Iceland Rise and western North Atlantic . . . . .	89
3.2 Chi-square analysis of compositional data from the Iceland Rise and western North Atlantic. . . . .	95
3.3 Least-square regression equations for light-scattering versus concentration correlations. . . . .	100
CHAPTER IV	
4.1 Sediment trap mooring data . . . . .	135
4.2 Box core data . . . . .	145
4.3 Mass of sediment trap samples . . . . .	149
4.4 Percentage of sediment trap samples by particle type .	159
4.5 Foraminifera in the sediment trap and surface sediment samples . . . . .	162
4.6 Percentage of surface sediments by particle type. . .	172
4.7 Semiquantitative mineralogy of surface sediments. . .	183
4.8 Carbonate, organic carbon and nitrogen from sediment traps . . . . .	195
4.9 Carbonate, organic carbon and nitrogen from surface sediments. . . . .	196
4.10 Calculated percentage of resuspended material from mass, carbonate and organic carbon . . . . .	210
4.11 Particle fall velocities from mooring 2, trap 10 mab .	217

## CHAPTER I

### INTRODUCTION

Voluminous sediment drifts in the northern North Atlantic (e.g., Feni, Gardar, and Hatton sediment drifts; Jones et al., 1970; Hollister et al., 1978; McCave et al., 1980) are evidence for the transport and redistribution of massive quantities of deep-sea sediments through geologic time. The working hypothesis of this thesis is that resuspension of deep-sea sediments continues to occur in the northern North Atlantic, specifically in the Iceland Rise region, and is measurable on time scales of days to months.

This investigation, to study present-day resuspension and its influence on the characteristics of suspended particulate matter, was principally conducted on the south Iceland Rise. This region is particularly suitable for three reasons: 1) Norwegian Sea Overflow Water flows roughly parallel to contours through the region at velocities in excess of 20 cm/sec (Steele et al., 1962; Shor, 1978). Laboratory experiments indicate that these speeds are capable of eroding cohesive shelf sediments and abyssal clays (Lonsdale and Southard, 1974; Young and Southard, 1978), and so they are probably capable of eroding the local sediments. 2) Near-bottom nepheloid layers are present with high concentrations of suspended particulate matter. The existence of these features is indicative of an ongoing process keeping material in suspension near the seafloor. 3) Geologic evidence indicates a continuation of sediment

erosion and redistribution through the Recent. For example, beneath the axis of the bottom current, the small amount of Recent sediment present is coarse-grained, winnowed of its fines. Also, the Katla Ridges (Malmberg, 1974), which are sedimentary features in the study area, have been constructed and shaped by both bottom currents and turbidity currents through geologic time (Shor, 1979). In addition, farther downstream lies the Gardar sediment drift, a huge pile of sediment formed by deposition from bottom currents (Hollister et al., 1978; McCave et al., 1980).

A large portion of this work focuses on the transport and properties of suspended particulate matter. Particulate matter in the water column was collected with both water bottles and sediment traps in two regions, the Iceland Rise and the continental rise southeast of New York. The suspended particulate matter was examined to determine and interpret the changes in particles that occur from mid-water depths through the near-bottom nepheloid layer. Surface sediments recovered in box cores were compared with trapped material to estimate the fraction of resuspended material and to assess the changes occurring to particles from transit through the water column to residence on the seafloor. Current-meter measurements and CTD lowerings were used to determine the spatial extent and magnitude of the bottom current, and together with measurements of the suspended particulate matter concentrations, to estimate the horizontal transport of particulate matter.

Specific questions addressed in this thesis are:

- (1) Where are the present bottom-current velocities sufficient to erode the local surface sediments?
- (2) What are the composition and characteristics of material settling from the surface waters, and how do they differ from those of material being transported in the near-bottom nepheloid layer?
- (3) What processes are responsible for the observed changes in suspended particulate matter in the water column?
- (4) What fraction of nepheloid-layer particles are resuspended?
- (5) How far can particles travel in single episodes of resuspension?

The structure of the thesis in answering these questions is as follows. Chapter II details the regional settings, summarizes the hydrography, and explains the rationale for the sampling schemes selected. Chapter III discusses the horizontal and vertical spatial variability in characteristics of suspended particulate matter in the Iceland Rise region and along the continental rise in the western North Atlantic. It emphasizes the existence and interpretations of the differences between near-bottom nepheloid waters and the overlying clear water. Chapter IV deals with resuspension and advection by bottom currents as inferred from a comparison between the composition of the contents of sediment traps in the lower portion of the water column and that of the surface sediments. Chapter V is a summary of the conclusions of the thesis.



## CHAPTER II

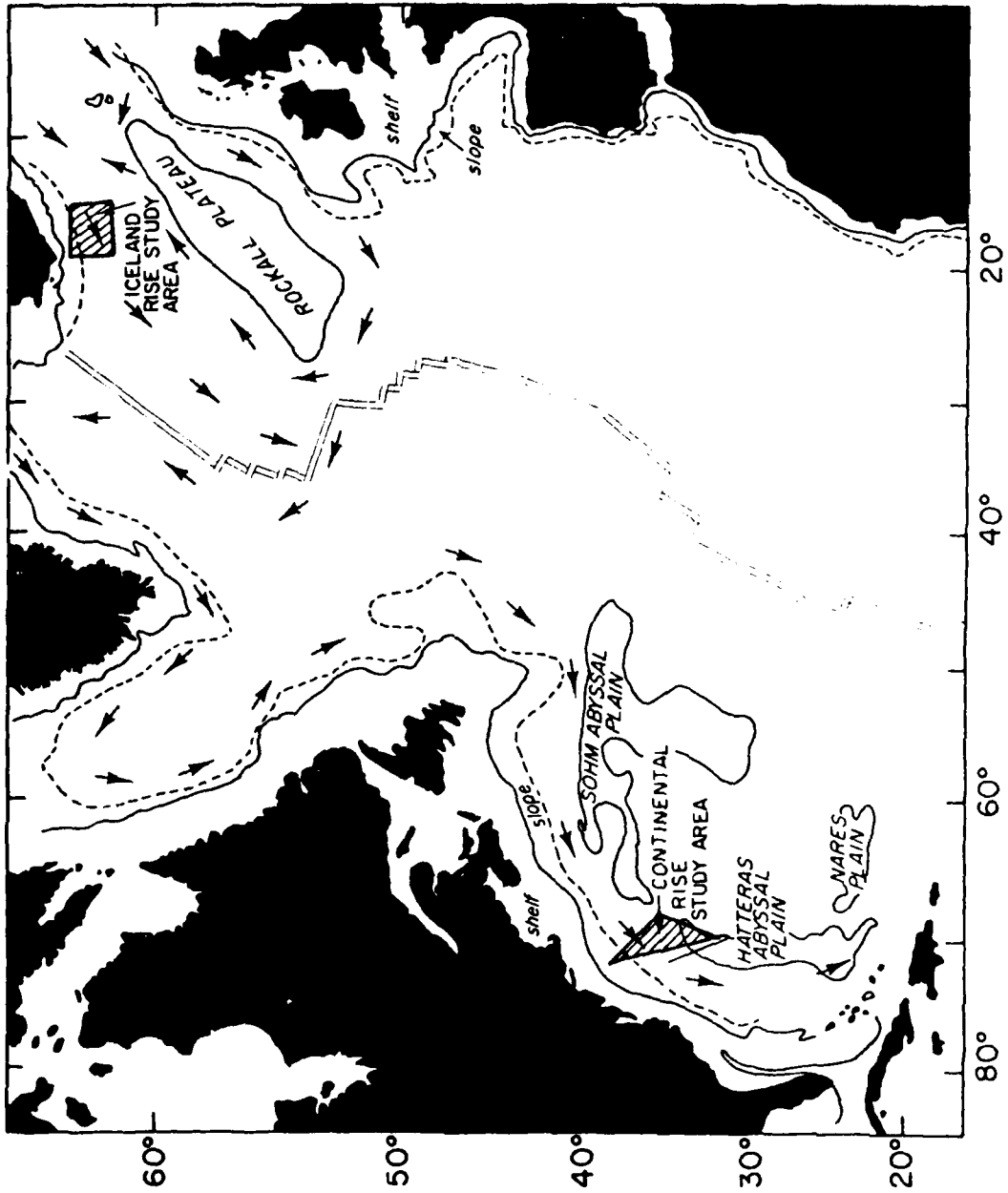
### REGIONAL SETTINGS, HYDROGRAPHY AND SAMPLING SCHEMES

The principal study region for this thesis work is the Iceland Rise. To broaden the scope of the work beyond a regional study, a comparison of the Iceland Rise results of suspended particulate matter is made with the results of a similar study in the western North Atlantic across the continental rise southeast of New York. This comparison allows the site-specific results to be differentiated from those perhaps more generally applicable. A detailed description of the Iceland Rise region and a summary of the applicable regional and hydrographic differences in the western North Atlantic continental rise region follows.

#### REGIONAL SETTING: ICELAND RISE

Previous investigations have shown that Norwegian Sea Overflow Water dominates the abyssal circulation of the northern and western North Atlantic (Figure 2.1; Lee and Ellett, 1965; Worthington, 1969; Worthington, 1976). In the Arctic basins and shelves north of Iceland, surface water is cooled and mixed downward by convective overturning in the winter (Peterson and Rooth, 1976). This cold, dense water mixes with warmer, more saline North Atlantic water as it cascades over sills in the ridge from Greenland to Scotland (Steele et al., 1962; Crease, 1965; Lee and Ellett, 1965; Worthington and Volkmann, 1965; Dietrich, 1967; Worthington, 1969;

Figure 2.1      Generalized western boundary, bottom-water circulation in the North Atlantic. Study areas south of Iceland and southeast of New York, denoted by the box and triangle respectively, are located in the path of a bottom current.



Swift et al., 1980). Water flows southward along the eastern flank of the Reykjanes Ridge, and westward through the Charlie-Gibbs Fracture Zone at approximately  $53^{\circ}\text{N}$  (Worthington and Volkmann, 1965; Garner, 1972; Schmitz and Hogg, 1978; Shor et al., 1980). From this latitude southward, the overflow water is mainly restricted to the western basin of the North Atlantic and flows along the western boundary.

The south Iceland Rise, the study area for this work (Figure 2.1), is directly in the path of the Norwegian Sea Overflow Water. This water flows southwestward through the region directed upslope from the contours of the East Katla Ridge by  $30^{\circ}$  to  $45^{\circ}$  (Figure 2.2; Steele et al., 1962; Worthington, 1970; Shor et al., 1977). Significant transport of Norwegian Sea Overflow Water, with current velocities on the order of 20-30 cm/sec (Shor, 1979), has been documented through this region.

Geologic effects of the Norwegian Sea Overflow Water are seen in abundance in the Iceland Basin region (Figure 2.3). Gardar Drift on the western side of the Iceland Basin, Feni Drift in Rockall Trough, and Hatton Drift on the western flank of Rockall Plateau are all thought to be formed and molded by deposition and redistribution of sediments from the overflow water (Johnson and Schneider, 1969; Jones et al., 1970; Davies and Laughton, 1972; Ellett and Roberts, 1973; Lonsdale and Hollister, 1979; McCave et al., 1980).

The detailed study region, the Katla Ridge province (Figure 2.2; Malmberg, 1974) in the south Iceland Rise, consists of two

Figure 2.2      Bathymetry of the Iceland Rise study area. Contours are in corrected meters. Current measurements were made along the northern transect across the eastern flank of the East Katla Ridge. Current velocities show westward to southwestward flow with an upslope component. The southern transect of stations extends from the nose of the West Katla Ridge into the Iceland Basin.

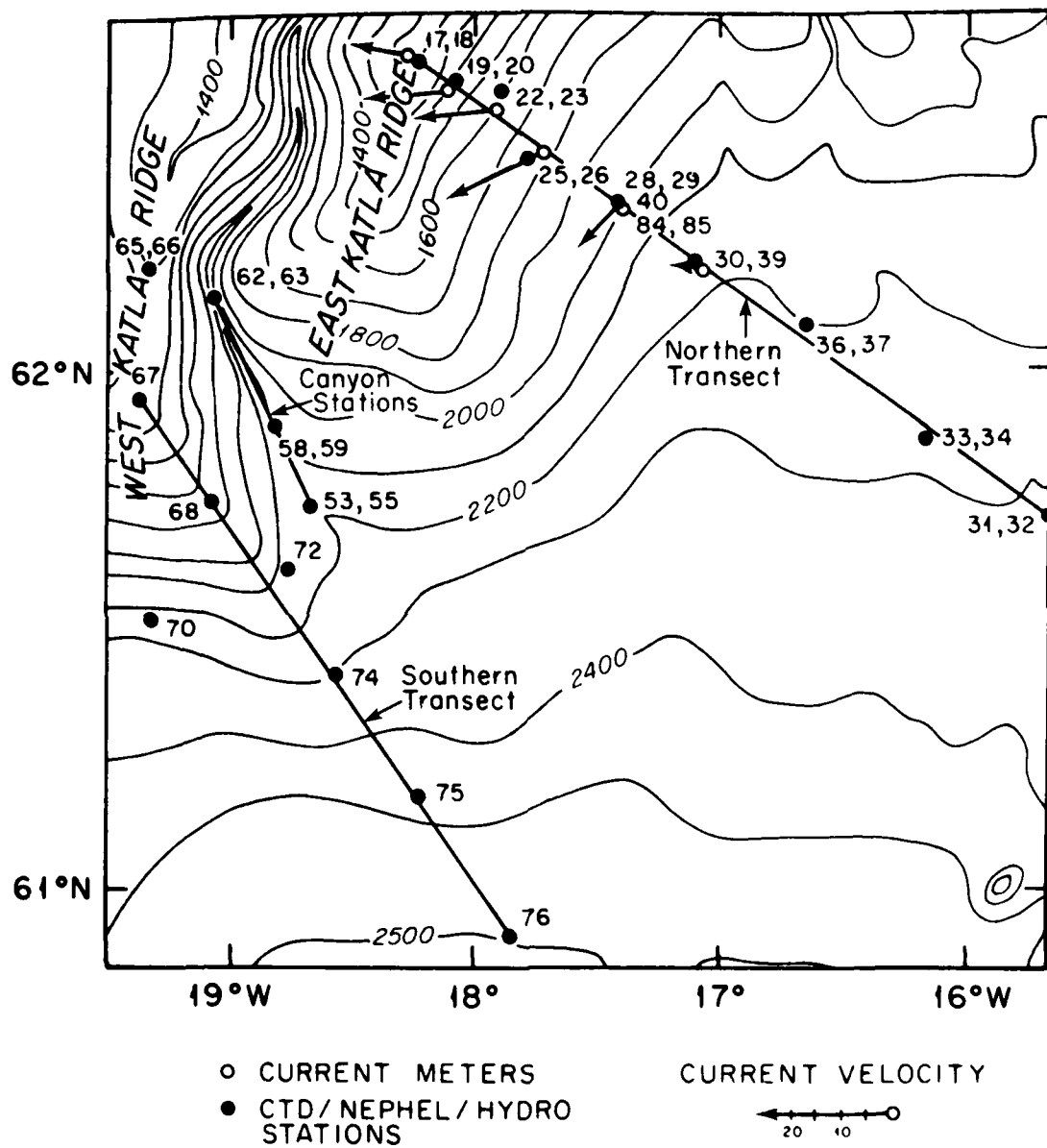
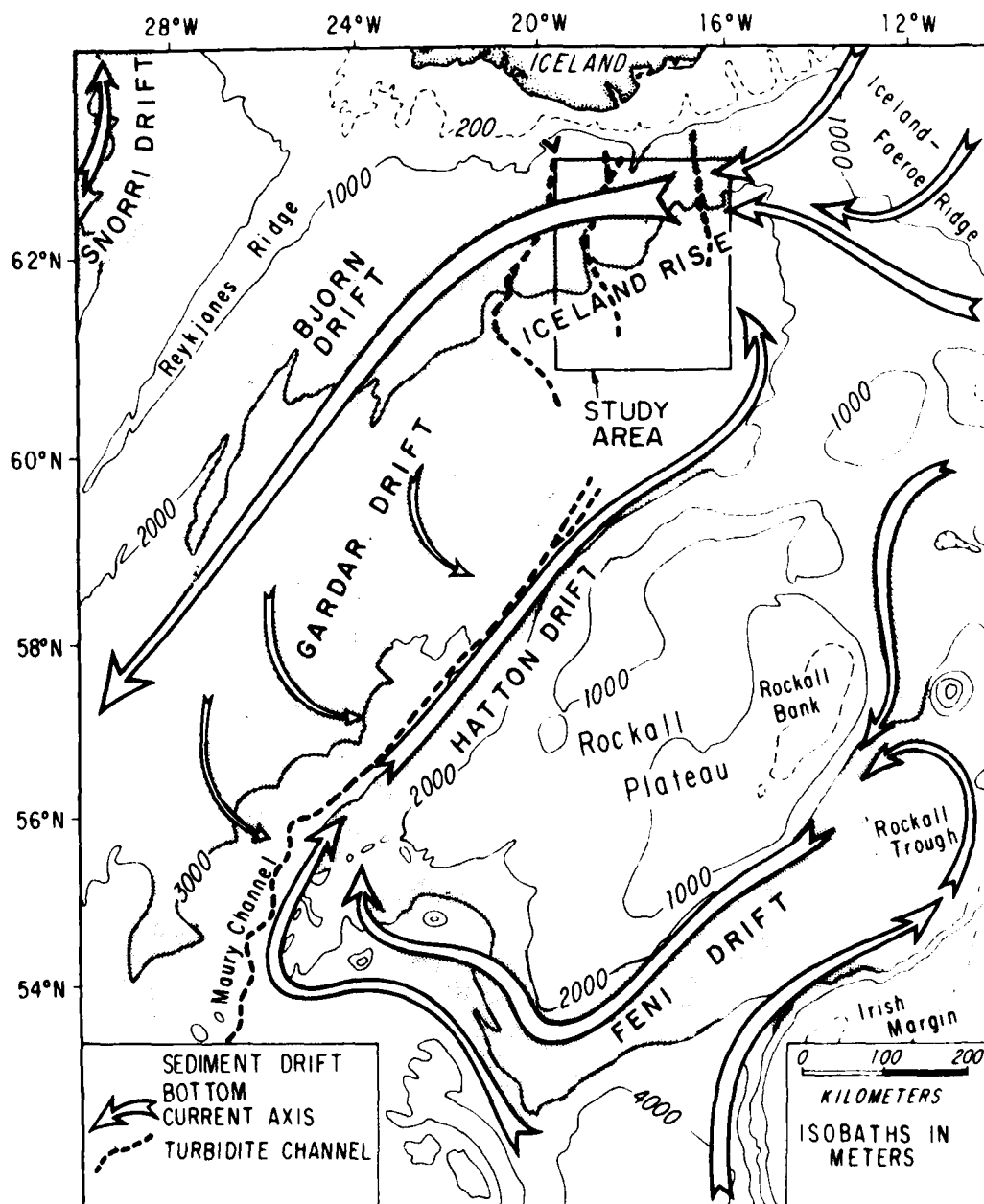


Figure 2.3      Location of the major sediment drifts in the northeastern North Atlantic. Arrows trace the flow of bottom water through the region. From McCave et al. (1980).





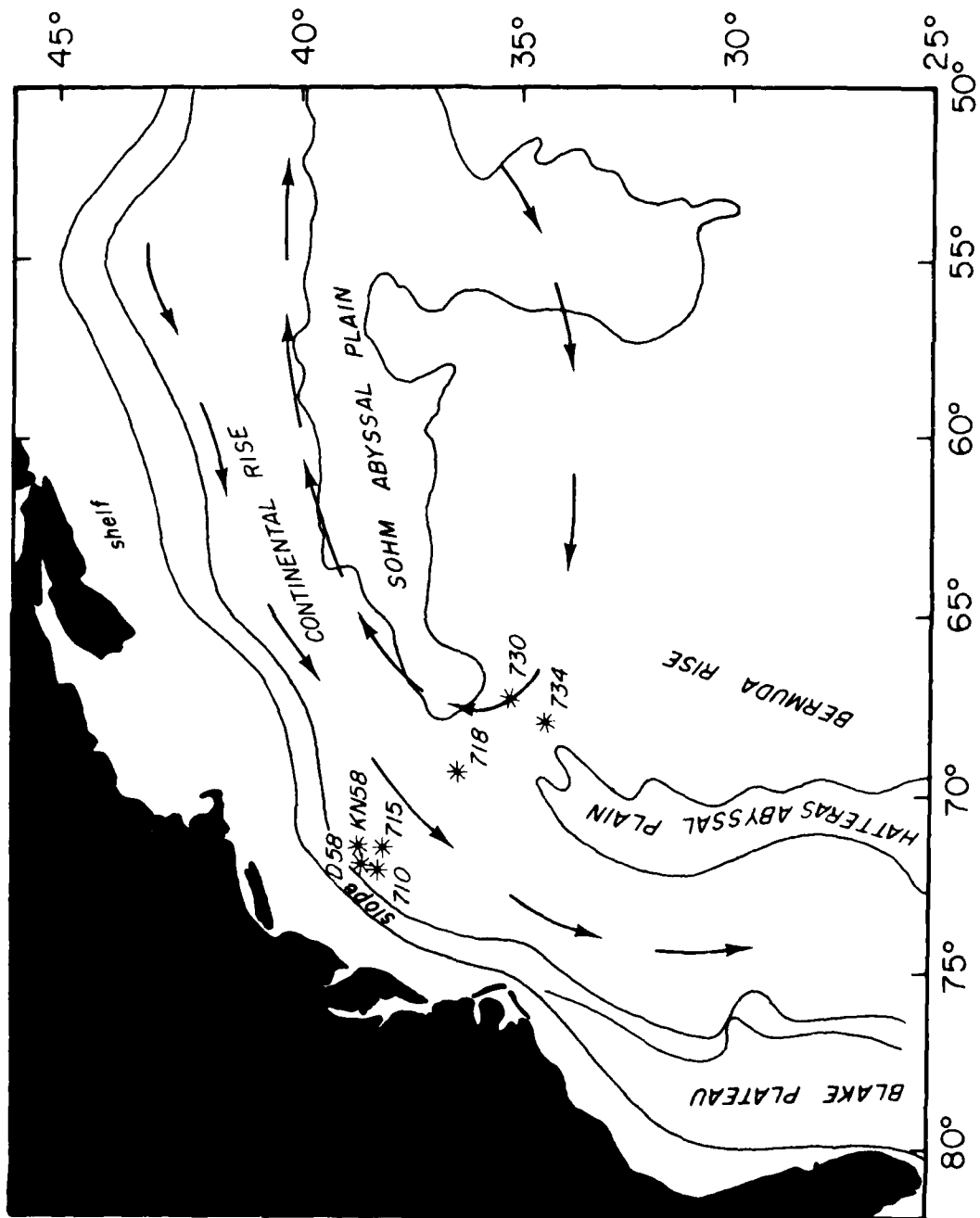
sedimentary ridges, the East and West Katla Ridges (Shor et al., 1977). The East Katla Ridge, striking NNE, has smooth parallel contours along its eastern flank from 1200-2100 m. Along this flank, the overflow water flows as a geostrophic current, roughly parallel to the regional contours (Steele et al., 1962). East Katla Ridge is separated from West Katla Ridge by a narrow turbidity-current canyon. The West Katla Ridge, oriented approximately N-S, has a wide, blunt nose and is separated from Gardar Drift to the southwest by a second turbidity-current canyon (Figures 2.2 and 2.3).

The south Iceland Rise is a region where both a strong surface source and a resuspended input of particulate matter are to be expected. Biogenic material in the surface waters and terrigenous material from volcanic and glaciofluvial sources are probable components of the flux of primary particulates (i.e. those of surface origin) through the water column. These sources are likely to have peak inputs during the spring and summer months, during the period of sampling for this study. The input of resuspended material is likely to be high due to the strong flow of Norwegian Sea Overflow Water through the region. The bottom current may be sporadic (Steele et al., 1962), but it has been observed in both winter and summer (Crease, 1965; Lee and Ellett, 1965; Shor, 1979). A mean velocity in the current core greater than 20 cm/sec was recorded during this study (Shor, 1979).

REGIONAL SETTING: WESTERN NORTH ATLANTIC

The area chosen for comparative study of the characteristics of particulate matter was the continental rise southeast of New York in the western North Atlantic (Figure 2.1). Hydrographically, this region is influenced by the deep northeastward-flowing Gulf Stream Gyre System (Worthington, 1976; Luyten, 1977; Laine and Hollister, 1980), and the southwestward-flowing Western Boundary Undercurrent (Figure 2.4; Hollister, 1967; Zimmerman, 1971; Richardson, 1977). Through geologic time, deep contour-following currents have shaped and developed the continental rise of eastern North America (Heezen et al., 1966; Field and Pilkey, 1971; Eittreim and Ewing, 1972; Hollister and Heezen, 1972). This continental boundary is dissected by many canyons which may have disgorged vast amounts of terrigenous debris into the deep sea during lower stands of sea level; presently, however, most of the sediment transported by rivers is trapped in estuaries and does not escape the continental shelf (Meade, 1972). Some terrigenous material may be supplied at mid-water depths by horizontal transport from the continental slope (Drake et al., 1972; Pierce, 1976). The introduction of biogenic material from the surface waters decreases rapidly from the highly productive, nutrient-rich slope waters to the unproductive Sargasso Sea. Particle input to the water column from the seafloor by resuspension and advection of sediments in this region, is possible from either the Gulf Stream Gyre System or the Western Boundary Undercurrent.

Figure 2.4      Locations of hydrographic stations in the western North Atlantic. Stations were taken from the base of the continental slope to the lower continental rise. Arrows indicate the abyssal flow of the Western Boundary Undercurrent and the Gulf Stream Gyre.



#### HYDROGRAPHY

The Iceland Rise study, of which this thesis work is a part, was a multidisciplinary, cooperative effort. As part of a comprehensive study of bottom currents and abyssal sedimentation south of Iceland, Shor (1979) described the hydrography of the region. The specifics of the instruments and methods used and calculations made for his work are contained in Shor (1979). A summary of his results which are pertinent to this study follows.

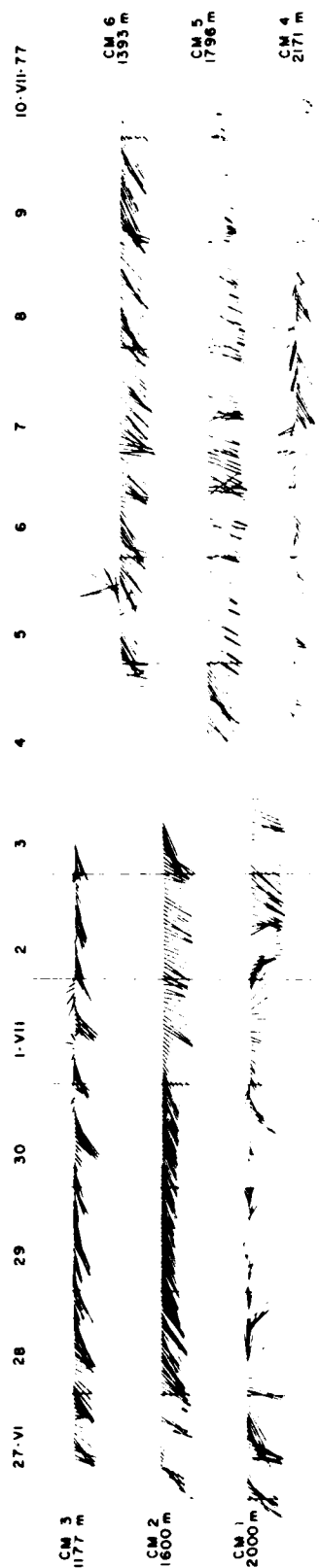
Six current meters were deployed for approximately one week, each during a two week period, at 10 m above bottom (mab) down the eastern flank of the East Katla Ridge from 1200 to 2171 m at 200 m isobath intervals (Figure 2.2). The meters between 1393 and 1796 m recorded velocities in excess of 20 cm/sec for the duration of the experiment (Table 2.1). The direction of flow was predominantly to the west-southwest, tending approximately  $30^{\circ}$  upslope with a maximum speed of 29 cm/sec (Figure 2.2). To the northwest and southeast of this inferred core of the overflow current, the mean current speed was 10 cm/sec or less, and flow directions were more variable. At the 2000 m mooring, the current record indicates velocities below threshold ( $<2$  cm/sec) for two days. Prior to and following this event, currents exceeded 20 cm/sec (Figure 2.5).

Current meter data are restricted to a single transect of stations across the region, referred to as the northern transect (see Figure 2.2). Photographic evidence of currents agrees well

TABLE 2.1: Current meter data. (from Shor, 1979)

	HT ABOVE		DURATION (hours)	VECTOR MEAN		MEAN SPEED (cm/sec)	VELOCITY @ 217° (cm/sec)
	BOTTOM (meters)			speed	direction		
CM 1	10		162	10.6 cm/sec	227°T	14.0	10.4
CM 2	10		151	20.9 cm/sec	226°T	21.0	13.7
CM 3	10		144	13.3 cm/sec	282°T	14.5	5.4
CM 4	10		156	5.8 cm/sec	273°T	8.8	3.2
CM 5	10		152	20.0 cm/sec	247°T	20.4	17.3
CM 6	10		132	18.7 cm/sec	265°T	21.5	12.5
				LATITUDE	LONGITUDE	WATER DEPTH	GMT
CM 1				62°17.4'N	17°24.6'W	2000 (meters)	2300/26 June- 1900/03 July
CM 2				62°28.3'N	17°53.5'W	1600	0400/27 June- 1330/03 July
CM 3				62°34.9'N	18°15.0'W	1177	0820/27 June- 1000/03 July
CM 4				62°10.8'N	17°03.6'W	2171	0300/04 July- 1800/10 July
CM 5				62°23.2'N	17°42.4'W	1796	0825/04 July- 1200/10 July
CM 6				62°30.8'N	18°04.8'W	1393	1930/04 July- 0800/10 July

Figure 2.5      Current velocity vectors plotted against time. Current meter locations are shown in Figure 2.2. Measurements are 30-minute averages. Tidal components have not been removed. Note the consistency of velocities in the three meters at 1393, 1600 and 1796 m, located in the core of the overflow water. From Shor (1979).





with actual measurements for this northern transect of stations. Bottom photographs indicate that currents are westward along the West Katla Ridge, and oscillating northerly and southerly flow, is indicated for canyon stations.

Geostrophic calculations made from hydrographic sections generally show southwestward velocities increasing with depth for individual pairs of stations. Calculated velocities are highest between 1600 and 1800 m for the northern transect and between 1800 to 2100 m for the southern transect, which corresponds with the minima in potential temperature (see Shor, 1979; Figures 2.5 and 2.6). Volume transport through the northern transect is calculated to be  $5.0 \times 10^6 \text{ m}^3/\text{sec}$ ; and through the southern line, is  $4.2 \times 10^6 \text{ m}^3/\text{sec}$ . A small eastward flow,  $0.8 \times 10^6 \text{ m}^3/\text{sec}$ , was indicated between stations 31 and 76.

Isothermal bottom mixed layers along the northern transect of stations were observed to be 30-50 m thick in the axis of the bottom current; off-axis and along the southern line, the layers were 10-20 m thick. These layers are thought to form by turbulent mixing at boundaries (Armi, 1978). In this study, the thickest mixed layers occur in conjunction with the highest velocities or in the canyon. Mixed layers are absent where current velocities are inferred from direct measurements and geostrophic calculations, to be low (see Shor, 1979; Figure 2.8).

## SAMPLING SCHEMES AND APPROACHES

A primary purpose of this thesis is to determine whether resuspension is presently occurring and to examine the influence of resuspension on the composition and characteristics of suspended particulate matter. Approaches to this problem and the rationale for using particular sampling schemes are discussed in this section.

## CURRENT COMPETENCE

Resuspension is generally acknowledged to be responsible for the existence of nepheloid layers in the deep sea (Heezen et al., 1966; Betzer and Pilson, 1971; Eittreim and Ewing, 1974; Biscaye and Eittreim, 1977). However, it is difficult to predict the conditions under which a deep-sea current is competent to actively resuspend seafloor sediments. Laboratory flume experiments have estimated critical erosion velocities for deep-sea clays and oozes to be in the range of 15-35 cm/sec (Southard et al., 1971; Lonsdale and Southard, 1974; Young and Southard, 1978). Within the axis of the overflow current, from 1400-1800 m along the flank of the East Katla Ridge, velocities were within this range for the duration of the experiment. Upslope and downslope of the axis, velocities are usually less than 15 cm/sec (Figure 2.5). This observation suggests that resuspension may be occurring during the entire time of the experiment in the current core, and occasionally when velocities exceed those critical for erosion, at the stations further removed.

Since the laboratory experiments of Southard and co-workers represent idealized circumstances and were not performed with sediment or biota from this particular study area, a comparison of the field and laboratory measurements alone cannot be used to conclusively establish that resuspension is actively occurring. Instead, it simply indicates that resuspension is likely. Suspended particulate matter in the study area was examined to determine whether changes in the composition and characteristics of the particles in the lower portion of the water column were indicative of resuspension.

#### SUSPENDED MATTER

Suspended particles are usually measured by filtration of water samples collected with Niskin bottles (Brewer et al., 1976). This method gives only an instantaneous point measurement of concentration, and with the small volume of water collected (5-30 liters), does not provide a representative sample of the rare larger particles in suspension (Bishop, 1977). Large particles may be major contributors to the mass flux of material through the water column (McCave, 1975). The two principal means of collecting these large particles are large-volume filtration systems and sediment traps (Bishop, 1977; Gardner, 1977a; Honjo, 1978; Spencer et al., 1978). Large-volume filtration has been restricted to shallow depths (<1500 m), precluding sampling in the deep-sea near-bottom nepheloid layer. Sediment traps can be used at all water depths.

Niskin bottles were used to collect the standing crop of small particles. Based on SEM photomicrographs of filtered samples and particle size distributions measured with a Coulter counter, most material collected in Niskin bottles below the surface water in the study region is less than 20  $\mu\text{m}$ . Based on the assumption of Stokes-law settling, the vertical fall velocities of particles in this size range, ( $5 \times 10^{-5}$  to  $1.3 \times 10^{-2}$  cm/sec), are more than three orders of magnitude less than the horizontal velocities in the core of the bottom current south of Iceland. This suggests that the material collected by the Niskin bottles in the high current areas of this study is a quasi-conservative property of the water.

Sediment traps were used to collect time-integrated samples of the suspended material in flux. The size of material caught by the sediment traps ranged up to a few millimeters, indicating that there are large particles in flux through the water column which are not collected by water bottles. However, sediment traps are not only large particle collectors: 5-42% of the trap samples are composed of particles less than 20  $\mu\text{m}$ . One problem with sediment traps is that the state of aggregation of particulate matter when it enters the traps is unknown. Loose aggregates may break up and with the high concentration of material on the floor of the sediment traps, aggregates may form. Size fractionation by sieving reveals small particles, particularly volcanic glass, adhered to large pteropods, foraminifera, diatoms, and organic matter. This agglomeration may have occurred in the sediment trap. The presence of intact and

collapsed fecal pellets on filters from the sieved fractions indicates that these aggregates maintain their integrity through wet-sieving, but filtration and drying of the samples may cause pellets to collapse.

Measurement of concentrations of suspended particulate matter from water bottles is limited by the number of bottles per cast. Nephelometers provide nearly continuous measurements of light scattering through the water column. To give a more detailed view of the distribution of suspended particulate matter, light-scattering observations were made during this study and correlated with concentrations of suspended matter from samples obtained at the same time.

These three instruments, Niskin bottles, sediment traps, and the nephelometer, were used to obtain information on suspended particulate matter during this study. The results are discussed in the following chapters.

CHAPTER III  
CHARACTERISTICS OF SUSPENDED PARTICULATE  
MATTER FROM NISKIN BOTTLES

INTRODUCTION

The distribution and redistribution of marine particulate matter is of great importance in interpreting the biological, chemical and geological processes acting in the deep sea. Particulate matter from the productive surface layer descends through the water column slowly by individual particle settling and rapidly by fecal-pellet transport, providing organic-rich food to the benthic communities. Adsorption of dissolved species and scavenging of chemical elements by the particulate matter may affect the distribution of chemical tracers and radioisotopes throughout the water column. Geologically, the suspended material in flux to the seafloor may ultimately become part of the sedimentary record.

Presently, a primary source of particulate matter to the deep ocean is the surface waters. Rivers, and off Iceland, glaciers, deliver high suspended loads of terrigenous material as well as dissolved nutrients necessary for the proliferation of plankton. Phytoplankton and zooplankton dominate the particles present in the surface waters. Their skeletons and pellets sink, comprising a large fraction of the material in transit through the water column. Other components, such as volcanic and wind-blown detritus, are regionally important constituents of the suspended matter.

Particles settling from the surface waters are constantly subjected to the physical, biological and chemical processes of aggregation, disaggregation, decomposition and dissolution. These processes are responsible for changing the characteristics of the particulate matter during descent through the water column to the seafloor.

Suspended material is also derived from the seafloor. Only infrequently does freshly deposited material become permanently incorporated into the sedimentary record at its first place of deposition. More commonly, animals living in and on the seafloor reprocess and transport the sediments through feeding and bioturbation. Deep-sea currents can also resuspend and transport the surface sediments. Both these mechanisms, animals and currents, re-introduce previously deposited material into the water column. This recurrent resuspension can result in vast redistribution of material (Ewing and Hollister, 1972).

Suspended matter originating from the surface waters may differ in its characteristics of particles from that originating at the seafloor. Assessing and interpreting the differences in particles settling from the surface waters versus those resuspended from the seafloor is the purpose of this chapter.

#### NEPHELOID LAYERS

In many areas of the oceans, after a decrease in concentration of suspended particulate matter (SPM) with depth due to dissolution,

decomposition, and consumption in the water column, there is an increase in the concentration of SPM near the seafloor. This layer of increased concentration of SPM (the near-bottom nepheloid layer) is thought to be due to resuspension of sediment from the seafloor (Heezen et al., 1966; Betzer and Pilson, 1971; Feely 1975; Brewer et al., 1977; Biscaye and Eittreim, 1977). The depth of minimum concentration of SPM above the near-bottom nepheloid layer is termed the "clear-water minimum" (Biscaye and Eittreim, 1977; Figure 3.1). Below this level, there is an increase in the resuspended component of the SPM. By sampling in clear water and the nepheloid layer below, the increasing influence of resuspended sediment can be examined.

#### HISTORICAL PERSPECTIVE

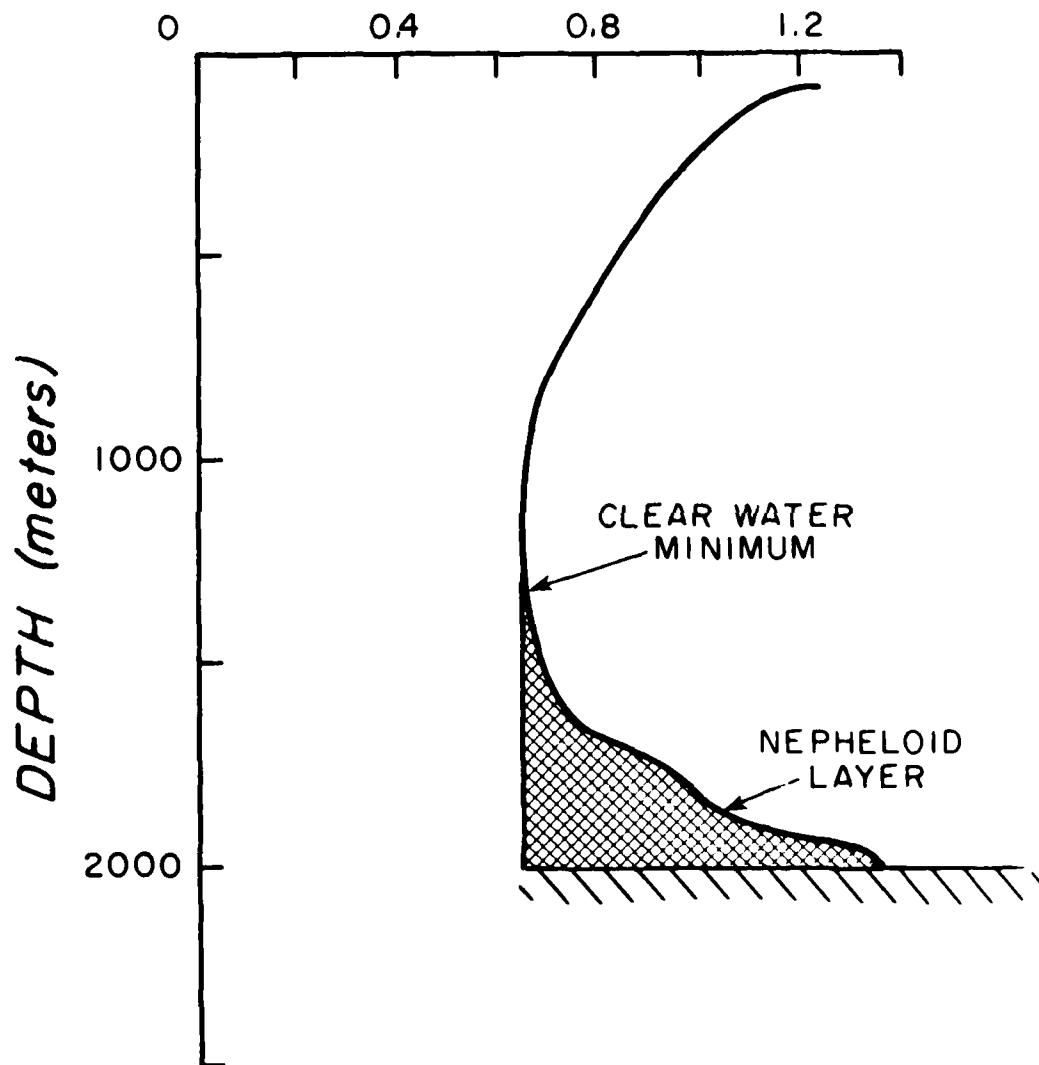
The characteristics of marine particulate matter have been studied extensively only in the past decade. With the initiation of the GEOSECS program, a detailed examination of the geochemistry of abyssal ocean water and SPM was begun. The GEOSECS program collected SPM for chemical, mineralogic, and microscopic analyses (Brewer et al., 1976). Since GEOSECS began, numerous techniques have been employed to determine the properties of suspended material. Compositional analyses have been performed with the scanning electron microscope for morphologic identification (Honjo et al., 1974; Honjo, 1976; Feely, 1976; Bishop et al., 1977), X-ray diffraction for mineralogy (Feely, 1975), and neutron activation and



Figure 3.1 Idealized nephelometer profile. The unit  $\text{Log } E/E_D$  is a measure of scattering made by comparing the scattered light to a direct beam. Cross-hatched area represents the near-bottom nepheloid layer. Note the location of the clear water minimum.

# LIGHT-SCATTERING

$\text{LOG } E/E_D$



atomic absorption for elemental determination (Spencer et al., 1972; Krishnaswami and Sarin, 1976; Bishop et al., 1977). Size distributions of suspended matter have been determined with instruments which count and discriminate particles by volume, e.g., a Coulter counter (Carder et al., 1971; Plank et al., 1972; Sheldon et al., 1972; Brun-Cottan, 1976). Optical devices, nephelometers and transmissometers, have been widely used to indirectly measure the concentration of SPM. Nephelometers, which measure scattered light, have been used to document the existence of near-bottom nepheloid layers in many areas of the world's oceans (Ewing and Thorndike, 1965; Eittreim et al., 1972; Eittreim and Ewing, 1972; Biscaye and Eittreim, 1974; Kolla et al., 1976; Biscaye and Eittreim, 1977). Transmissometers, which measure transmitted light (a function of both absorption and scattering by SPM and water), have been used to monitor variations in the quantity of SPM, particularly in surface waters (Pak and Zaneveld, 1977; Bartz et al., 1978). Using data on SPM concentration and size, models have been formulated for the vertical flux of particles in the ocean (McCave, 1975; Bishop, 1977).

These techniques have been used to gain a global perspective of the distribution of SPM, gross compositional information, and preliminary ideas about its dynamics. Now that this base-line information has been established, it is possible to examine in detail those characteristics of marine particulate matter that may yield insight into its behavior and provenance.

#### OBJECTIVES

Geological and physical-oceanographic data were obtained in the North Atlantic along the Iceland Rise (cruise ATLANTIS II-94) and in the western North Atlantic along the continental rise (cruises DALLAS, KNORR-58, and OCEANUS-6) with the following objectives in mind:

- (1) to determine the differences between clear-water particles and nepheloid-layer particles with respect to size distribution, composition, density, and light-scattering characteristics in limited study regions;
- (2) to identify properties of particles which might be useful in distinguishing their prior source;
- (3) to determine whether differences observed between properties of nepheloid-layer particles and clear-water particles are regionally site-specific;
- (4) to identify those processes which most strongly influence particle characteristics, e.g., dissolution, decomposition, deposition, and resuspension.

#### OBSERVATIONAL TECHNIQUES

This investigation is a comparison of the characteristics of the SPM in two regions: the Iceland Rise and the continental rise southeast of New York (Figure 2.1). A total of thirty-two hydrographic stations and twenty-four nephelometer stations were

occupied on the Iceland Rise during June and July 1977 (Figure 2.2), and seven hydrographic stations were occupied in the western North Atlantic along a transect southeast of New York in the summer of 1976 (Figure 2.4). Each hydrographic station employed six to twelve 5 or 30 liter Niskin bottles for collection of SPM. Samples were collected from the lower portion of the water column from both clear water and the near-bottom nepheloid layer. Reversing thermometers were used to obtain accurate records of sample depth in mid-water; a pinger was used to determine the height of the bottom bottles above the sea floor. Simultaneous nephelometer profiles using an L-DGO-Thorndike deep-sea photographic nephelometer (Thorndike, 1975) were taken at most Iceland Rise stations to ensure that samples were from a known position relative to the nepheloid layer (if present).

#### CONCENTRATION OF SPM

A 250 ml aliquot was taken from the Niskin bottles immediately on retrieval for size distribution determination of SPM. The remaining water was filtered with an in-line vacuum filtration system through a preweighed 47 mm diameter, 0.4  $\mu$ m Nuclepore filter. Filters were washed ten times with filtered distilled water to remove salt and reweighed upon return to the laboratory to determine the mass of particles. For the Iceland Rise, water beneath the spigot was filtered onto a separate filter to collect the "dregs" (Gardner, 1977b). For the western North Atlantic, the entire water bottle was filtered onto one filter by tilting the

bottle to remove all the water. Concentrations reported as "corrected" concentration include this "dregs" material. Combined errors in filter weighing and volume readings amount to  $\pm 9\%$  for concentrations of  $20 \mu\text{g/l}$  and  $\pm 5\%$  at  $100 \mu\text{g/l}$ .

#### SIZE DISTRIBUTIONS

Size distribution of SPM was determined with a Model TA II Coulter counter. With this instrument, particles suspended in an electrolyte (seawater) are drawn through a small aperture. When a suspended particle passes through the aperture, it decreases the volume of electrolyte in the aperture, thereby increasing the resistance and decreasing the current in the circuit. The percent current change is proportional to the ratio of the particle volume to the aperture volume. This relationship is linear for particles having diameters between 2% and 40% of the aperture diameter (Sheldon and Parsons, 1967).

Coulter-counter data are recorded in terms of either total number or total volume of particles counted and are subdivided into logarithmically increasing size grades, each grade representing a doubling of volume. A  $50 \mu\text{m}$  aperture and a 2.0 ml sample size were used in this study to measure the size distribution of particles having equivalent spherical diameters from 1-20  $\mu\text{m}$ .

### LIGHT SCATTERING

Light-scattering was measured with a L-DGO-Thorndike deep-sea photographic nephelometer (Thorndike, 1975), designed to measure relative forward light scattering from  $8^{\circ}$  to  $24^{\circ}$ . Although light scattering is dependent on all the optical properties of the particles (Jerlov, 1968), forward scattering is most sensitive to variations in concentration of SPM and least sensitive to variations in particle size and index of refraction (Thorndike, 1975).

The nephelometer is composed basically of a light source and a camera lens. An attenuator is situated between the source and lens to calibrate direct light. Scattered light as well as the attenuated direct light are measured by the nephelometer. A ratio is formed between the intensity of the scattered light,  $E$ , and that of the attenuated direct light,  $E_D$ , to form a scattering index,  $E/E_D$ . Forming this ratio circumvents problems involved in correcting the scattering values due to variation in the intensity of the source and direct beam attenuation losses. Nephelometer readings are most often reported in terms of  $\log(E/E_D)$ .

Nephelometers are optical instruments and cannot directly yield absolute concentrations of SPM. However, nephelometer readings in a few instances have been calibrated by sampling and filtering water for SPM from nephelometer lowerings (Beardsley et al., 1970; Baker et al., 1974; Carder et al., 1974; Sternberg et al., 1974). The L-DGO-Thorndike nephelometer has been calibrated by Biscaye and Eittrheim (1974) through their work in a limited region of the

Blake-Bahama Outer Ridge and the Hatteras Abyssal Plain (BBOR-HAP). A slightly different calibration for this instrument was obtained by them from the eastern North American lower continental rise (LCR) (Biscaye and Eittrheim, 1977).

#### COMPOSITIONAL ANALYSES

Composition of the SPM collected from the near-bottom nepheloid layer and overlying clear water was studied by photographing sections of filters with a scanning electron microscope. Five stations in the Iceland Rise area and two along the western North Atlantic transect were selected for quantification of the composition of SPM. A sample from the nepheloid layer and one from clear water for each station were photographed for optical identification of the SPM. Four or five random photographs were taken in each of four sections of a filter to determine homogeneity of the SPM on the filters.

Additionally, "dregs" filters from two of the Iceland Rise samples were photographed and counted to allow a valid comparison with the western North Atlantic samples, where the entire sample was collected on one filter. A comparison of "dregs" composition to that of the above-spigot sample was made for the Iceland Rise samples to examine the differentiation of the SPM while settling in the water samplers (Gardner, 1977b).

Twelve classes of particles were identified and counted: small coccoliths ( $<4 \mu\text{m}$ ), large coccoliths ( $>4 \mu\text{m}$ ), centric diatoms,



pennate diatoms, dinoflagellates, organic matter, plankton fragments, fecal pellets, aggregates, clays, mineral matter, and unidentified particles (Plate 3.1). Particles smaller than two microns were not included in the counts since positive identification was impossible.

Chi-square analysis of the compositional data was performed:

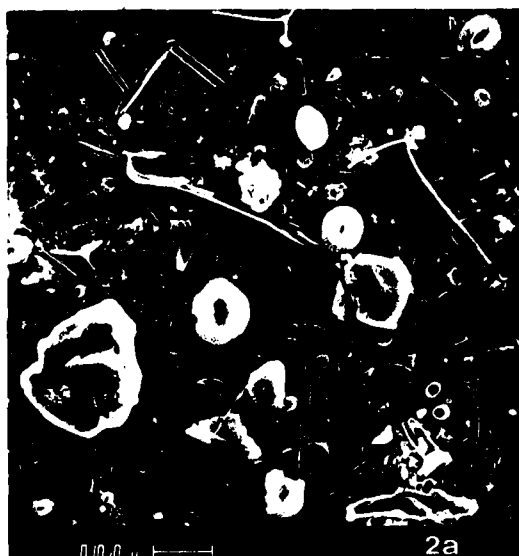
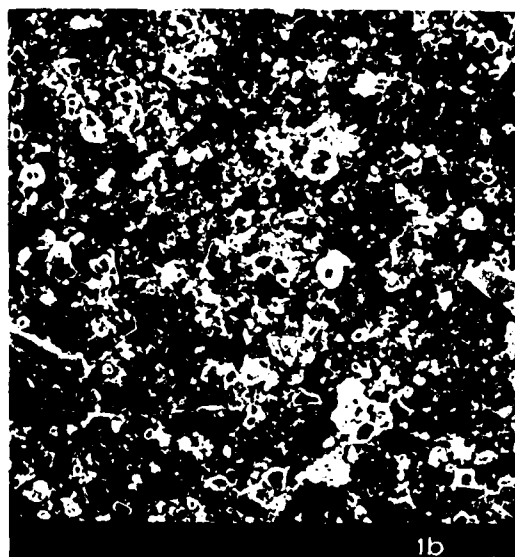
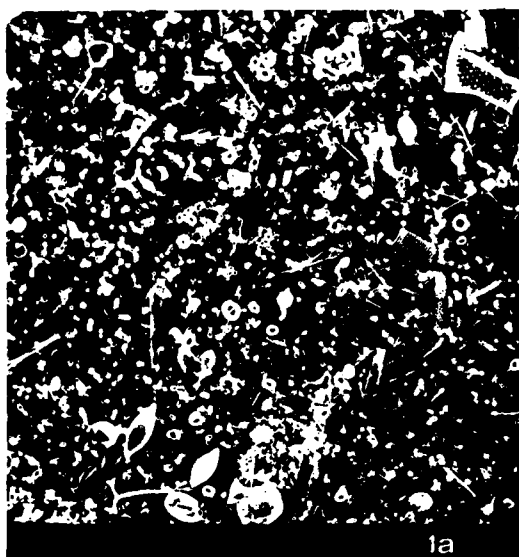
- a) to determine whether the random photographs represented subsamples of a homogeneous population of material on the filters;
- b) to determine whether compositional differences between clear-water samples and nepheloid-layer samples for individual stations were statistically significant; c) to determine whether the clear-water samples from all stations were statistically different from each other and whether the nepheloid-layer samples from all stations were statistically different from each other; and d) if all the above are true, to determine whether collectively the clear-water samples statistically differ from the nepheloid-layer samples.

## RESULTS

### SPM CONCENTRATION

High concentrations of SPM in the lowest few hundred meters of the water column extend from the sill depths along the Greenland-Scotland ridge, at approximately 62°N, southward along the western side of the North Atlantic basin outlining the path of

Plate 3.1 SEM photographs of suspended particulate matter. Samples (1a,1b) are taken from clear water (a) and the nepheloid layer (b) from the western North Atlantic. Note the decrease in percentage of small coccoliths and increase in percentage of clays and mineral matter between these two samples. Samples (2a,2b) are "dregs" filters from the Iceland Rise. Note the aggregates of coccoliths and diatoms and the large mineral grains. Approximate scale is given below each photograph. X 1100.



bottom-water flow (Figure 3.2; Brewer et al., 1976). This detailed study of SPM across the bottom-current axis south of Iceland and along a transect across the western North Atlantic margin is an attempt to compare SPM characteristics from areas widely separated, but perhaps influenced by the same bottom current.

#### Iceland Rise

Profiles of concentration of SPM were obtained in the lower 1000 m of the water column along two transects across the axis of the bottom current from the crests of the East and West Katla Ridges (1200 and 1500 m) into the Iceland Basin (2500 m)(Figure 2.2). In water depths greater than 2000 m the profiles are characterized by low concentrations ( $<30 \mu\text{g/l}$ , corrected concentration of  $\sim 40 \mu\text{g/l}$ ) in mid-water depths with sharp increases in concentration in the lowest hundred meters of the water column (Figure 3.3). Shallower than 1800 m, concentrations in mid-water are higher ( $\sim 50 \mu\text{g/l}$ , corrected concentration of  $\sim 70 \mu\text{g/l}$ ) with thicker nepheloid layers (up to 300 m)(Figure 3.3).

Stations 29, 40, and 85 are reoccupations of a station at approximately 2000 m. The character of the SPM profile changed dramatically over a ten-day period (Figure 3.4), even at mid-water depths. Station 29 showed a gradual increase in concentration towards the seafloor to concentrations up to  $120 \mu\text{g/l}$  (corrected concentration  $>200 \mu\text{g/l}$ ). Mid-water concentrations exceed  $40 \mu\text{g/l}$  (corrected concentration of  $\sim 50 \mu\text{g/l}$ ). Four days later, station 40

Figure 3.2      Distribution of suspended particulate matter in the western Atlantic Ocean. High concentrations in the nepheloid layer, seen from the Denmark Straits to 45°N, outlines the flow of the Norwegian Sea Overflow water. From Brewer et al. (1976).

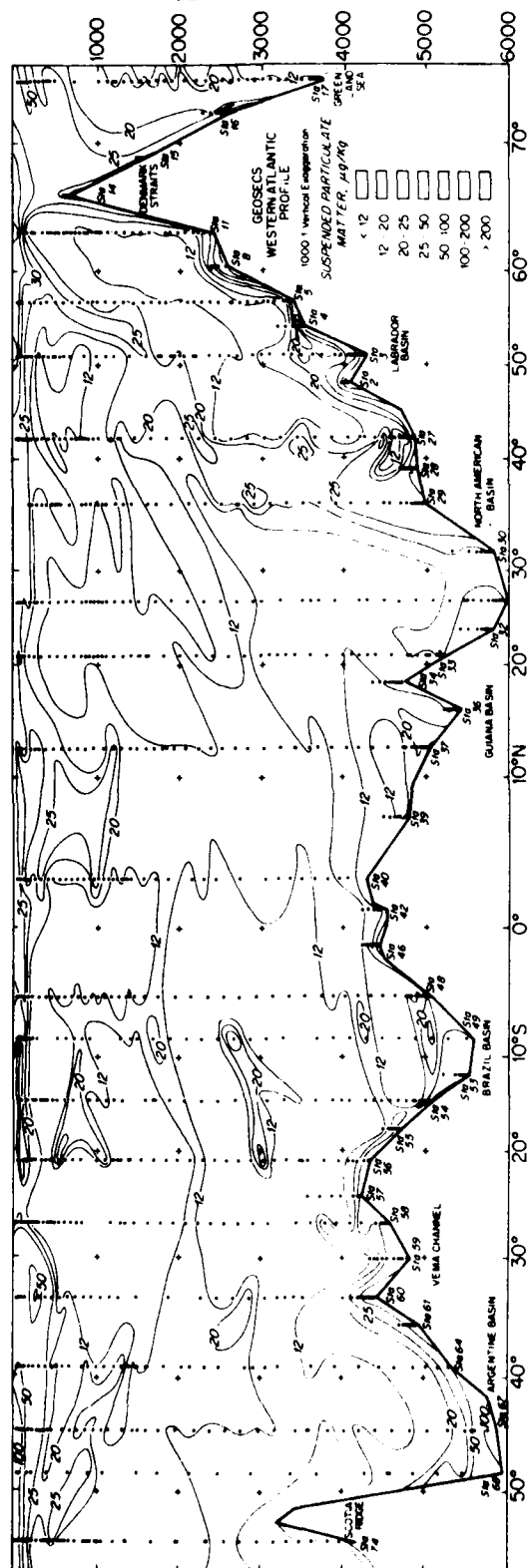
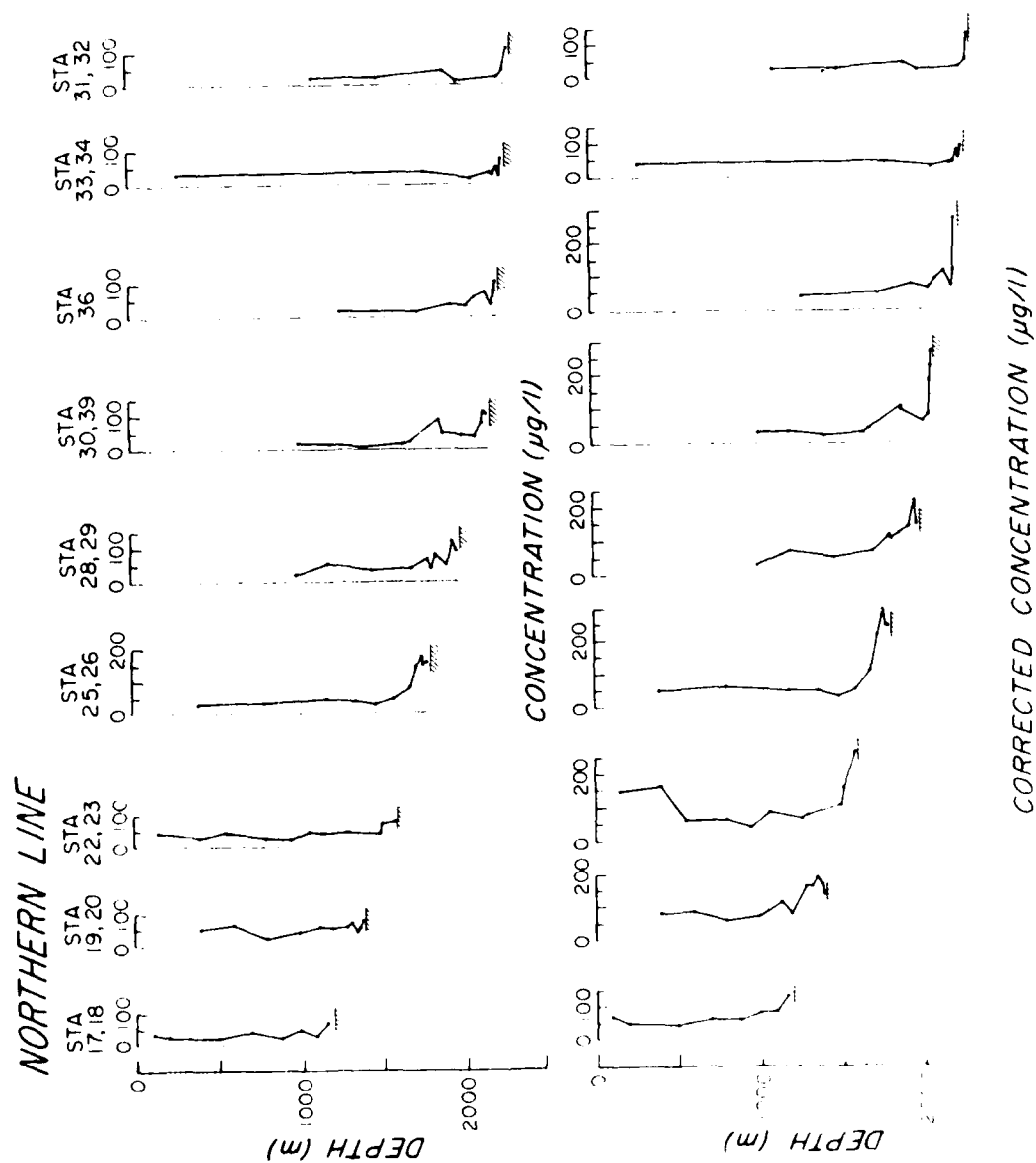


Figure 3.3      Profiles of suspended particulate matter from the Iceland Rise. Most profiles show nepheloid layers.  
a) Stations from the northern transect, both standard and corrected concentrations; b) stations from the southern line with standard and corrected concentrations.

d





b

# *SOUTHERN LINE*

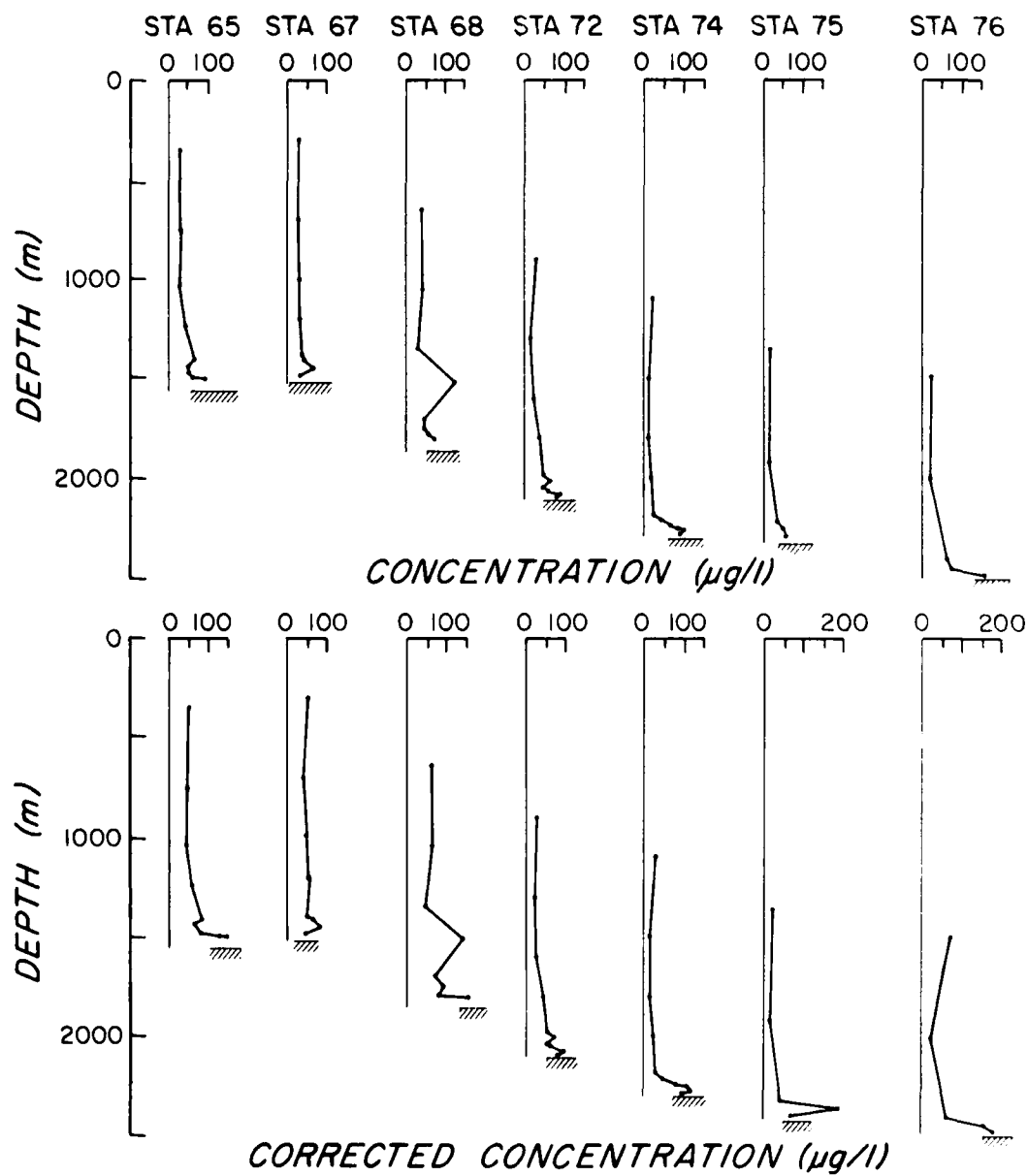
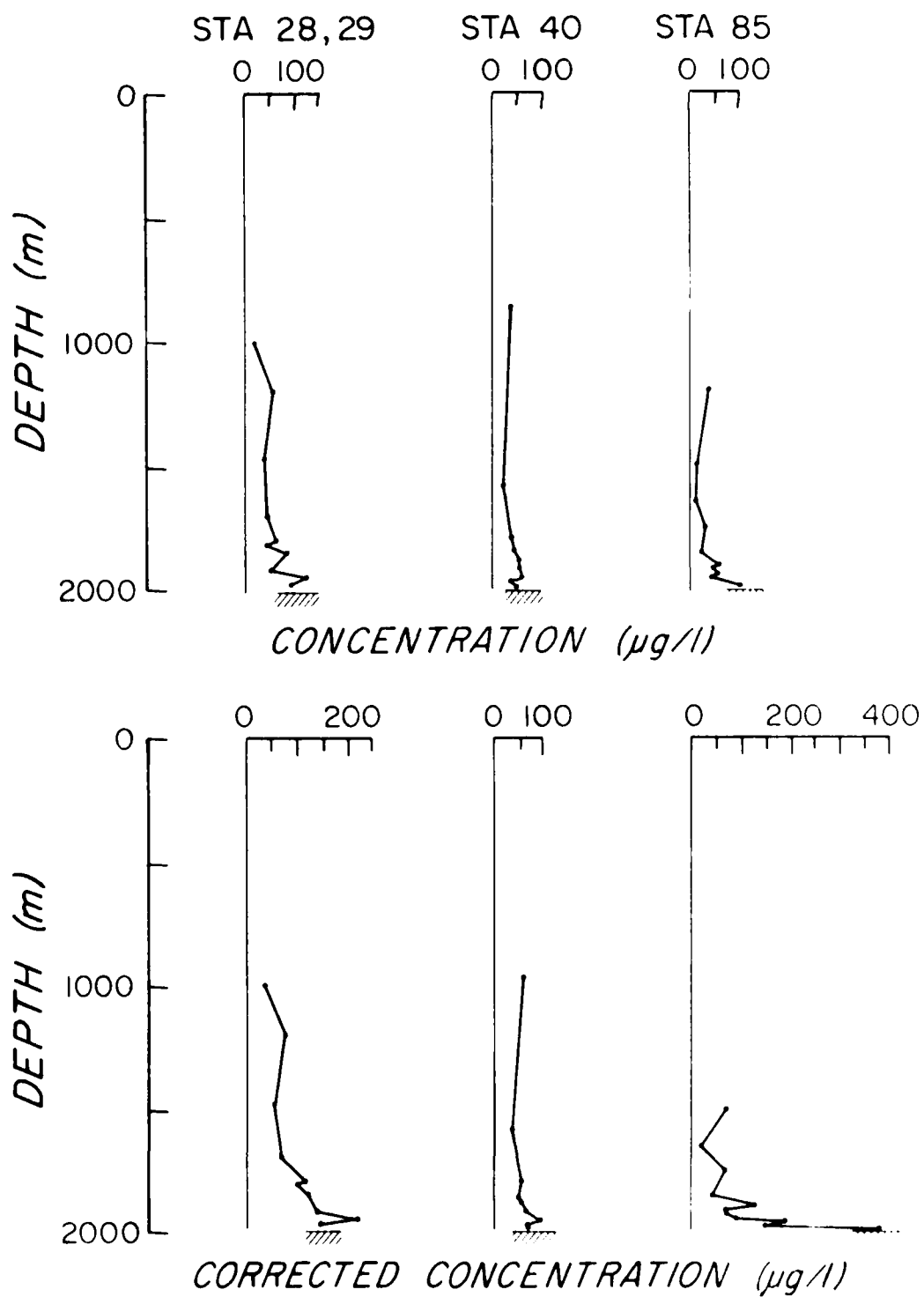


Figure 3.4      Profiles of suspended particulate matter from reoccupation of the station at 2000 m from the Iceland Rise. Note the temporal variability in both mid-water concentrations and nepheloid layer concentrations over a ten-day period.

# REOCCUPATIONS OF THE 2000 m STATION



had both lower mid-water concentrations ( $\sim 20 \mu\text{g/l}$ , corrected concentration of  $\sim 40 \mu\text{g/l}$ ) and nepheloid-layer concentrations ( $< 60 \mu\text{g/l}$ , corrected concentration of  $\sim 90 \mu\text{g/l}$ ). For the final reoccupation, mid-water values remained low ( $< 20 \mu\text{g/l}$ , corrected concentration of  $20\text{--}70 \mu\text{g/l}$ ), but nepheloid concentrations increase to greater than  $90 \mu\text{g/l}$  (corrected concentration  $> 300 \mu\text{g/l}$ ).

Concentration maxima are seen in mid-water near the crest of the Katla Ridges (Figure 3.5). These features are above the near-bottom nepheloid layers and may be detached turbid waters laterally advected from upstream (Armi, 1978).

#### Western North Atlantic

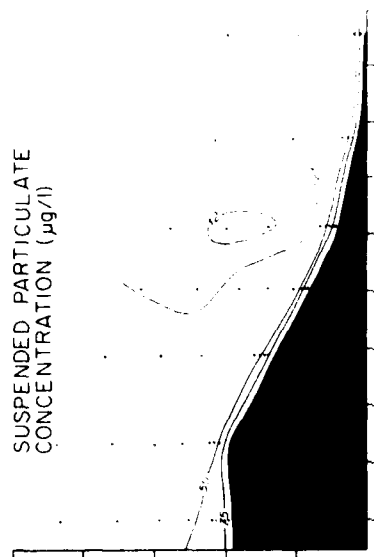
A single hydrographic section was made across the continental rise southeast of New York (Gardner, 1977a). Nepheloid-layer corrected concentrations on the slope and upper rise did not exceed  $100 \mu\text{g/l}$ , while above the lower rise and abyssal plain, nepheloid-layer corrected concentrations consistently exceeded  $100 \mu\text{g/l}$  (Figure 3.6). Mid-water maxima in particle concentrations in slope and upper rise waters are interpreted as being caused by material advected horizontally outward from the slope.

#### LIGHT-SCATTERING OBSERVATIONS

Information on SPM concentration from water bottles is limited to a small number of discrete samples per station. In order to obtain a continuous vertical profile of SPM, light-scattering

Figure 3.5      Cross-sections of suspended particulate matter for the Iceland Rise region. Dots indicate sample locations. Corrected concentrations include the "dregs" (Gardner, 1977b). Highest concentrations in the near-bottom water occur in the bottom current axis, along the flanks of the ridges.

ICELAND RISE  
SOUTHERN SECTION



ICELAND RISE  
NORTHERN SECTION

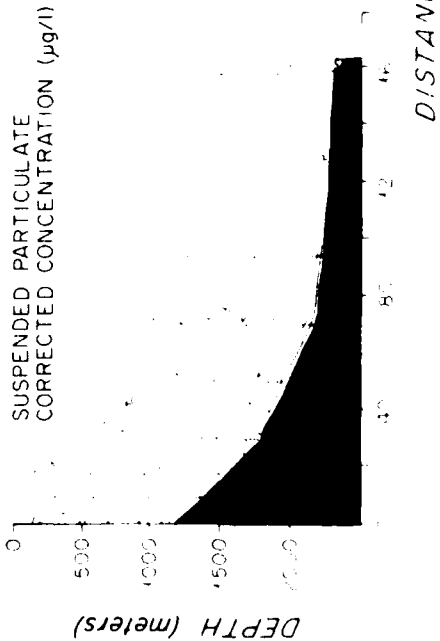
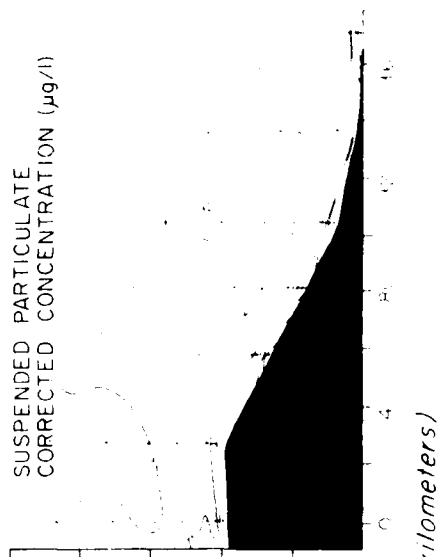
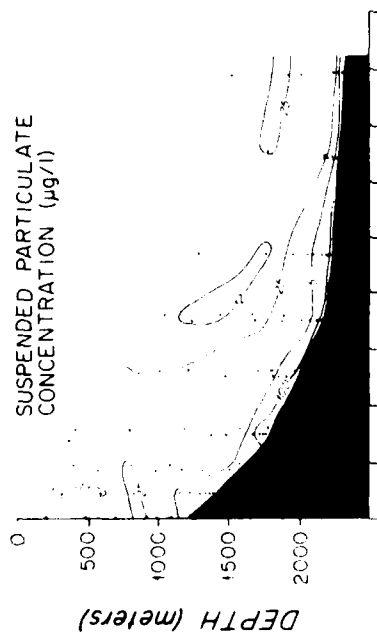
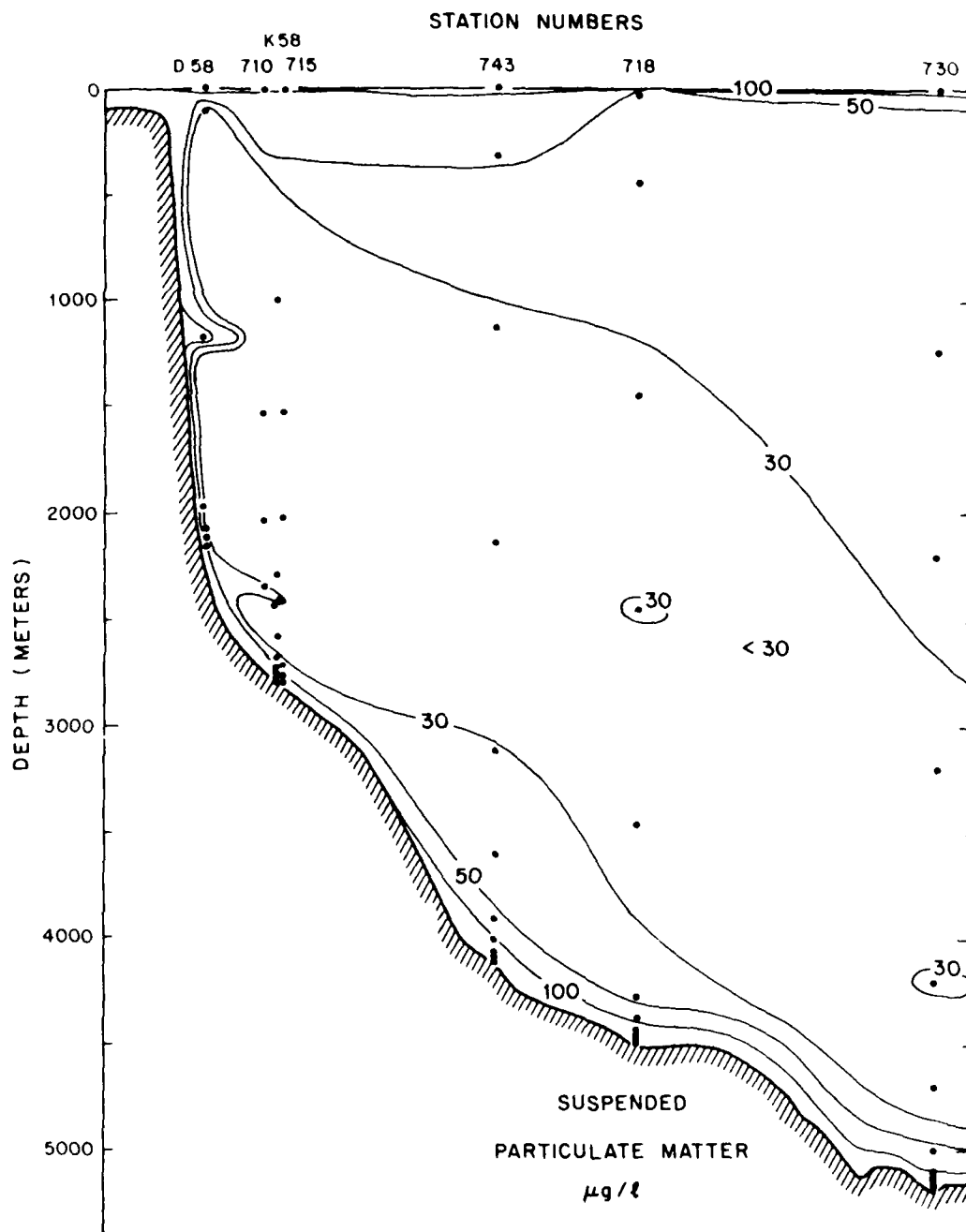


Figure 3.9 Cross-section of suspended particulate matter along the continental rise southeast of New York. Concentrations are corrected for "dregs." Note the occurrence of some high concentrations in mid-water which may reflect advection of material from the slope. From Gardner (1977a).





measurements, which can be calibrated in terms of SPM concentrations, were made at most of the hydrographic stations in the Iceland Rise region (Figure 3.7).

The nephelometer profiles exhibit features similar to those of the SPM, but being more detailed, the nephelometer profiles allow the vertical extent and structure of the nepheloid layer to be more clearly defined. Lowest clear-water values ( $0.34 \log E/E_D$ ) are found over the basin; highest near-bottom values ( $1.43-1.55 \log E/E_D$ ) occur along the ridge flank and over the basin in water depths greater than 1800 m.

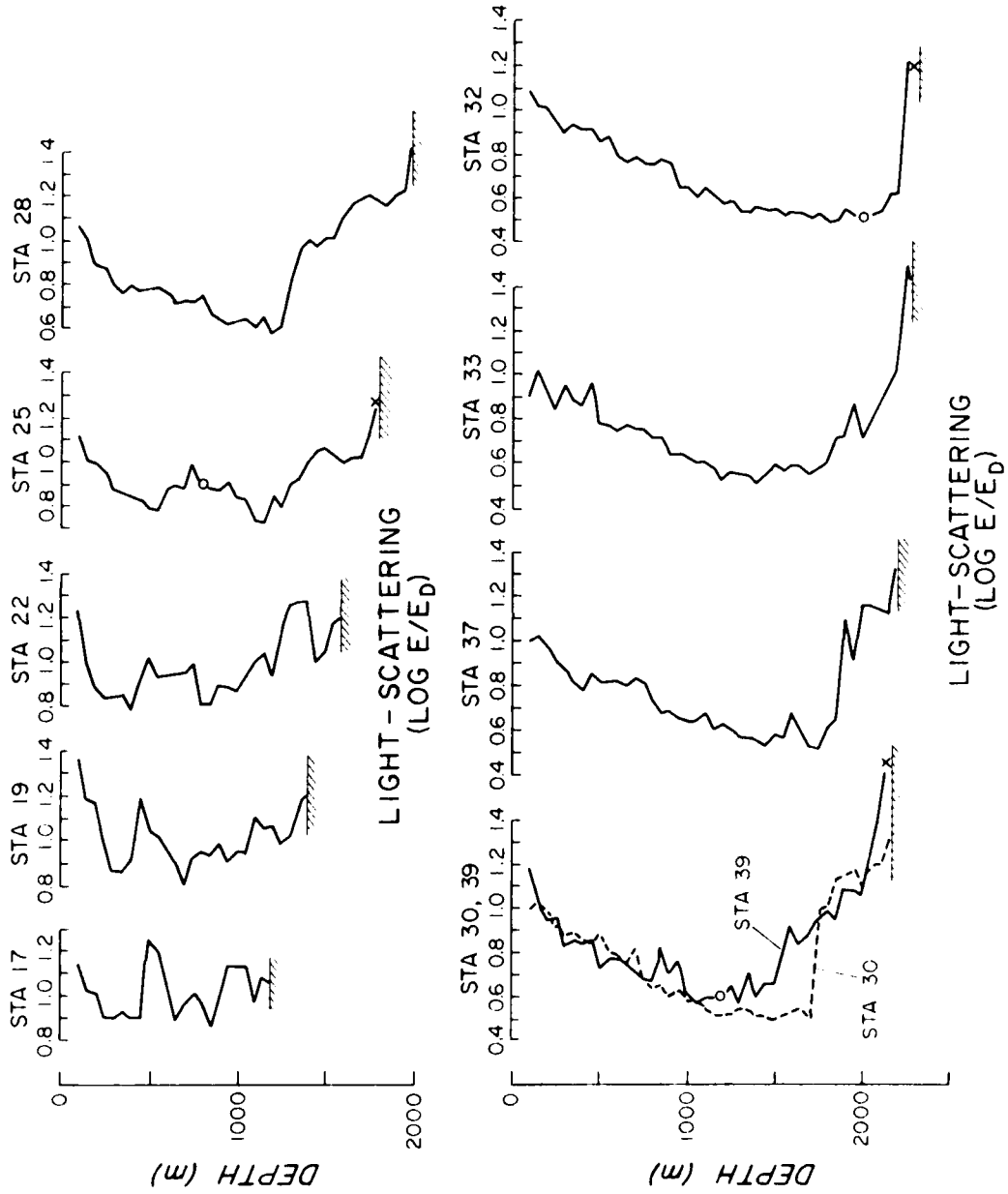
The character of the nephelometer profiles changes substantially from the crest of the ridge eastward into the basin. The ridge-crest profiles show variable light scattering throughout the water column, generally in excess of  $0.5 \log E/E_D$ . At station 67, no clearly defined nepheloid layer is observed. To the east, along the ridge flank (1600-2200 m) nepheloid layers up to 700 m thick are developed. Clear-water values decrease below those from the ridge crest. The nepheloid layers for the last profile of each transect, located over the basin, are thin (<100 m), but show a very sharp gradient from clear water to the nepheloid layer.

Profiles taken within the canyon between the two ridges are somewhat erratic. A general increase in light scattering from mid-water to the seafloor is observed, but the nepheloid layer is not as well-defined as it is along the ridge flanks (Figure 3.7). Light scattering is fairly high ( $>0.6 \log E/E_D$ ) for these profiles throughout the entire water column.

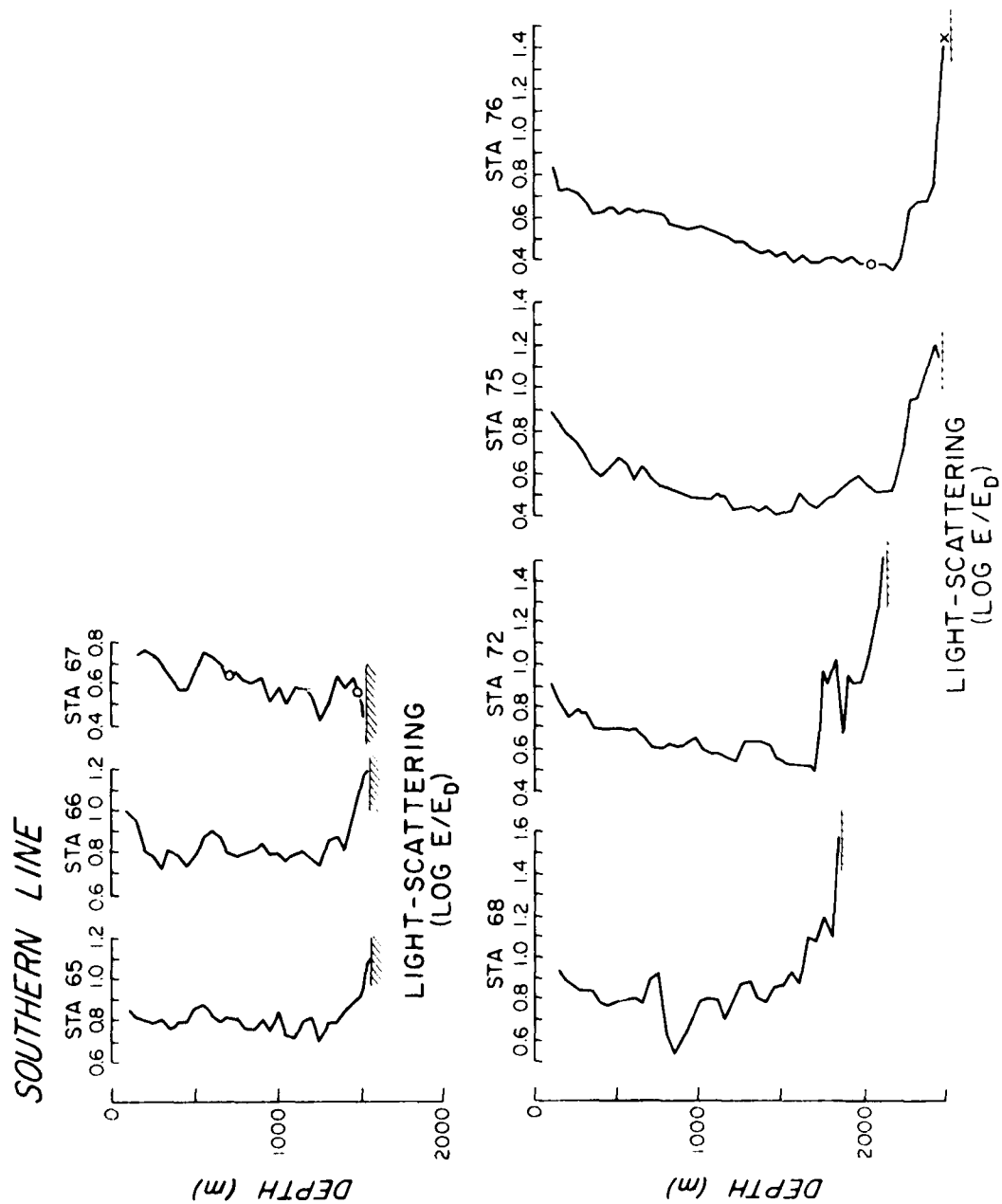
Figure 3.7 Nephelometer profiles from the Iceland Rise region. Nepheloid layers are sharper and thinner with increasing depth. Location of samples taken for suspended particle size analysis is indicated by (o) for clear water samples and (x) for nepheloid layer samples. a) Northern section; b) southern section; c) canyon stations.

d

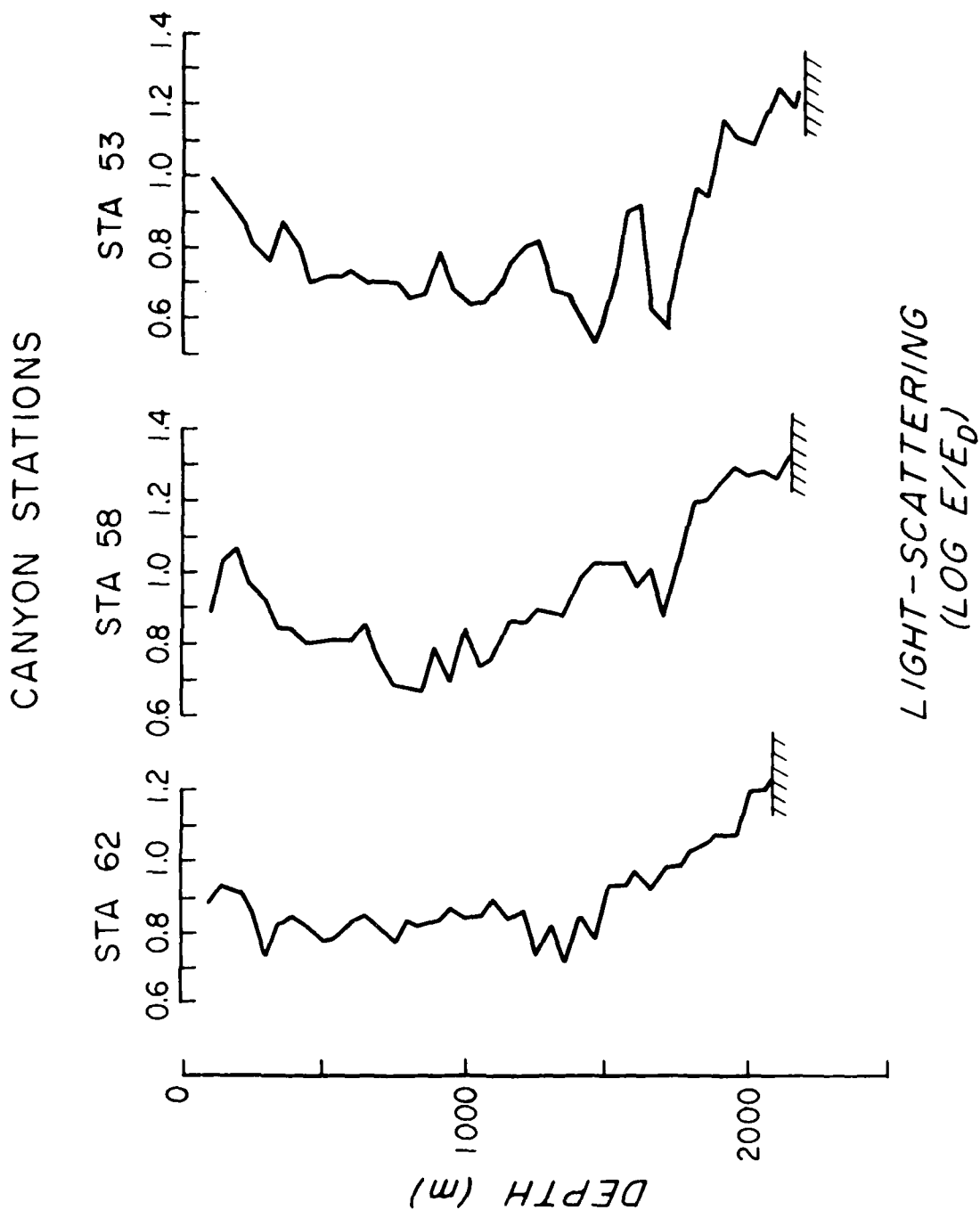
NORTHERN LINE



b



C



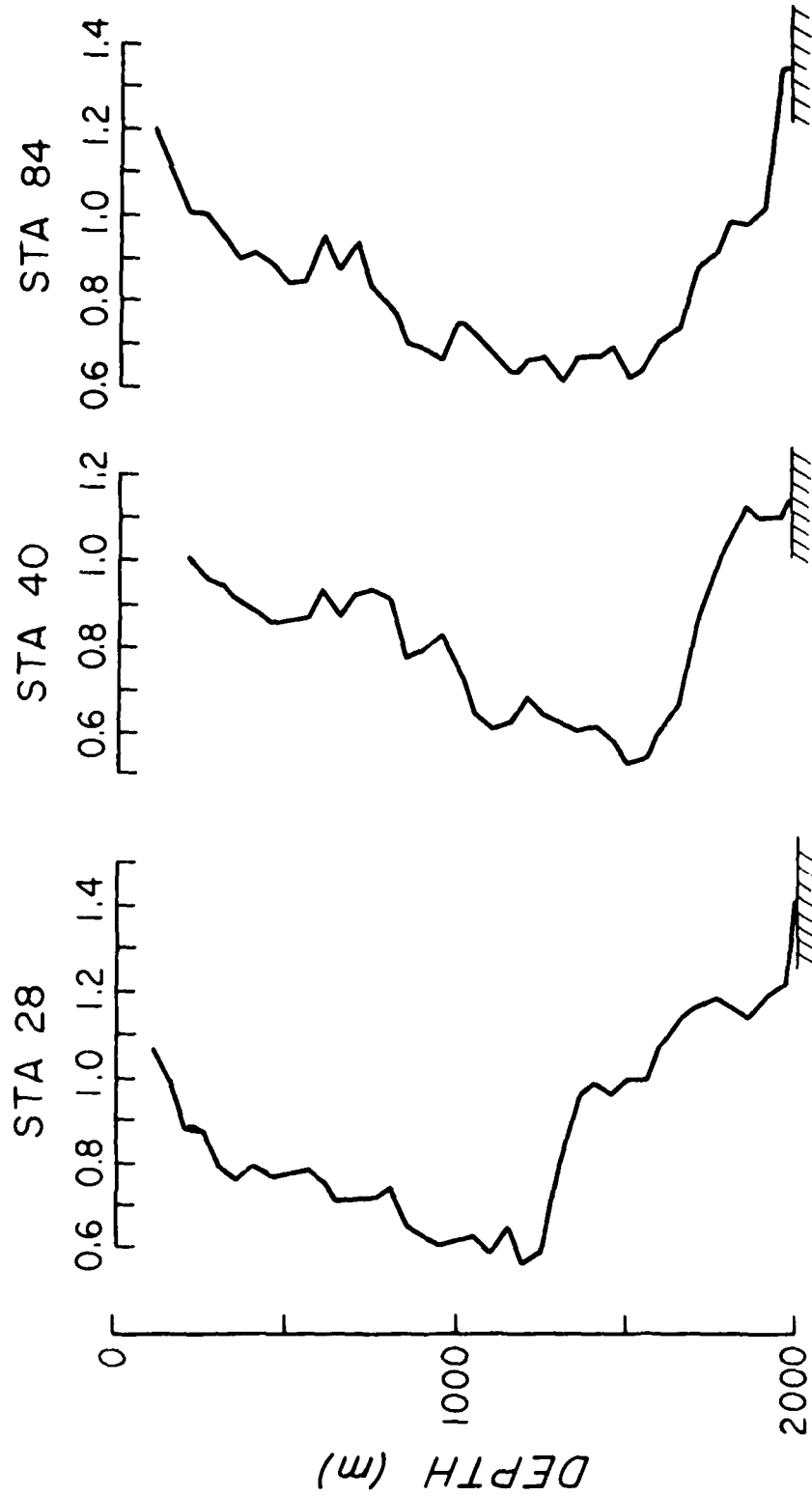
The two reoccupations of station 28 (2000 m) gives some idea of the temporal variability of the nepheloid-layer structure over 10 days (Figure 3.8). The first occupation shows a sharply defined nepheloid layer, 700 m thick, with a second increase in light scattering in the deepest 10 m of the water column. Station 40, taken 4 days later, has a much thinner (400 m) nepheloid layer. The nepheloid layer is characterized by a gradual increase with depth leveling off to a constant value for the final 150 m. The second reoccupation (Station 84) has a nepheloid layer 450 m thick with a sharp increase with depth in light scattering in the lowermost 30 m. These reoccupations demonstrate that light scattering in the region is highly variable over the time scale of ten days.

The nephelometer profiles have been compiled to give cross-section distributions of light-scattering values (Figure 3.9). These cross sections show the extent and influence of the bottom current in the region. In the axis of the current (1600-2000 m), the nepheloid layer is several hundred meters thick, but diffuse, suggesting mixing of material up into the water column. In the basin, the nepheloid layer is thin, perhaps reflecting the lesser influence of the bottom current.

High values of light scattering in the surface waters are probably caused by both high biological productivity and Icelandic terrigenous input. The general decrease in clear-water values from the ridge crests into the basin is a function of the distance from Iceland.

Figure 3.8 Nephelometer profiles from reoccupation of the station at 2000 m from the Iceland Rise, showing the temporal variability in the thickness and structure of the nepheloid layer over a ten-day period.

# REOCCUPATION OF THE 2000 m STATION

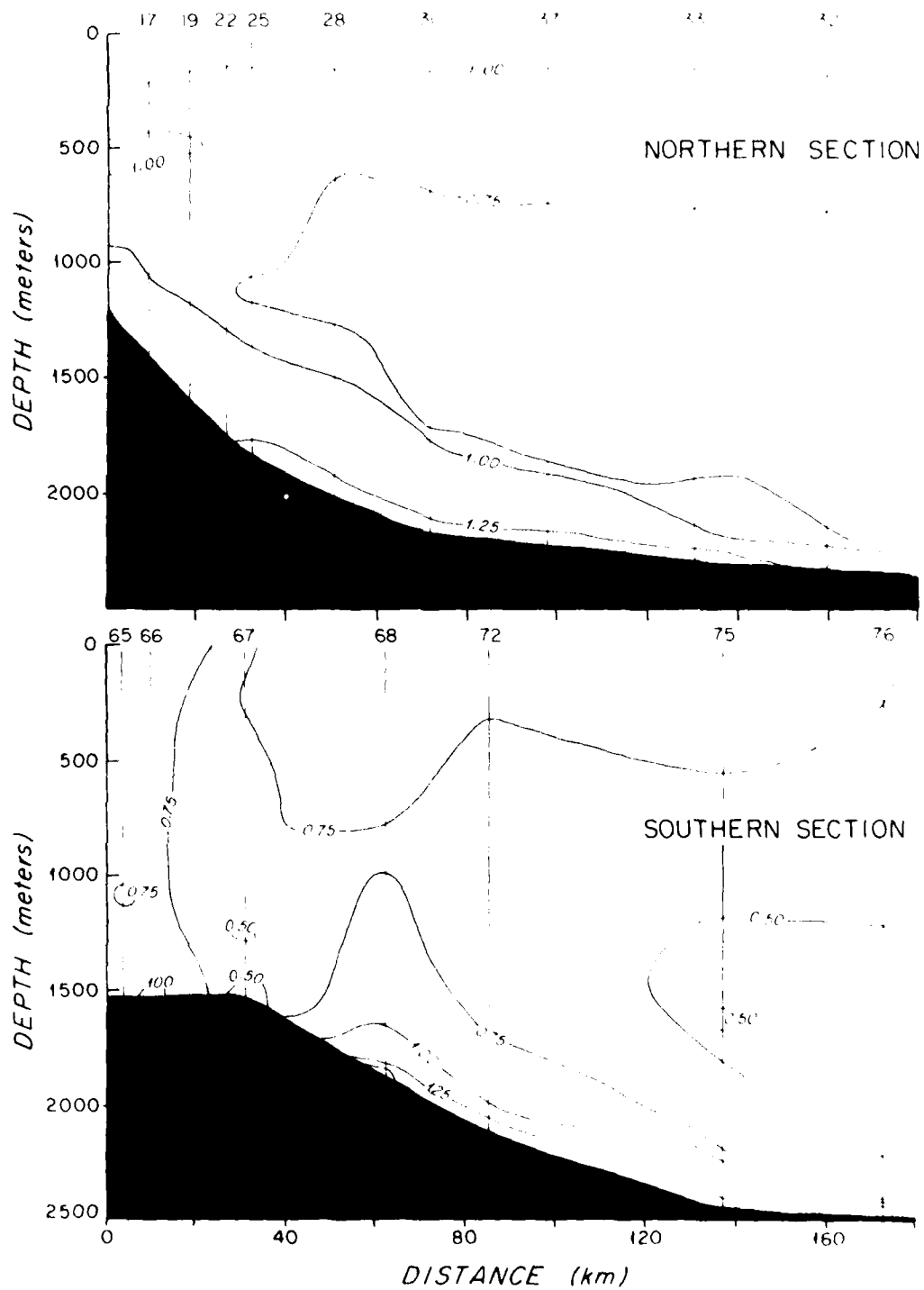


LIGHT-SCATTERING  
(LOG E/E<sub>0</sub>)



Figure 3.9 Cross-sections of light-scattering for the northern and southern lines on the Iceland Rise. Vertical lines indicate station control. Light-scattering readings were made at 25 m intervals.

LIGHT SCATTERING ( $\text{LOG } E/E_D$ )  
ICELAND RISE



#### SIZE DISTRIBUTION ANALYSES

SPM size distributions have been examined throughout the oceans, but primarily in the surface waters (Sheldon et al., 1972). The presence and patchiness of biological components in the surface waters dramatically affects the size distributions of SPM. For this reason, both latitudinal and seasonal variations have been noted (Sheldon et al., 1972). Below the surface waters (upper few hundred meters) the particle size distributions change. Distributions in surface waters are often characterized by a predominant modal size, whereas in deep water the particle size spectrum is one of approximately equal amounts of material in logarithmically increasing size grades (Sheldon et al., 1972), at least up to the 100  $\mu$ m size studied.

Particle size distributions are most often displayed in terms of number, volume, or weight of particles per logarithmic size grade. Since this work deals with volume or weight concentrations rather than numbers of particles, all of the data will be displayed in terms of volumetric measurements.

#### Iceland Rise

Water samples were obtained from above and within the near-bottom nepheloid layer in order to compare characteristics of the SPM. Two stations (25 and 39) are used here as examples to demonstrate the differences in the percent volume size distributions between clear water and the nepheloid layer. Station 25 is located

along the northern section in the Iceland Rise region at 1804 m, in the axis of the bottom current. A nephelometer profile obtained at the same site (Figure 3.7) was compared with SPM concentrations from the water bottles to verify which bottles were within the nepheloid layer. The size distribution from bottle 1 at 1780 m, within the nepheloid layer, shows a distribution with low variance (Figure 3.10). The modal size is an equivalent spherical diameter of 5.6  $\mu\text{m}$ . The shape of this distribution stands in marked contrast to the more typical deep-water profile of equal volumes of material in the size grades from 1-20  $\mu\text{m}$  (Sheldon et al., 1972). This more typical distribution, with high variance, is seen in bottle 4 (790 m), in clear water at the same station (Figure 3.10).

Similar features are seen at Station 39 at 2163 m, farther down the ridge flank (Figure 3.11). The nephelometer profile for this station (Figure 3.7) shows a sharply defined nepheloid layer. From this profile, two bottles, B1 and B5, were selected for comparison of particle size distributions. Bottle B5 at 2145 m shows a low variance distribution as does the nepheloid-layer sample at Station 25, but the modal size of this distribution is larger ( $\sim 9 \mu\text{m}$ ). Bottle B1, at 1205 m, has an irregular, high variance distribution, as does the clear-water sample from Station 25.

#### Western North Atlantic

Size distributions were also compared for clear- and nepheloid-layer waters in the western North Atlantic. In this region,

Figure 3.10 Coulter counter volumetric size histograms from station 25 in the Iceland rise region. See Figure 3.7 for the location of the clear-water and nepheloid-layer samples with respect to the light-scattering profile. Note the lower variance of the nepheloid-layer sample.

# STATION 25

1804m

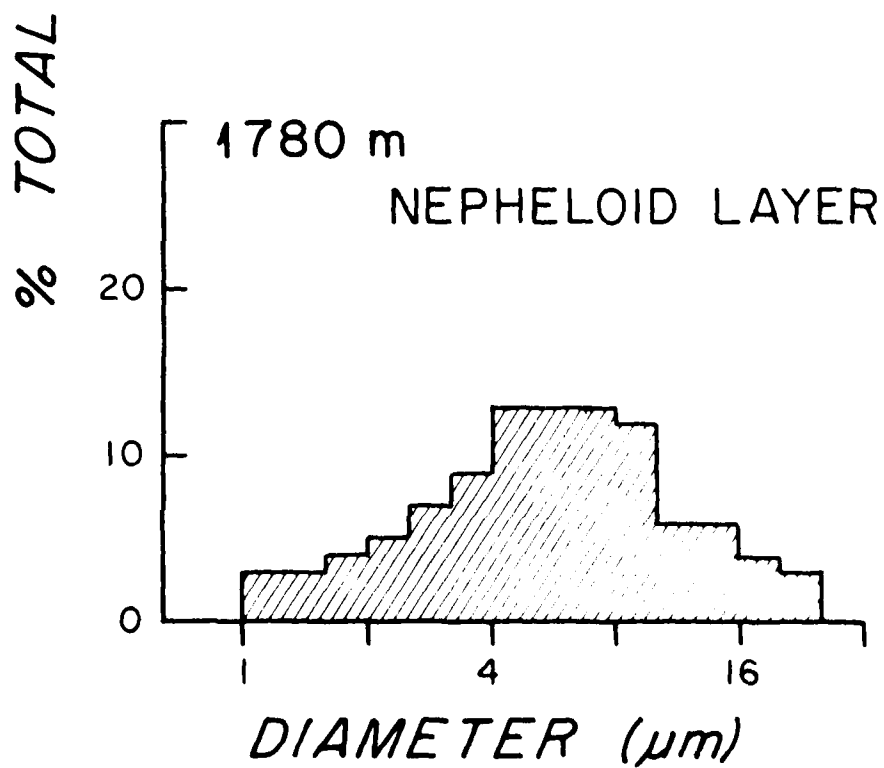
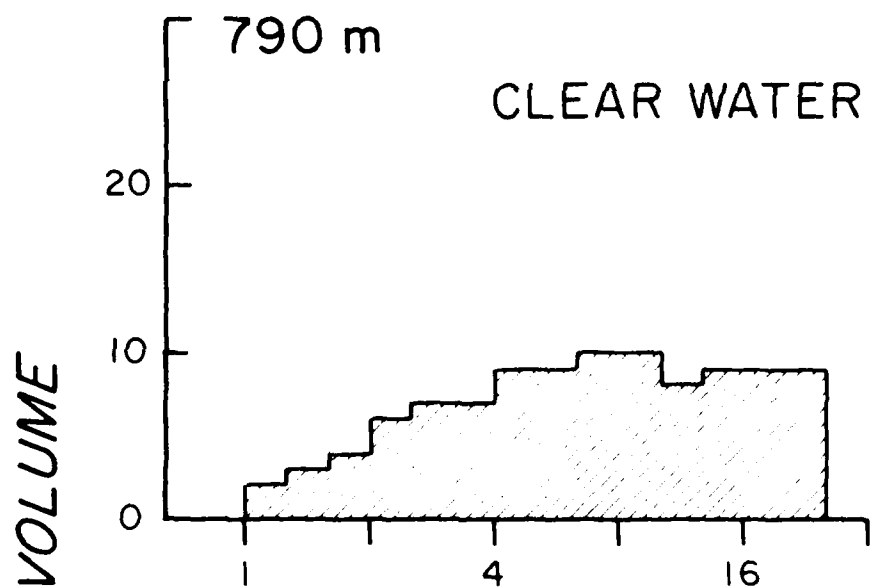
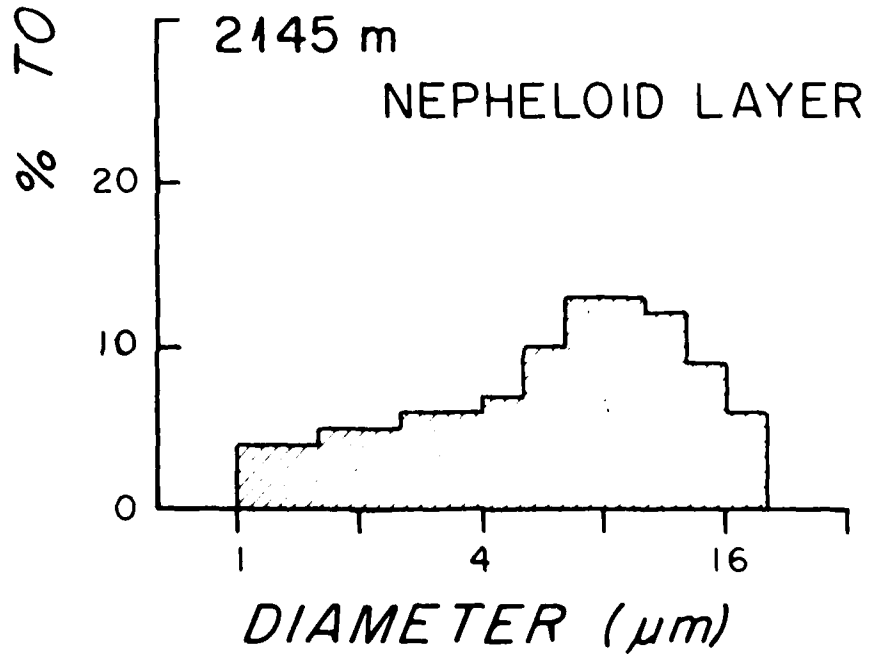
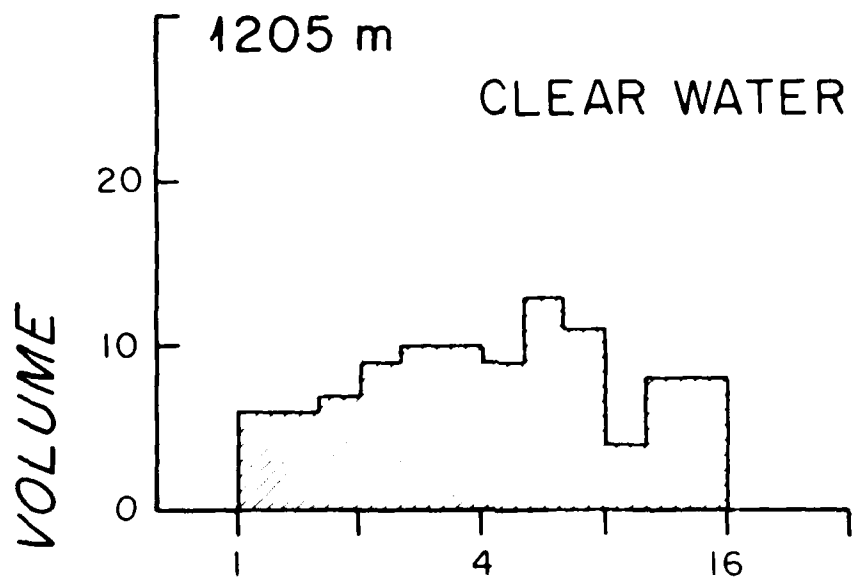


Figure 3.11 Coulter counter volumetric size histograms from station 39 in the Iceland Rise region. See Figure 3.7 for the location of the clear-water and nepheloid-layer samples with respect to the light-scattering profile. Note the lower variance of the nepheloid-layer sample.

# STATION 39

2163m





nephelometer profiles were not available at the hydrographic stations, so the nepheloid layer was judged to begin at the sharp increase in concentration in the near-bottom waters. The general results of the comparison made between clear-water and nepheloid-layer samples are similar to those from the Iceland Rise. The nepheloid-layer samples (e.g., OC6, 718, bottle 1, 4462 m) have low variance distributions with the modal size at 3  $\mu$ m, whereas clear-water sample distributions have higher variance (Figure 3.12).

Both standardly drawn samples and "dregs" samples were counted with the Coulter counter for nepheloid-layer samples. The nepheloid-layer "dregs" samples exhibit the low variance type distribution even more strongly than do the standard nepheloid-layer samples (Figure 3.12).

#### COMPOSITION OF SPM

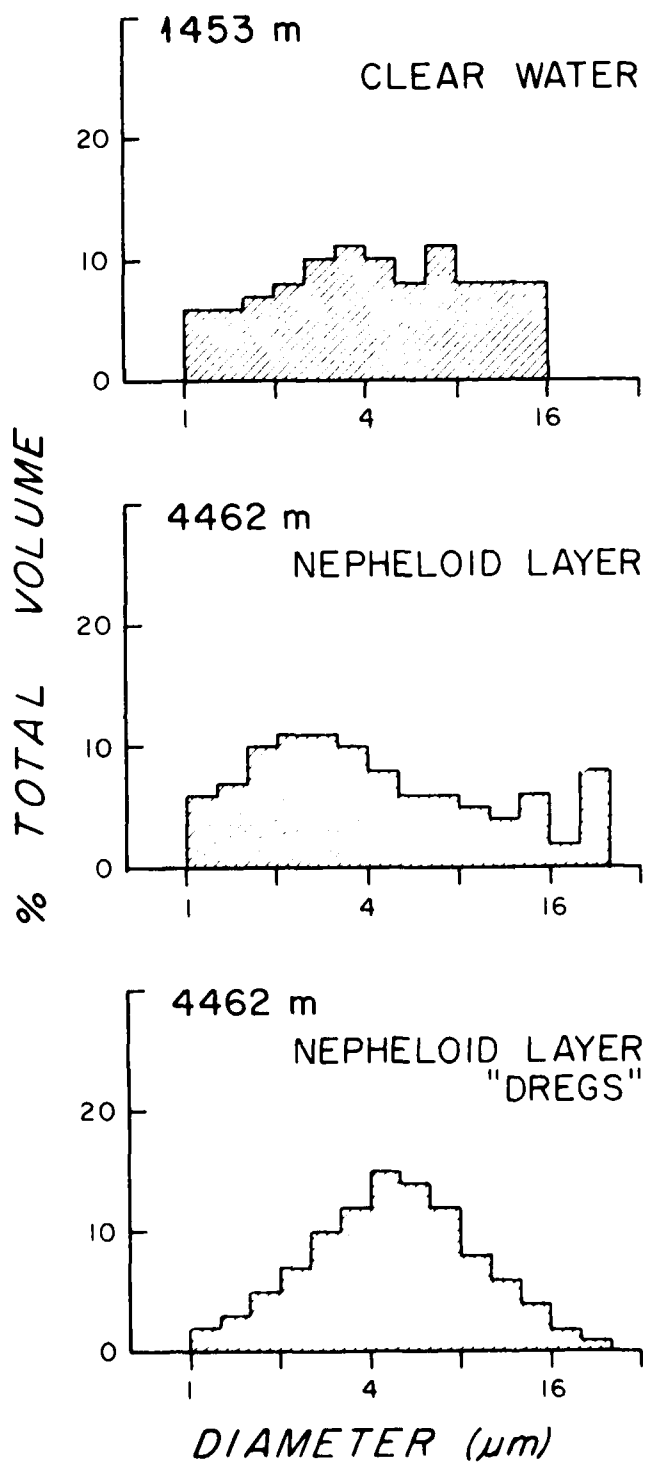
Particles on SEM photomicrographs were counted in this study to determine the difference in composition between the clear-water material and the nepheloid-layer material.

#### Iceland Rise

Five stations were selected for compositional analysis in the Iceland Rise region (25, 31, 39, 67, and 76; see Figure 2.2) as being representative of the various hydrographic conditions. Station 25 is in the axis of the bottom current; Station 39 is off-axis along the same transect. Stations 31 and 76 are in the

Figure 3.12 Coulter counter volumetric size histograms from station 718 in the western North Atlantic. Samples are from clear water, the nepheloid layer and the "dregs" water from a nepheloid layer sample. Note the lower variance of the nepheloid-layer standard and "dregs" samples.

STATION 718  
4485m



interior of the basin, at the ends of the northern and southern lines, respectively. Station 67 is located on the nose of the West Katla Ridge and exhibits no nepheloid layer. Instead, concentrations vary erratically with an overall general decrease with depth. Two samples were taken from each station, one in clear water at mid-depths and one in the nepheloid layer or within fifty meters of the seafloor.

The results of the particle counts for these stations are given in Figure 3.13 and Table 3.1. These compositional studies (Plate 3.2) show that by number, small coccoliths are the largest component of the samples (up to 62%). Pennate diatoms, mineral matter, and clays follow in order as the next largest fractions of the sample. These are also the components which show major differences between clear-water and nepheloid-layer samples. Nepheloid-layer samples have fewer small coccoliths and more pennate diatoms, clays, and mineral matter than do clear-water samples (Figure 3.13). These same differences are observed whether or not particles from the "dregs" water are included. In comparison to the standard, above-spigot samples, "dregs" samples have fewer small coccoliths, less organic matter and mineral matter, and more large coccoliths, centric diatoms, and pennate diatoms. The smaller percentage of mineral matter in the "dregs" samples is difficult to understand. One would expect that the larger and denser particles would settle to the bottom of the bottle. A differentiation is seen for the biogenic particles, but does not hold for the mineral matter.

Figure 3.13    Compositional variability of suspended particulate matter from the Iceland Rise. Counts were made of the different components from scanning electron microscope photomicrographs and normalized to total number of particles counted. Identifiable fragments were included in the counts. Greatest differences between clear-water and nepheloid-layer samples are in small coccoliths, pennate diatoms, and mineral matter.

# COMPOSITIONAL VARIABILITY OF SUSPENDED PARTICULATE MATTER ICELAND RISE

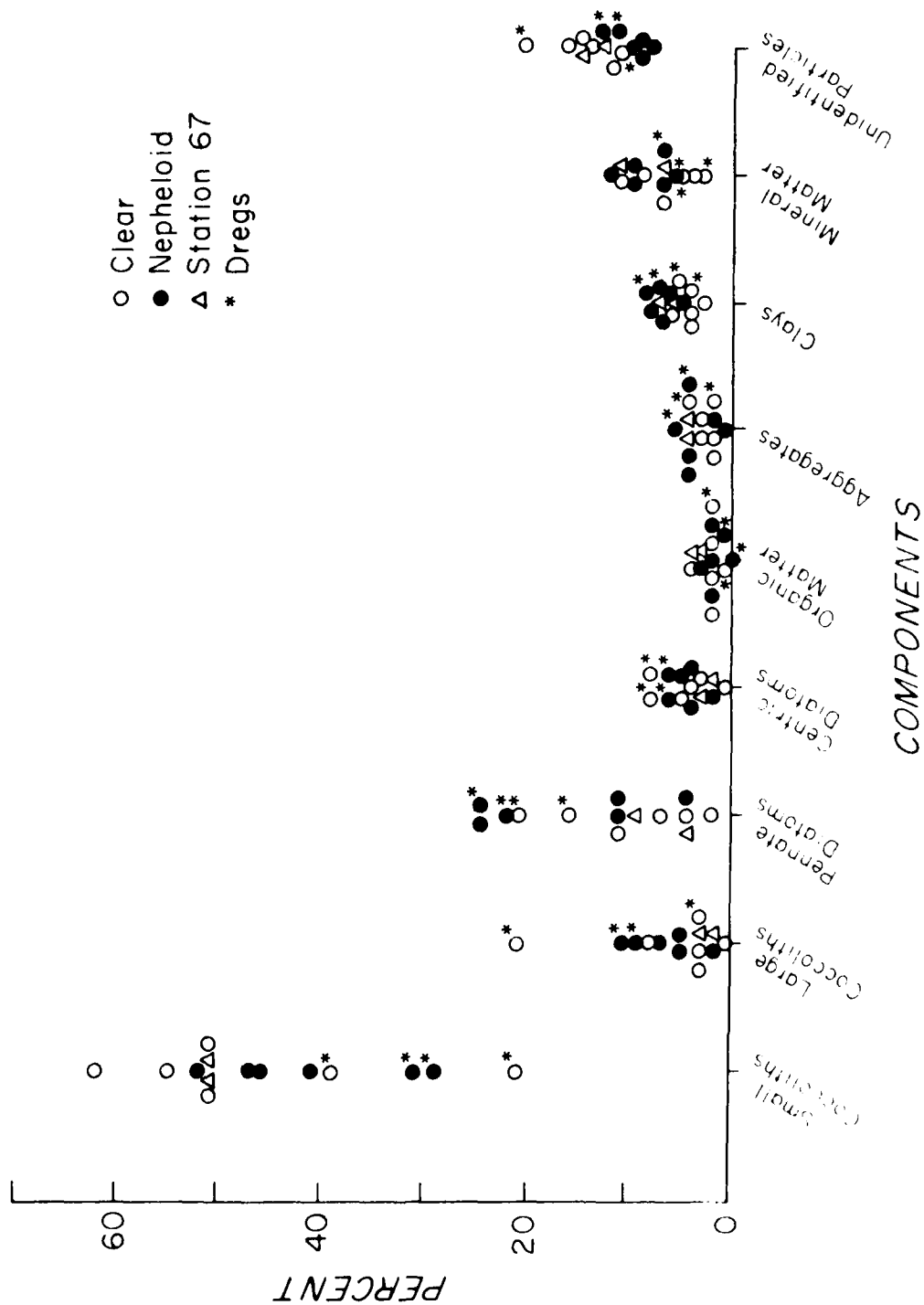


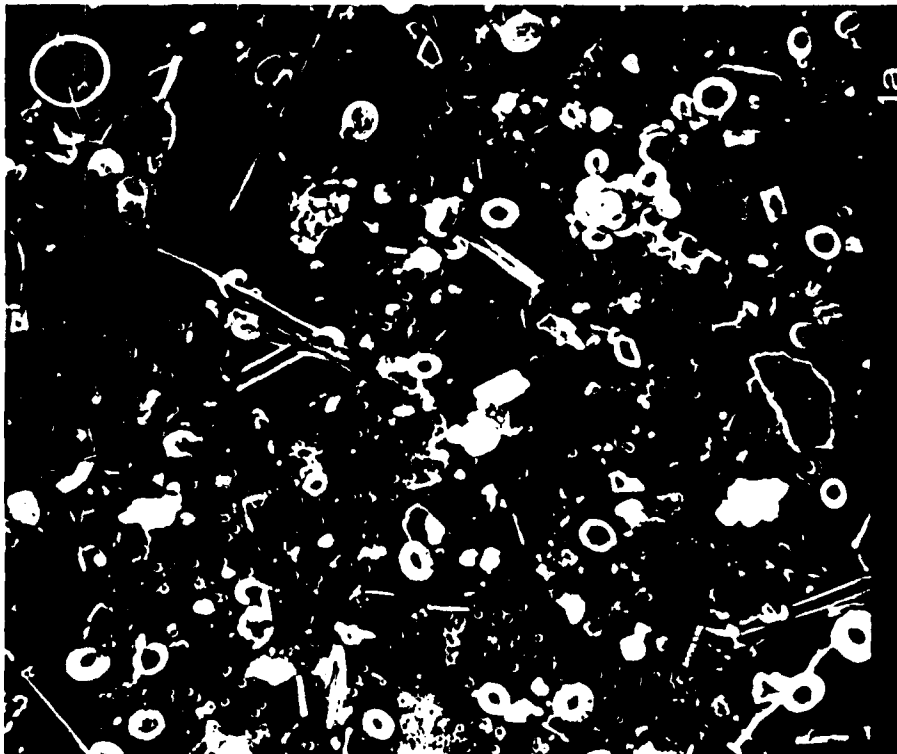
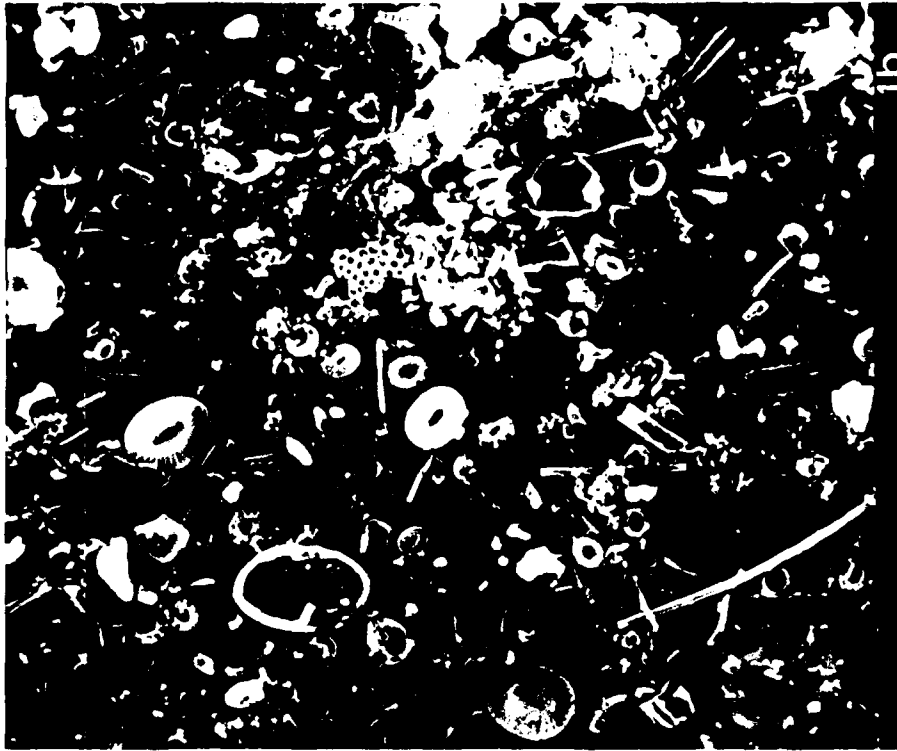
Table 3.1

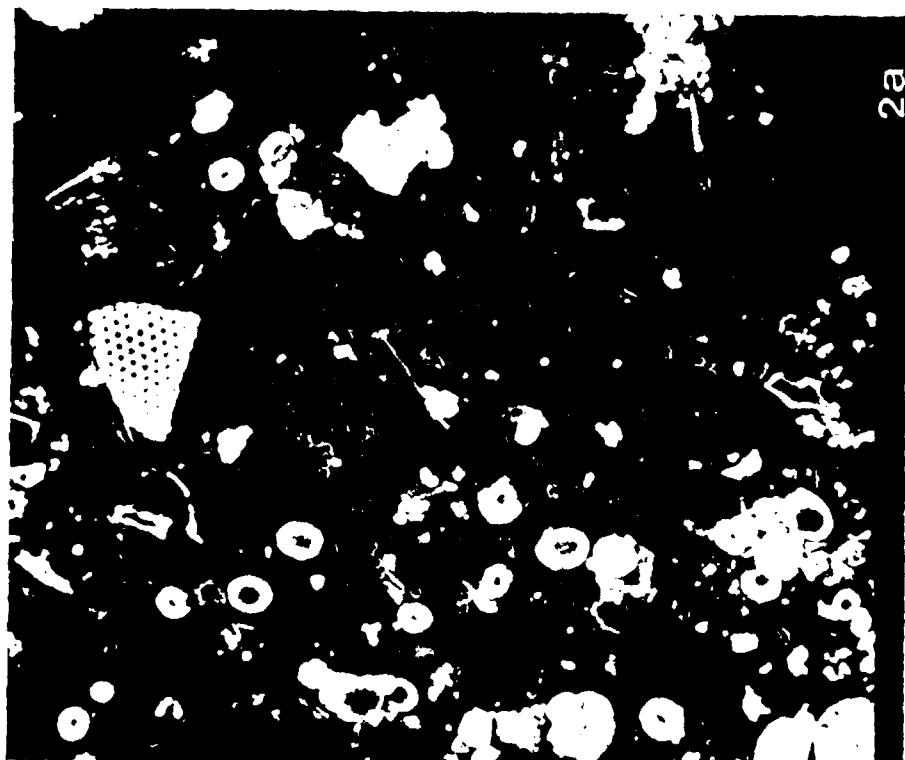
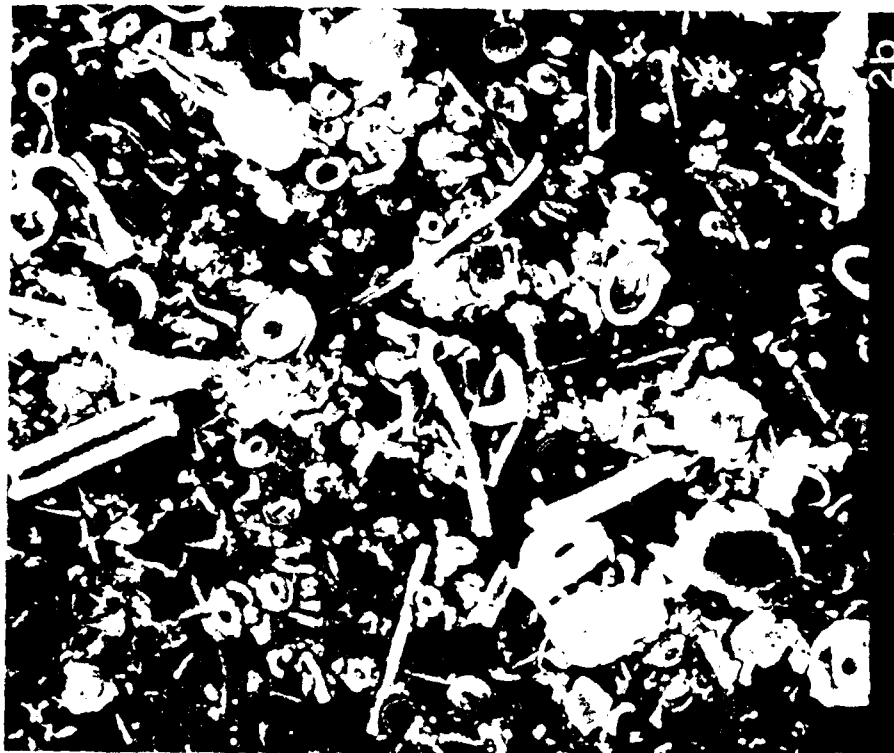
DECONTAMINATED SOIL BY AIR LAKE TYPE FROM THE ICELAND RISE  
AND LOST TO WASTE MATERIAL

Sample No.	Location	Depth (m)	Volume (L)	Particle Size (mm)	Plantation Fragments	Fossil Pellets	Aggregates	Clays	Mineral Matter	Unidentified Particles	Total
1	1	1	1	1	1	0	0	4	11	11	22
2	2	2	2	2	2	0	0	4	5	11	16
3	3	3	3	3	3	0	0	4	10	11	25
4	4	4	4	4	4	1	4	5	12	9	35
5	5	5	5	5	5	1	4	7	6	11	34
6	6	6	6	6	6	1	4	6	11	9	31
7	7	7	7	7	7	0	0	0	4	10	14
8	8	8	8	8	8	1	3	0	3	11	25
9	9	9	9	9	9	1	3	0	3	11	28
10	10	10	10	10	10	0	0	0	10	7	17
11	11	11	11	11	11	0	0	0	7	10	17
12	12	12	12	12	12	0	0	0	9	10	19
13	13	13	13	13	13	0	0	0	7	10	17
14	14	14	14	14	14	0	0	0	7	7	14
15	15	15	15	15	15	0	0	0	7	11	18
16	16	16	16	16	16	0	0	0	11	11	22
17	17	17	17	17	17	0	0	0	9	10	19
18	18	18	18	18	18	0	0	0	10	10	20
19	19	19	19	19	19	0	0	0	3	10	13
20	20	20	20	20	20	0	0	0	26	10	36
21	21	21	21	21	21	0	0	0	9	10	19
22	22	22	22	22	22	0	0	0	9	11	20

Plate 3.2 SEM photomicrographs of suspended particulate matter from clear water and the nepheloid layer from the Iceland Rise. 1a and 2a are clear-water samples; 1b and 2b are from the nepheloid layer. Sample 1 is from Station 25, and sample 2, from Station 76. Sample 3 is from Station 67, which has no nepheloid layer. 3a is from mid-water; 3b, from the near-bottom water. See text for interpretation of these samples.  
X 1200.







AD-A092 231

WOODS HOLE OCEANOGRAPHIC INSTITUTION MASS

F/G 8/10

COMPOSITION AND CHARACTERISTICS OF PARTICLES IN THE OCEAN: EVID--ETC(U)

NOV 80 M J RICHARDSON

N00014-79-C-0071

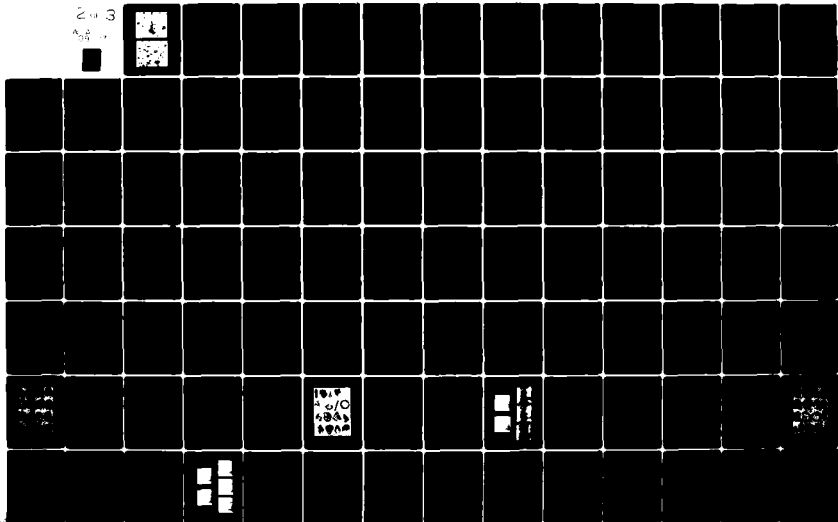
UNCLASSIFIED

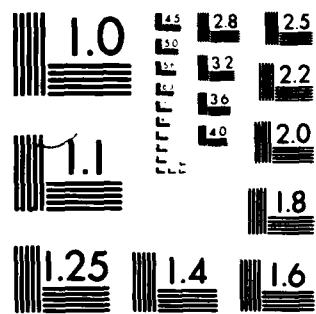
WHOI-80-52

NL

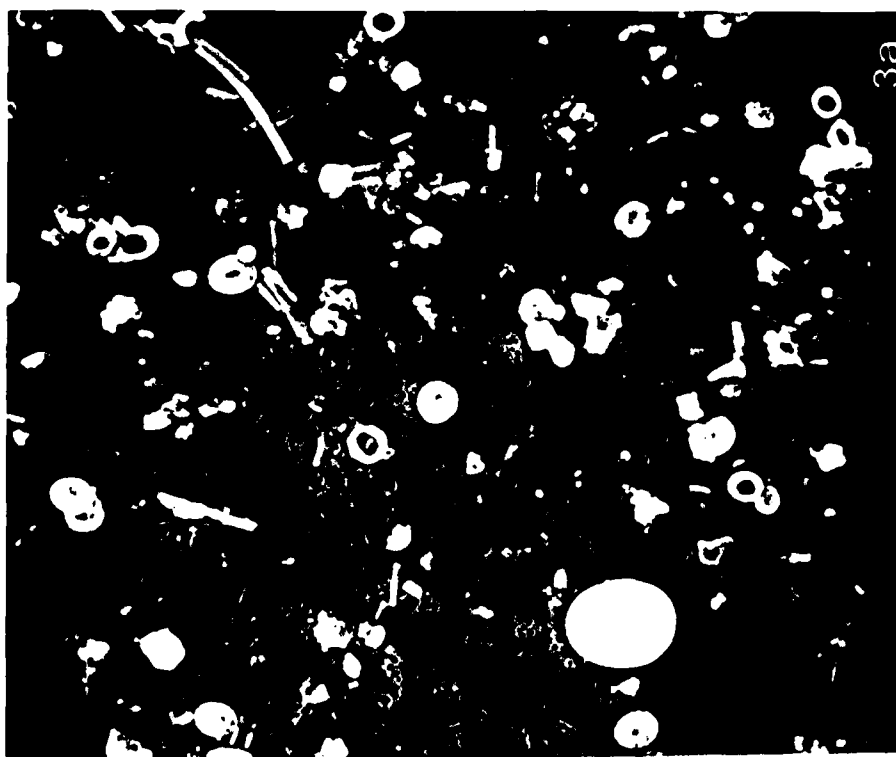
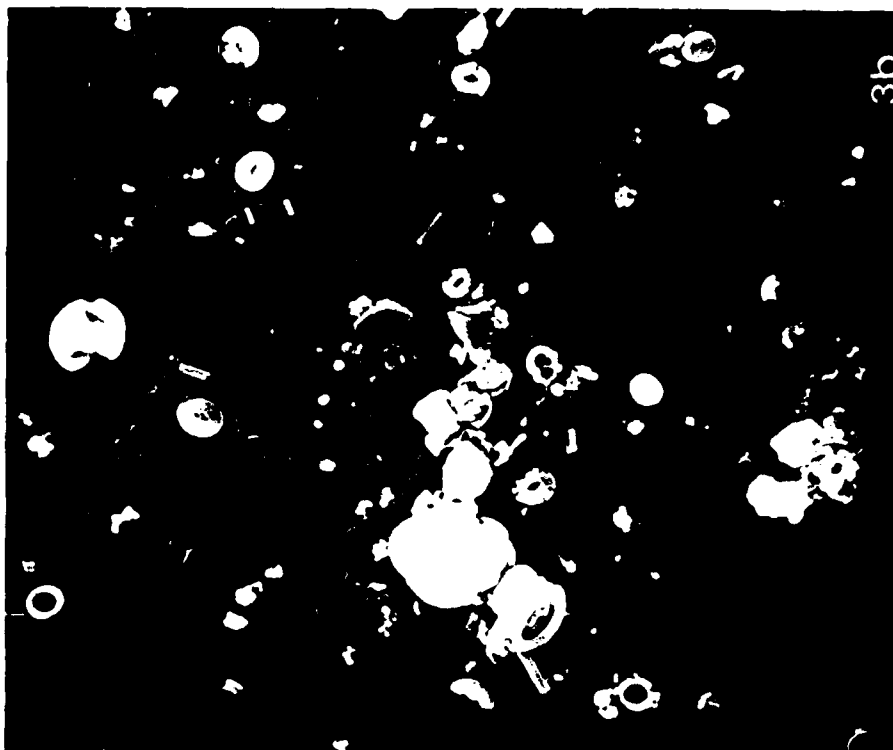
2-3

A-10





MICROCOPY RESOLUTION TEST CHART  
NATIONAL BUREAU OF STANDARDS 1963 A



Perhaps the mineral matter is contained in organic aggregates of low density. The results of the chi-square analysis (statistics after Crow et al., 1960) on the compositional data summarized in Table 3.2 indicate that at the 95% confidence level, the random photomicrographs of the filters are representative subsamples of a homogeneous population of material. This result allows summing the counts from many photomicrographs to make additional comparisons. The second chi-square test performed was to determine whether clear-water and nepheloid-layer samples from individual stations are statistically different. This was found to be true at the 95% confidence level. The differences observed were outlined above. Another chi-square test was performed to determine whether the clear-water samples from all stations were statistically different from each other, and whether the nepheloid-layer samples from all stations were statistically different from each other. This hypothesis was also found to be true at the 95% confidence level. The variability between stations is perhaps related to proximity to Iceland. The two stations in the basin generally have less mineral matter and fewer clays and aggregates than the stations along the flanks. For mineral matter, this is true only for the nepheloid-layer samples, indicating that the variability may also be caused by resuspension of mineral matter by the bottom current into the nepheloid layer for the stations along the flanks.

TABLE 3.2

CHI-Square Analysis of Compositional Data from the Iceland Rise  
and Western North Atlantic

Station -Bottle	Clear - C Nepheloid - N	Degrees of Freedom	Calculated CHI-Square	95% Confidence Interval
TESTS FOR HOMOGENEITY OF FILTER SAMPLES				
25-4	C	27	35.16	40.11
25-1	N	27	39.83	40.11
39-B1	C	27	25.83	40.11
39-B5	N	27	23.98	40.11
32-4	C	27	31.95	40.11
32-1	N	30	28.93	43.77
67-B6	C	27	19.29	40.11
67-B1	C	27	41.30*	40.11
76-B6	C	24	25.50	36.42
76-B1	N	30	14.15	43.77
TESTS FOR STANDARD VERSUS DREGS SAMPLES				
25-4	C	10	32.70*	18.31
25-1	N	11	70.03*	19.68
39-1	C	10	103.12*	18.31
39-5	N	10	73.96*	18.31
TESTS FOR CLEAR WATER VERSUS NEPHELOID LAYER SAMPLES				
25	C/N	11	38.62*	19.68
39	C/N	10	50.16*	18.31
32	C/N	10	131.90*	18.31
67	C/C	9	16.52	16.92
76	C/N	10	24.07*	18.31
SAME INCLUDING DREGS				
25	C/N	11	48.34*	19.68
39	C/N	10	64.36*	19.68
718	C/N	8	37.46*	15.51
734	C/N	8	145.50*	15.51
TESTS FOR ALL CLEAR WATER SAMPLES				
all clear	C	45	197.28*	61.63
TEST FOR ALL NEPHELOID LAYER SAMPLES				
all nepheloid	N	33	326.15*	45.69

\* Significant at 95% confidence interval

### Western North Atlantic

Compositional identification and quantification of particles for two stations in the western North Atlantic were performed in a similar fashion to that for the Iceland Rise samples. The dominant components of these samples are small coccoliths, clays, and mineral matter (Figure 3.14, Table 3.1). The variations seen between clear-water and nepheloid-layer samples are also most pronounced for these components. The percentage of small coccoliths drops sharply from clear-water to nepheloid-layer samples, whereas the percentages of clay and mineral matter rise dramatically (Figure 3.14).

A chi-square test to examine the similarity of the clear-water and nepheloid-layer samples verifies that these samples are statistically different at the 95% confidence level (Table 3.2).

## DISCUSSION

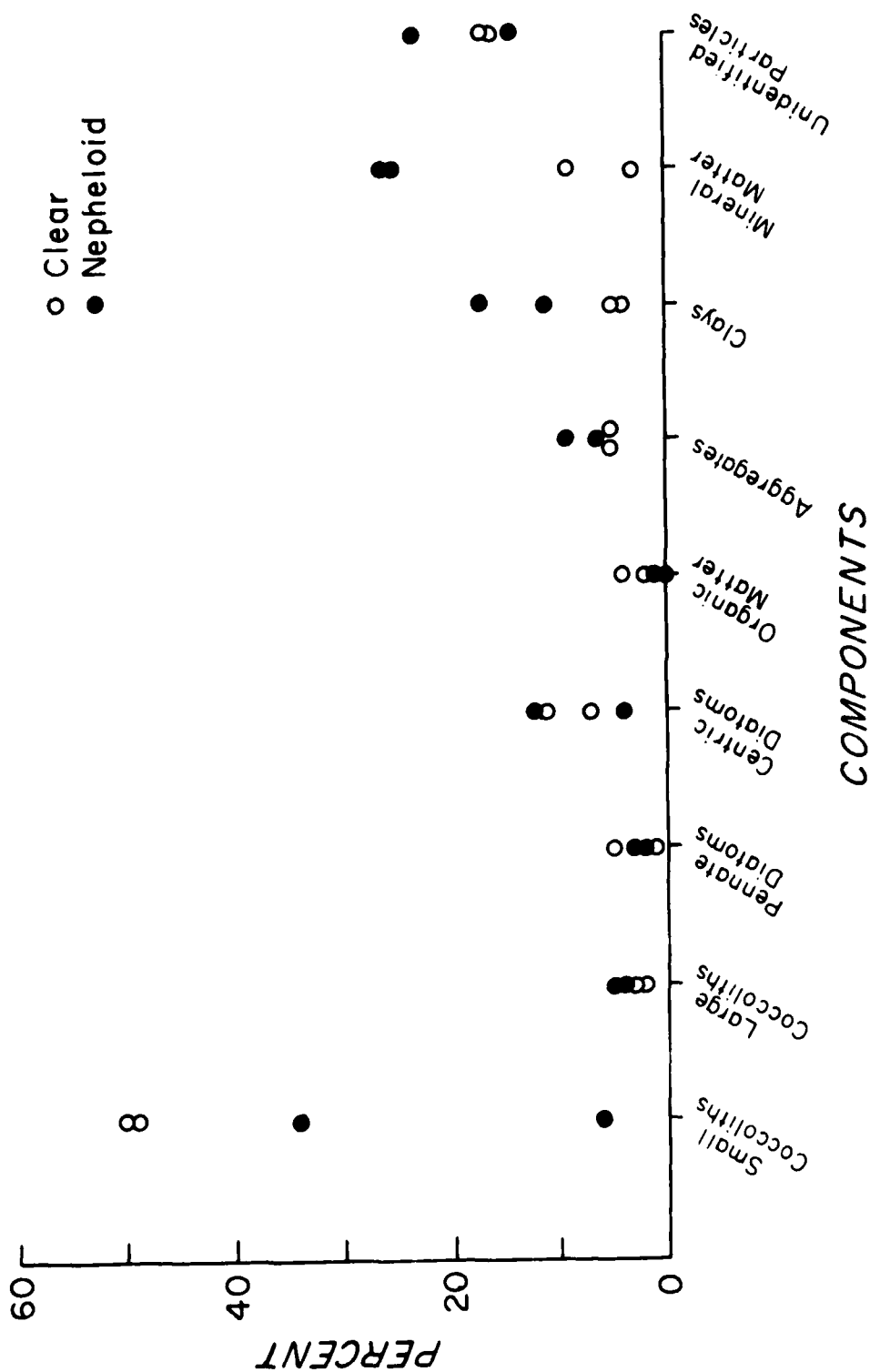
### CORRELATION OF LIGHT-SCATTERING MEASUREMENTS WITH SPM CONCENTRATIONS

A correlation of light-scattering measurements with concentrations of SPM has been used for several years to calibrate L-DGO nephelometer profiles in quantitative terms (Biscaye and Eittreim, 1974; 1977). As part of this study, a relationship was sought between light-scattering observations and SPM concentrations (uncorrected for "dregs" particles) for clear-water samples, nepheloid-layer samples, and the entire water column. Uncorrected



Figure 3.14    Compositional variability of suspended particulate matter from the western North Atlantic. Note the pronounced differences in percentages of small coccoliths, clays and mineral matter between clear water and the nepheloid layer.

# COMPOSITIONAL VARIABILITY OF SUSPENDED PARTICULATE MATTER WESTERN NORTH ATLANTIC



concentrations were used so that a comparison of the relationships given by Biscaye and Eittreim (1974; 1977) to those obtained south of Iceland could be made (Table 3.3).

There are two important comparisons to be made with these regression correlations: first, the comparison between clear-water and nepheloid-layer samples in the Iceland Rise area, and second, the regional comparison between the Biscaye and Eittreim curves and the combined Iceland Rise data.

Analysis of the regression lines for clear-water and nepheloid-layer data shows a statistically significant difference in these two curves at the 95% confidence level (Figure 3.15). This can be interpreted in two ways: either the nephelometer responds differently to the particles in the nepheloid layer versus those in clear water, or the relationship between light scattering and SPM concentration is nonlinear for the full range measured. Theory suggests nephelometers are responsive to particle characteristics other than concentration, such as size and composition from differences in index of refraction (Jerlov, 1968). It has been shown here that the size and composition of suspended material differs between clear-water and nepheloid-layer samples in the Iceland Rise region. Both of these factors are likely to influence the response of the nephelometer; however, it is not yet possible to determine the magnitude of their influence.

The considerable scatter about the regression lines for the Iceland Rise data may originate from numerous sources of error.

Table 3.3

LEAST SQUARE REGRESSION EQUATIONS FOR LIGHT SCATTERING  
VERSUS CONCENTRATION CORRELATIONS

BBOR-HAP from Biscaye and Eittreim (1974)	$\log Y = 1.19 \log X + 0.13$	( $r = 0.91$ )
LCR from Biscaye and Eittreim (1977)	$\log Y = 1.0 \log X + 0.50$	( $r = 0.84$ )
Clear water this study	$\log Y = 0.63 \log X + 0.94$ $S_b = 0.106$	( $r = 0.62$ )
Nepheloid layer this study	$\log Y = 0.36 \log X + 1.35$ $S_b = 0.055$	( $r = 0.52$ )
All data this study	$\log Y = 0.65 \log X + 0.98$	( $r = 0.76$ )

Y = concentration ( $\mu\text{g/l}$ )  
X = light-scattering ( $E/E_D$ )  
r = correlation coefficient  
 $S_b$  = standard error of the regression coefficient, b

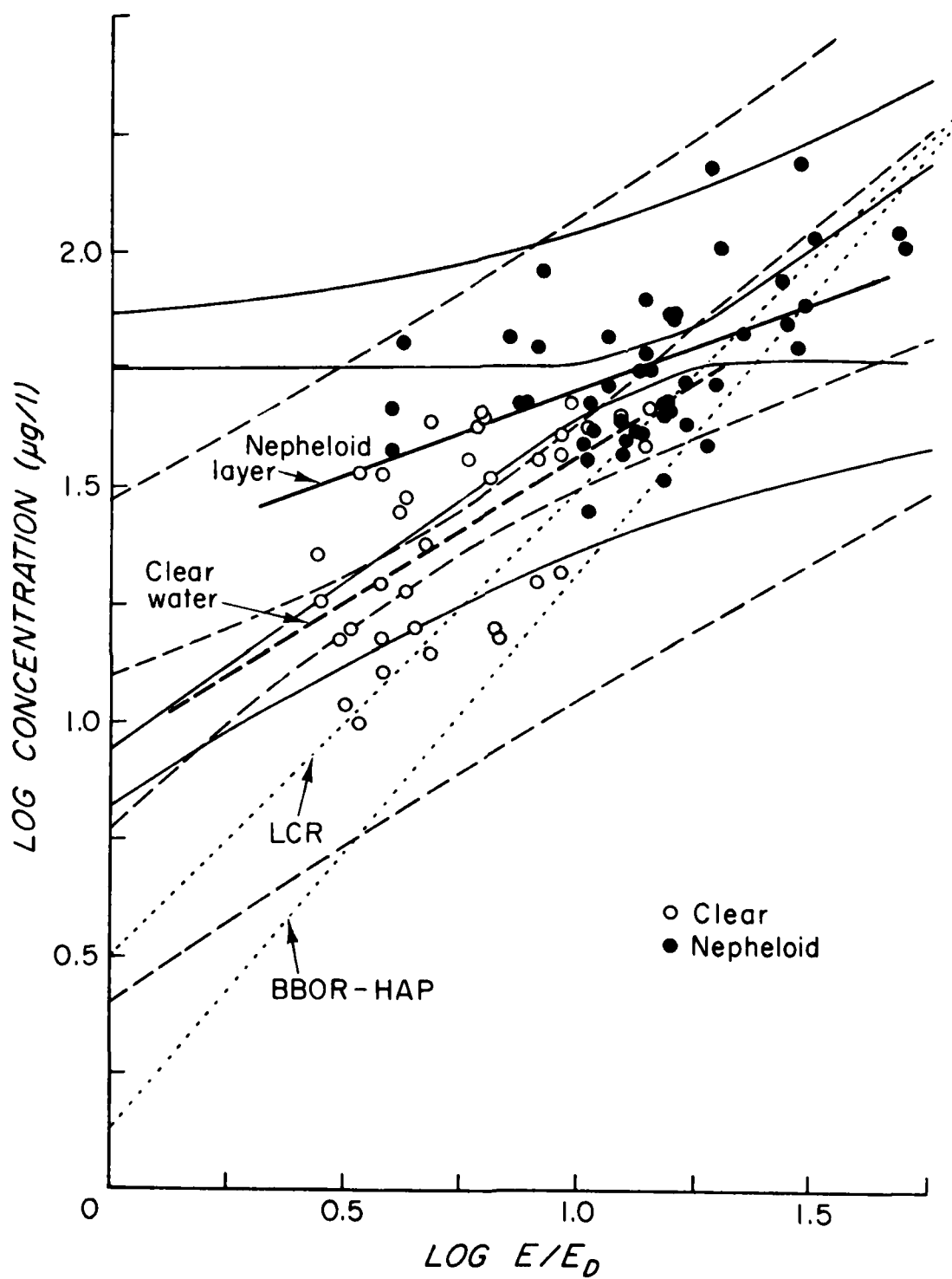
test for similarity between clear water and nepheloid layer lines

$$t = \frac{b_1 - b_2}{S_{b_1 - b_2}} = \frac{0.63 - 0.36}{0.0124} = 21.77$$

Reject the hypothesis at the 5% significance level that the two regression lines are the same

statistics after (Crow et al., 1960)

Figure 3.15 Correlation of light scattering and standard concentration for the Iceland Rise area. The dashed line is the regression line for the clear-water samples. The inner pair of dashed curves are the 95% confidence limits for clear-water concentration values. The outer pair represent the 95% prediction interval for this regression. The solid line is the regression line for the nepheloid-layer samples. The solid curves are the same as for the clear-water samples. The regression lines for clear water and the nepheloid layer, are statistically different at the 95% confidence level. The dotted lines are the regressions for the BBOR-HAP and LCR of Biscaye and Eittreim (1974; 1977).

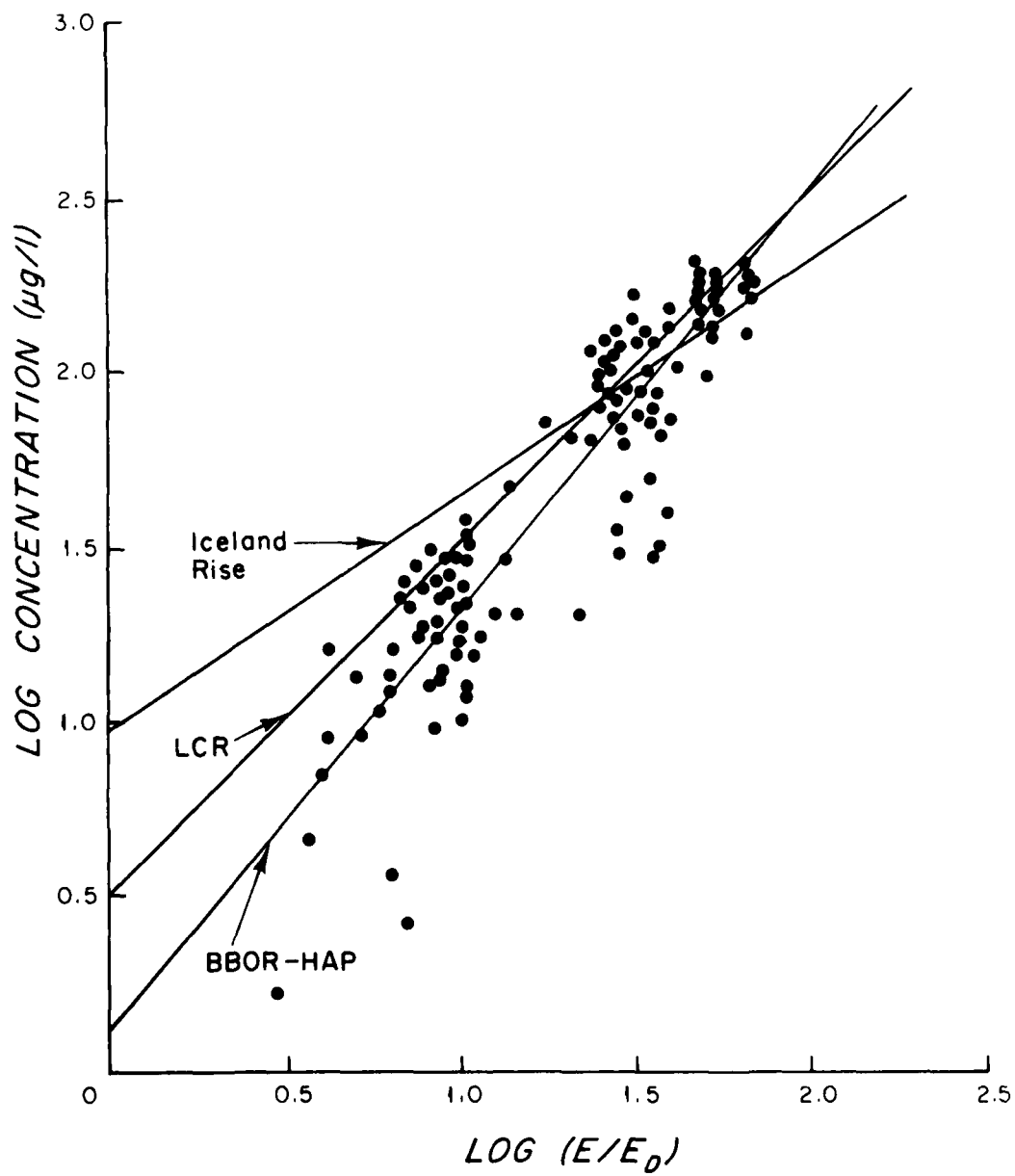


There is analytical error in the concentration measurements (outlined earlier), error in the light-scattering determinations, and error in relating the depth of the nephelometer measurements to the depth of the bottle samples. Perhaps larger than any of these is the basic difference in the volume of water being examined by each method. The SPM concentration data are obtained with 5 or 30 liter Niskin bottles, which sample over a vertical scale of one-half to one meter. The nephelometer, on the other hand, measures light scattering that is integrated over a vertical distance of 25 meters. In a region of active currents like the Iceland Rise, temporal variability over a half hour and patchiness in the concentration of particles in near-bottom water are likely and could cause differences between the point values of the Niskin bottles and the integrated values measured by the nephelometer.

Although the Biscaye and Eittreim curves (Figure 3.16) yield good first-order approximations of SPM concentration, their calibration curves differ from those of this data set. Calibrations apparently differ regionally. The data south of Iceland produce a curve with a gentler slope and a larger intercept than those obtained by Biscaye and Eittreim (1974; 1977). This reflects smaller changes in concentration for the same increase in light scattering when compared with their study. The difference in the intercepts of these curves indicates that in the BBOR-HAP and LCR regions, less material is needed for detection of measurable scattering than south of Iceland. This may be due to a nonlinear

Figure 3.16    Correlation of light scattering and standard concentration for the BBOR-HAP, from Biscaye and Eittreim (1974). The BBOR-HAP line is the least-squares regression line through the data shown. Also shown are the regression lines for the LCR from Biscaye and Eittreim (1977), and that for the entire Iceland Rise data set.





response of the nephelometer, or to a difference in the nature of SPM in the two regions. A comparison of the SPM off Iceland to that along the continental rise off New York indicates that more clays and mineral matter occur at the latter location.

Most light-scattering values observed in these studies fall in the range 0.5 to 1.5  $\log E/E_D$ . Over this range of light-scattering values, the differences in prediction of the SPM concentration from the different regression lines vary by a factor of 3.4 for low values of light scattering and by a factor of 1.3 for high values. This appears to indicate significant differences in prediction from the curves. However, the 95% prediction limits for the Iceland Rise data span at least this much variability (Figure 3.15). Information for these limits for the Biscaye and Eittreim curves is not available. Therefore, although there are regionally significant differences in the response of the nephelometer to SPM, used as a predictive tool, the particular correlation employed is unimportant, since the prediction limits are so large.

#### SIZE DISTRIBUTION VARIATIONS

Particle size distributions were analyzed from clear water and the nepheloid layer from south of Iceland and compared to those from the western North Atlantic to determine whether variation in the size spectra were site specific.

### Volumetric Histograms

Histograms of normalized particle volume versus equivalent spherical diameter depict the variations in the distributions between clear water and the nepheloid layer (Figures 3.10, 3.11, 3.12). The clear-water distributions in both regions have relatively constant volumes of material in logarithmically increasing size grades, from 1-20  $\mu\text{m}$ , i.e., distributions with high variance. In contrast, the particles in the nepheloid layer generally have low variance distributions. These variations in particle size distributions between clear water and the nepheloid layer are noted in both areas, and may be due to either differences in the state of aggregation or the composition of the suspended material. Filters of SPM were examined to determine which alternative was more likely.

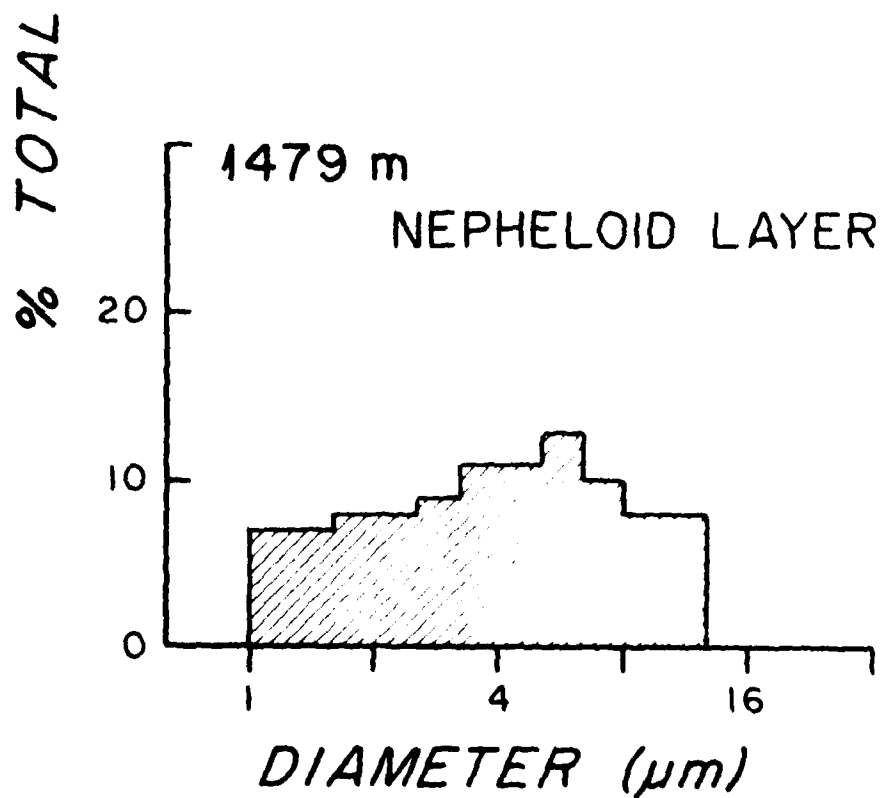
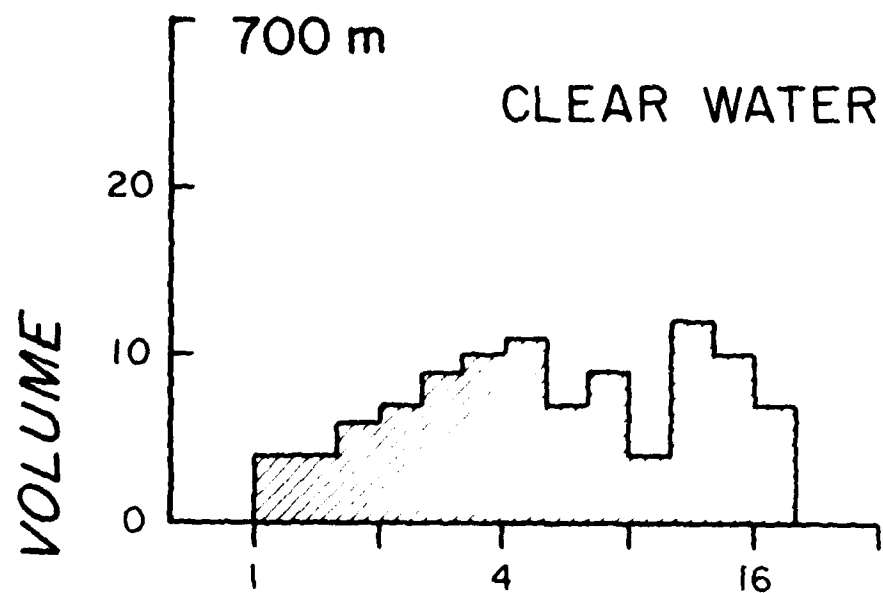
The percentage of aggregates does not change substantially between clear water and the nepheloid layer for either region. Composition of the SPM does change. Both regions show an increase in relative proportion and total concentration of the clays and mineral matter in the nepheloid layer in comparison to clear water.

The variations in particle size distributions between clear water and the nepheloid layer occur wherever a nepheloid layer is present. In the few stations where nepheloid layers are absent, the size distributions retain a clear-water characteristic, high variance, even near the seafloor (Figure 3.17). This suggests that nepheloid layers are areas of introduction into the water column of material with a given, (site-specific) predominant modal size. With

Figure 3.17 Coulter-counter volumetric size histograms from station 67 in the Iceland Rise region. See Figure 3.7 for the location of the mid-water and deep-water samples with respect to the light-scattering profile. Station 67 does not show a well-defined nepheloid layer.

# STATION 67

1522m



an increasing quantity of resuspended material, a distribution of lower variance with a more well-defined mode develops.

#### Differential Volume Distributions

Data on marine particle-size distributions are usually expressed as the slope of the cumulative number distribution (Bader, 1970; Carder et al.; 1971, Brun-Cottan, 1971; Sheldon et al., 1972; McCave, 1975; Brun-Cottan, 1976). A slope of minus three is indicative of a distribution with equal volumes of material in logarithmically increasing size grades, the type described here for clear-water samples. In this study of concentration, size, composition, and density, most of which are related to weight or volume of material, the parameters mass and volume are more useful than number. For this reason, the normalized differential volume of particles is used in interpretation rather than the cumulative number distribution. For comparison with other studies, a slope of minus one for a normalized differential volume distribution is equivalent to a slope of minus three for a cumulative number distribution (Figure 3.18).

Slopes from the normalized differential volume distributions were plotted versus depth for all stations from the Iceland Rise region (Figure 3.19). Nepheloid-layer and clear-water points were distinguished to determine trends within these subgroups. It is seen from the plot that the data have too much scatter to reveal any depth-dependent or clear-water versus nepheloid-layer distinctions.

Figure 3.18 Particle size distributions and associated parameters. Graph 1a represents a particle size distribution with equal volumes of material in logarithmically increasing size grades. Graph 1b shows the associated differential and cumulative number distributions. Graph 1c shows the associated volume distribution normalized by the size grade interval. Graph 2a illustrates an idealized nepheloid-layer, volumetric distribution of lower variance. Graph 2b, similar to 1b, demonstrates the variability of slope through the distribution, but overall having slopes very similar to those in 1b. Graph 2c, similar type to 1c, shows both positive and negative slopes through the distribution, with the overall slope similar to 1c.

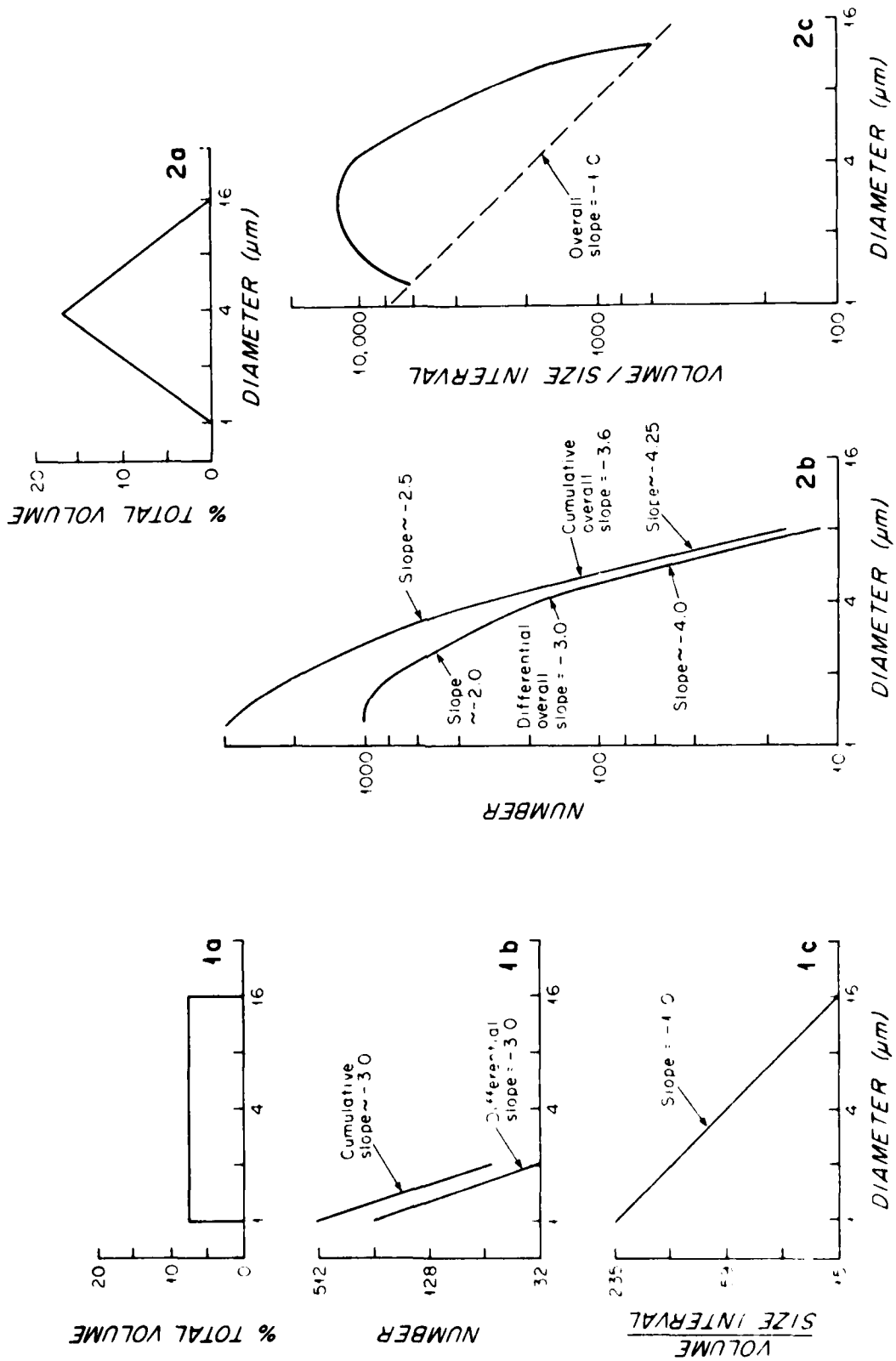
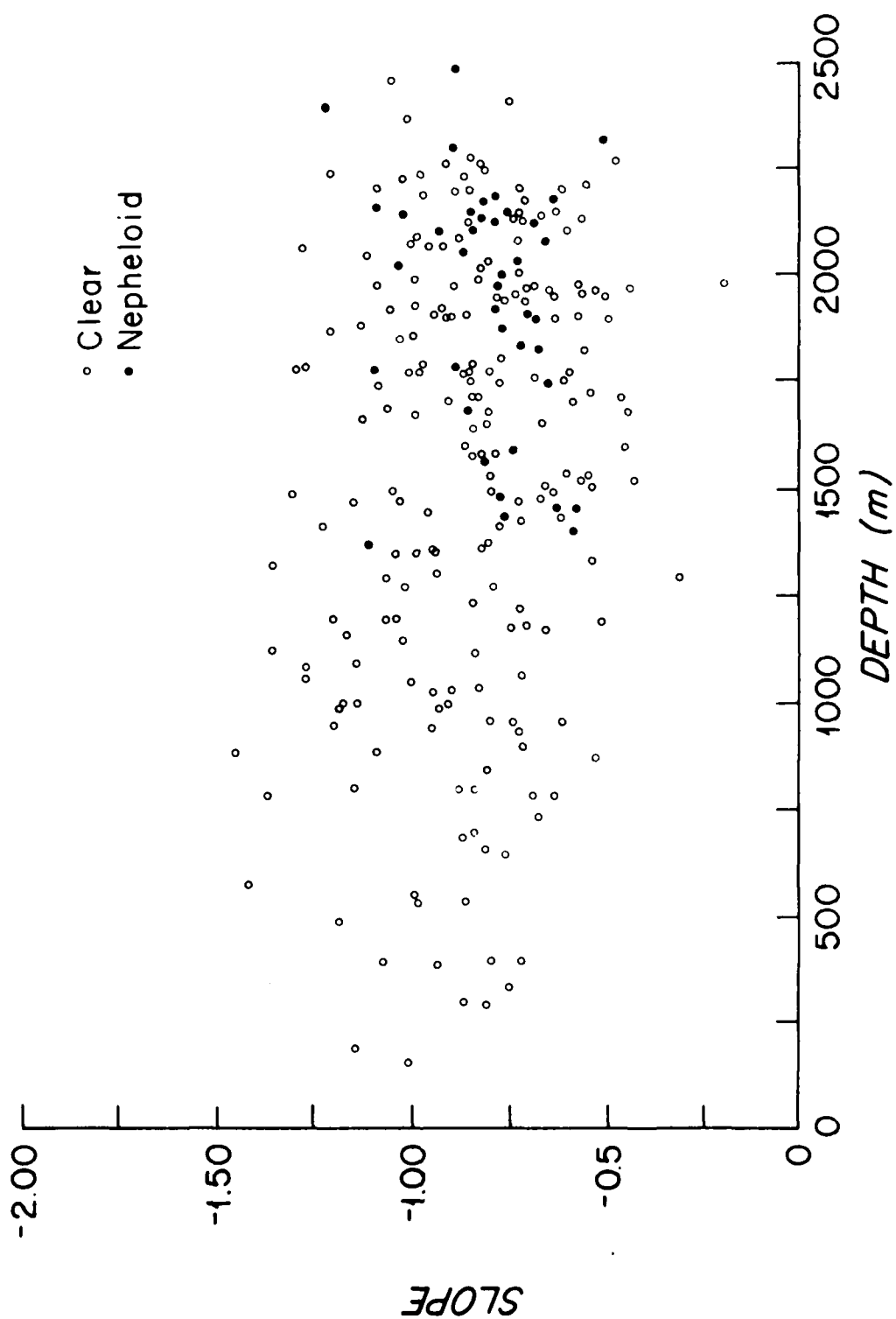




Figure 3.19 Scatter plot of the slopes of the curves of the normalized differential particle volume versus particle diameter, with depth for the Iceland Rise region. Slopes of two idealized distributions are shown in Figure 3.18.



Insight into this phenomenon is gained in examining the slopes of individual profiles (Figure 3.20). Clear-water distributions are well represented by single lines having slopes of approximately -0.9. Nepheloid-layer distributions as single-line representations have slopes similar to those of clear water, but much more scatter. An explanation for the similarity in slopes between clear-water and the nepheloid-layer samples is seen in examining idealized distributions (Figure 3.20). Both idealized clear water (high variance, flat distributions) and idealized nepheloid layer (low variance distributions) have the same slopes of minus 1. However, the nepheloid-layer distributions are much better expressed as two-slope distributions with a slope break at the modal point of the particle volume histograms.

This break in slope has previously been reported for shallow-water data (<200 m)(Bader, 1970; Brun-Cottan, 1971; McCave, 1975) and is here shown to be a feature also of the deep-water nepheloid layer. In shallow water, the meaning of the slope break is unexplained. In this case, for deep water, the two-slope distribution is interpreted to be due to an introduction of resuspended clays and mineral matter into the nepheloid layer.

#### APPARENT DENSITY

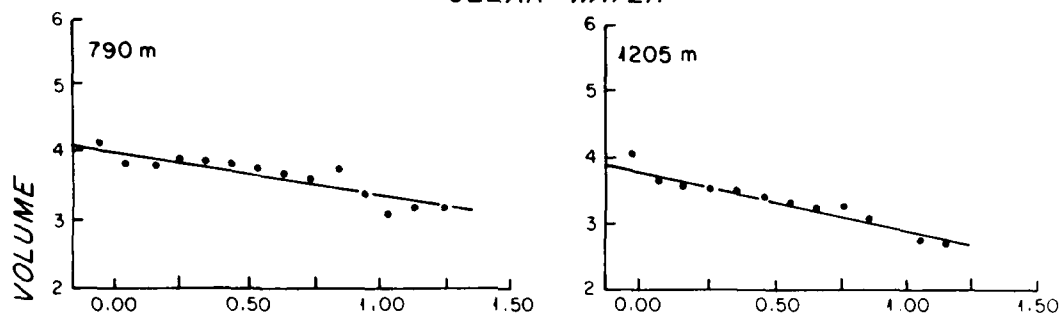
One of the characteristics of suspended particles most difficult to determine is their in-situ bulk density. However, measurements related to the density of SPM may be useful in providing insight

Figure 3.20 Individual profiles of normalized differential particle volume versus particle diameter for the clear-water and nepheloid-layer samples plotted in Figures 3.10 and 3.11. Clear-water samples are seen to be well represented by a single line through the data. Nepheloid-layer samples are better represented as a two-slope distribution.

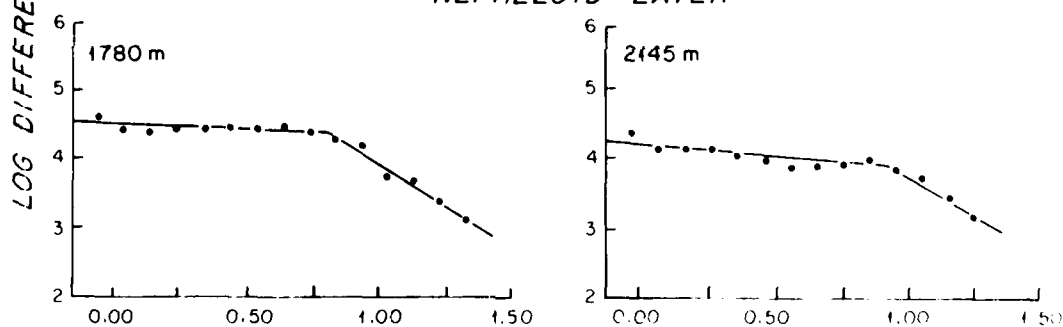
STA 25

STA 39

CLEAR WATER



NEPHELOID LAYER



LOG DIAMETER ( $\mu m$ )

into the differences between clear-water and nepheloid-layer samples. Biogenic organic-rich matter has a density close to that of seawater, whereas mineral grains have a density approaching  $2.5 \text{ g/cm}^3$ . However, few marine particles are composed solely of either organic matter or mineral grains. Organic-rich matter, fecal pellets, and aggregates are often composed of varying percentages of skeletons of plankton, organic matter, and clays.

Contents of organic-matter in SPM drop substantially from 25-50% in the water column to <2% in surface sediments (Baker et al., 1979; Rowe and Gardner, 1979). This difference may be useful in identifying resuspended material, which would tend to have a lower organic-matter content and therefore a higher density.

Although in-situ particle density cannot now be measured, an apparent density can be calculated. This parameter is the ratio between mass and volume concentrations of a sample of SPM. The mass concentration is determined by filtration and the volume concentration, by the Coulter-counter analysis. Filtration of SPM gives a measurement of dry weight of particles per volume of seawater. The Coulter counter gives a measurement of wet volume of particles per volume of seawater. The ratio of the two gives a dry weight of material per wet volume of material.

It is evident that numerous sources of error are included in estimates of this type. The specific errors in filtration and Coulter-counter analysis have been detailed previously. The three major additional sources of variability in this parameter lie in the

difference in the quantity, range, and nature of the measurements. First, filtration integrates over at least 5 (and up to 30) liters of water, whereas the volume of seawater analyzed with the Coulter counter was only a 2 ml aliquot. Second, the Coulter counter was used to measure particles only between 1 and 20  $\mu\text{m}$ , whereas filtration includes all particles greater than 0.4  $\mu\text{m}$ , and some smaller particles are probably collected as well. Third, filtration is a measurement of a dry weight of particles; Coulter-counter analysis measures a wet volume. These sources of error indicate that apparent density cannot be interpreted in terms of actual bulk densities, but it may be a useful parameter for comparative purposes.

#### Iceland Rise

A plot of mass concentration versus wet particle volume (Figure 3.21) reveals no distinction in the data between the apparent density (the ratio of the two plotted parameters) of the nepheloid-layer and clear-water samples, except that nepheloid-layer samples plot in the upper portion of the graph due to their higher concentrations. The fifty-two clear-water samples give a mean apparent density of  $2.00 \pm 1.39 \text{ g/cm}^3$ , whereas the nepheloid-layer samples yield a statistically indistinguishable  $2.38 \pm 1.23 \text{ g/cm}^3$ .

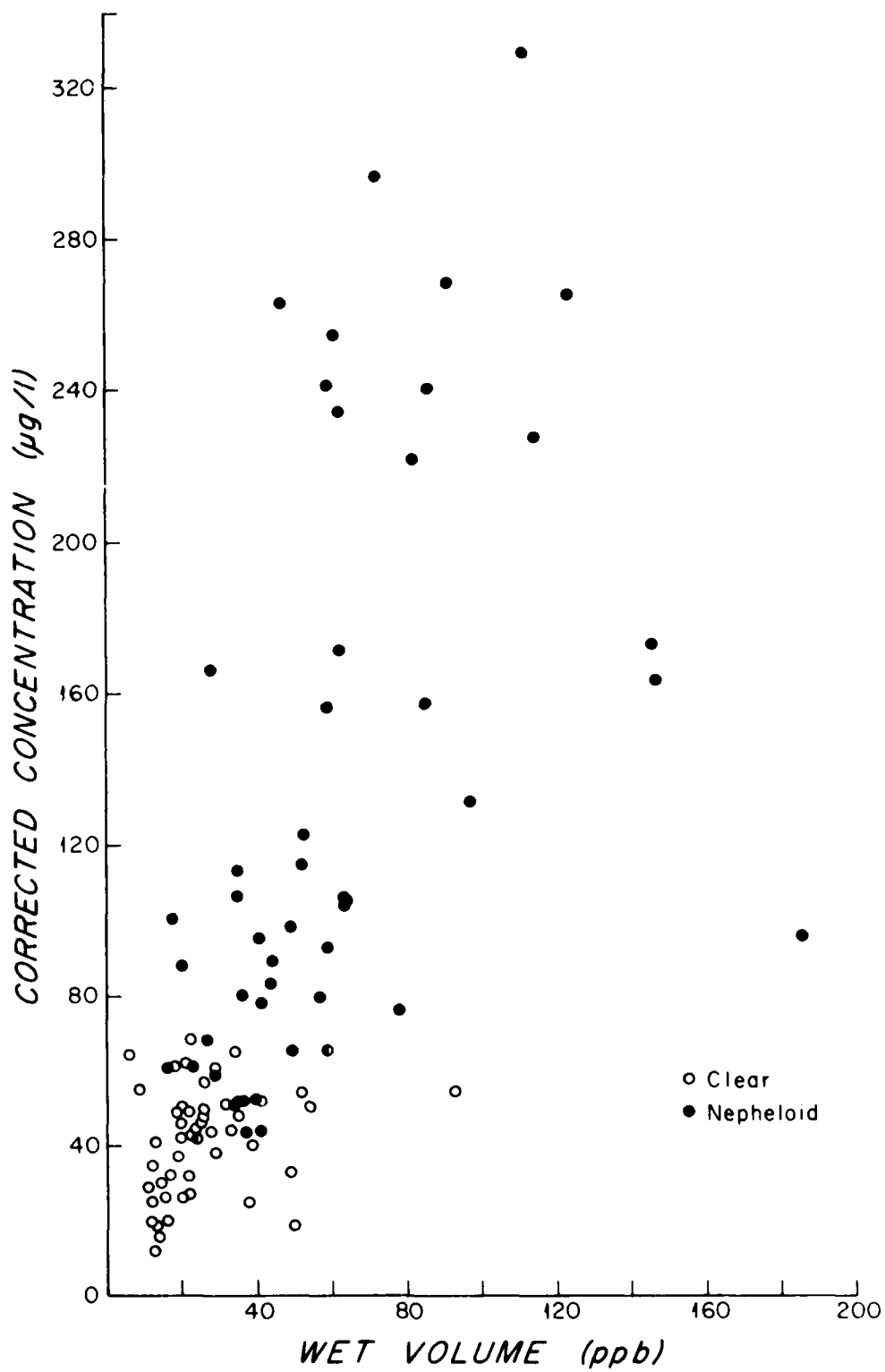
#### Western North Atlantic

A similar study was made of the apparent density of particles from the western North Atlantic continental rise. A plot of

Figure 3.21    Apparent density of samples from the Iceland Rise. No differentiation by apparent density is evident between clear-water and nepheloid-layer samples.



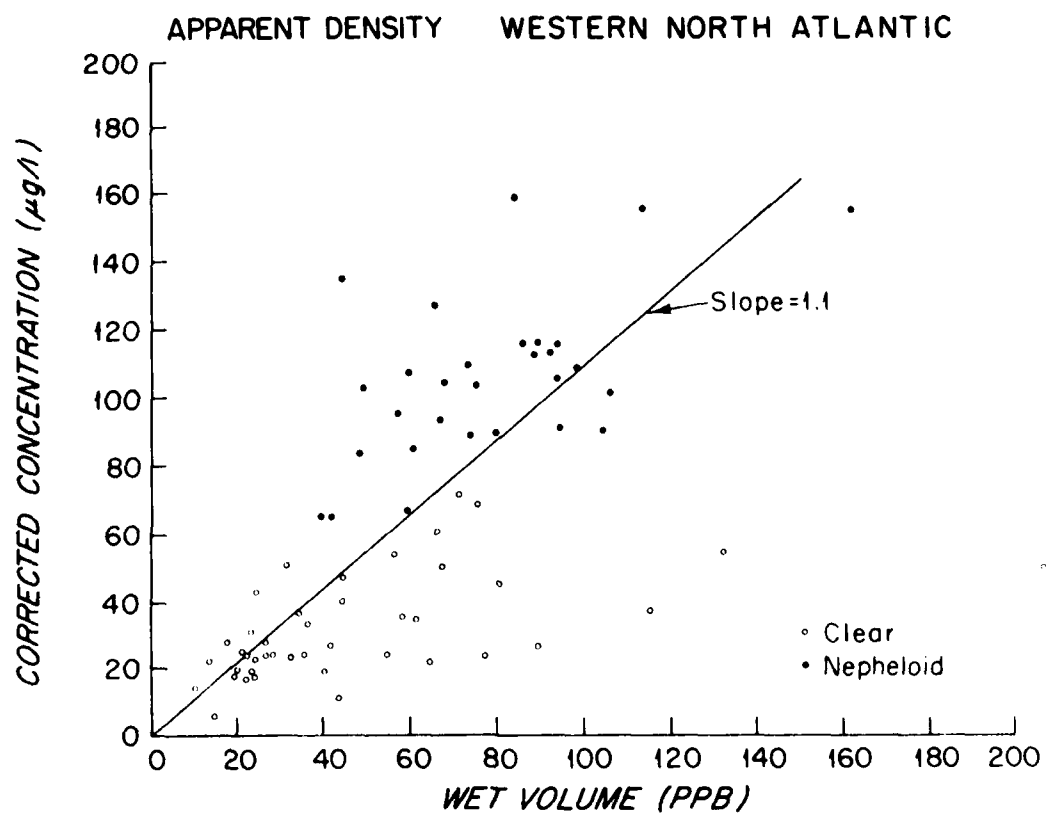
# APPARENT DENSITY - ICELAND RISE



apparent density (Figure 3.22) suggests that the nepheloid-layer particles have an apparent density greater than that of clear-water particles. Clear-water samples have a mean apparent density of  $0.83 \pm 0.40 \text{ g/cm}^3$ , whereas nepheloid-layer samples have significantly larger values ( $1.34 \pm 0.46 \text{ g/cm}^3$ ). A line of apparent density at  $1.10 \text{ g/cm}^3$  effectively separates most of the nepheloid-layer samples from clear-water samples.

An explanation for why differences in apparent density between particles in clear water versus nepheloid water are seen in the western North Atlantic and not south of Iceland lies in the composition of the particulate matter. Both regions have statistically significant differences in the composition of SPM between clear-water and nepheloid-layer samples. However, the differences for the western North Atlantic samples are much more pronounced (Table 3.1). They have a dramatic 16-43% decrease in coccoliths, a 16-23% increase in mineral matter, and a 6-13% increase in clays between clear water and the nepheloid layer. The increase in the clays and mineral matter in the nepheloid layer serves to increase the apparent density of these particles with respect to clear-water particles. Compositional variations for the Iceland Rise samples are not as large. Coccoliths have a 5-6% decrease; pennate diatoms, a 0-6% increase; clays, a 2% increase; and mineral matter, a 1-5% increase, between clear water and the nepheloid layer. These compositional differences are not sufficient to reflect differences in the apparent densities.

Figure 3.22    Apparent density of samples from the western North Atlantic. Clear water samples have apparent densities smaller than those for nepheloid-layer samples. A line with slope  $1.1 \text{ g/cm}^3$  effectively separates the two groups.



### COMPOSITIONAL DIFFERENCES

Filters of SPM from both regions were examined to look for compositional differences between clear-water and nepheloid-layer particles, and to determine whether composition or state of aggregation is a likely cause of the differences in particle size distributions. In the previous section, compositional differences were suggested as an explanation for apparent density changes in the western North Atlantic samples.

#### Iceland Rise

Chi-square analyses of the compositional results indicate that particles from clear water and the nepheloid layer at individual hydrographic stations differ at the 95% confidence level. In order to determine whether these differences are due to processes causing nepheloid layers, or are simply evidence of dissolution, decomposition, and consumption of particles with increasing water depth, a station with no nepheloid layer was sampled. A chi-square test was made on samples from Station 67 (no nepheloid layer; Figure 3.7) taken from 700 m and 1479 m where the total water depth is 1522 m. The result indicates that at the 95% confidence level these samples are from the same population. These data support the hypothesis that the variability between clear-water and nepheloid-layer samples is due to the existence of the nepheloid layer, and is not simply a function of depth or depth-related processes.

For comparative purposes, the percentages, rather than numbers, of particles in the different compositional classes were used to eliminate the effects of concentration differences between clear water and the nepheloid layer (Figure 3.13). The major variations seen in composition were a decrease in the percentage of small coccoliths and an increase in the percentage of diatoms (particularly Rhizosolenia), clays, and mineral matter in the nepheloid layer relative to clear water. The increase in the percentages of diatoms, clays, and mineral matter is probably caused by resuspension of these components, which are abundant in the local surface sediments into the nepheloid layer. The decrease in the percentage of small coccoliths reflects dilution. The number of small coccoliths does not decrease in the nepheloid layer, but the percentage does (Table 3.1, Figure 3.13). Therefore, the other components of the SPM in the nepheloid layer are preferentially added, resulting in the decrease in percentage of small coccoliths.

State of aggregation of particles was also studied. Aggregates were found in both the clear-water and nepheloid-layer samples, with the percentage of aggregates in both samples being very similar (Table 3.1). Aggregates are sometimes difficult to detect on filters, because drying of the samples removes water and collapses organic matter which may act a binding agent. In clear-water samples, collapsed aggregates were readily detected because there was little material on the filters (Plate 3.2). However, for nepheloid-layer samples, filters were usually covered with material,

in some cases more than a single layer, which made estimation of aggregates more difficult. Therefore, aggregates may have been underestimated in the nepheloid-layer samples.

From the studies on composition and state of aggregation, it appears that compositional differences between clear water and the nepheloid layer, particularly the increases in diatoms and mineral matter, may account for the differences in particle size distributions. Aggregations of particles in the nepheloid layer may be of secondary importance.

The possibility of inorganic flocculation being a contributor to aggregate formation in the nepheloid was assessed on theoretical grounds. Inorganic flocculation occurs by Brownian motion, local shear and differential settling. Einstein and Krone (1962) report equations to calculate the probability of successful collisions by particles in salt water resulting in flocculation. From their equations, and using Iceland Rise data, collisions by Brownian motion would occur once every six months to two years; collisions by local shear would occur once every twenty to eighty days; and differential settling may be important for particles larger than  $5.4 \mu\text{m}$  which comprise <1% by number of the suspended particles. These calculations indicate that inorganic flocculation is not likely to be responsible for aggregate formation in the nepheloid layer on the Iceland Rise. However, organic flocculation may be important.

### Western North Atlantic

The compositional differences between particles in clear water and the nepheloid layer are more pronounced in the western North Atlantic region than for the Iceland Rise. This is probably due to the different inputs and processes in the two regions. At present, the Iceland Rise region has a high surface input of both terrigenous and biogenic components, whereas the western North Atlantic has a smaller terrigenous input. For the western North Atlantic, the clear-water samples are mostly composed of biogenic material; the nepheloid-layer samples contain a larger fraction of clays and mineral matter (Figure 3.14). Changes between clear water and the nepheloid layer include a decrease in percentage of small coccoliths and organic matter and an increase in mineral matter, clays, and aggregates.

Water depths are much greater in the western North Atlantic than in the Iceland Rise area. In these increased depths carbonate dissolves at the seafloor (Takahashi, 1975; Broecker and Takahashi, 1978). The coccoliths observed in the nepheloid-layer samples are frequently partially dissolved. Dissolution at the seafloor, and subsequent resuspension, certainly could account for the dramatic decrease in coccoliths from clear water to the nepheloid layer. The increase in clays and mineral matter in the nepheloid layer is partially due to the decomposition and dissolution of other components at the seafloor. However, advection of nonbiogenic material into the region in the bottom boundary layer is another probable cause.



Since current velocities were not measured during this study, assessing the probability of local sediment input is difficult.

Composition and state of aggregation change from clear-water to nepheloid-layer samples. Both of these may cause the differences observed in the particle size distributions. Mineral grains and clays increase substantially in the nepheloid layer. These components usually range in size from 3 to 8  $\mu\text{m}$  and therefore may account for the peak of material in the nepheloid-layer particle size distributions (Figure 3.12). Aggregates observed tended to be larger ( $>10 \mu\text{m}$ ), and therefore are not as likely candidates for explaining the size changes observed.

#### CONCLUSIONS

(1) Analysis of light scattering versus SPM concentration from the Iceland Rise gives three principal results: a) clear-water and nepheloid-layer samples show different relationships of concentration to light scattering, indicating that although the first-order response of the L-DGO nephelometer is a function of particle concentration, second-order responses due to other SPM characteristics such as particle size and composition are not negligible, and/or the response is nonlinear with increasing concentration; b) comparison of the correlation obtained south of Iceland to the BBOR-HAP and LCR regression lines (Biscaye and Eittrheim, 1974; 1977) demonstrates that the correlation is somewhat site-specific, with predicted concentrations differing by up to a

factor of 3.4 for light-scattering  $\log E/E_D$  values between 0.5 and 1.5; and c) but as a means of predicting SPM concentration from light scattering the correlation curves for the two regions are indistinguishable. Limits for prediction of a further observation for the Iceland Rise data include the Biscaye and Eittrheim curves for  $\log E/E_D$  values greater than 0.5.

(2) Particle size analyses show that clear-water and nepheloid-layer samples have different distributions. Clear-water samples are characterized by high variance distributions of roughly equal volumes of material in logarithmically increasing size grades. Nepheloid-layer samples have lower variance distributions with a mean modal size between 3 and 9  $\mu\text{m}$  in the two areas studied. Expressed in terms of normalized differential volume curves, nepheloid layers are shown to have a two-slope distribution, previously reported only in shallow waters. The variations in particle size observed between clear-water and nepheloid-layer samples are interpreted as being due primarily to resuspension of sediment into the nepheloid layer and advection of material into the region in the bottom boundary layer.

(3) Determinations of apparent density from the Iceland Rise area show no differentiation between clear-water and nepheloid-layer samples. However, plots of apparent density from the western North Atlantic do show a marked increase for nepheloid-layer samples. The interpretation of this phenomenon is that the compositional differences for the western North Atlantic samples are much greater

than for the Iceland Rise samples. The dramatic decrease in coccoliths and increase in mineral matter and clays between clear water and the nepheloid layer serves to increase the apparent density of these particles with respect to clear-water particles.

(4) Microscopic examination of filtered particles and application of a chi-square test to the data obtained show that samples from the nepheloid layer are statistically different from clear-water samples. For the Iceland Rise, compositional differences include a decrease in the percentage of small coccoliths and an increase in the percentage of diatoms, clays, and mineral matter in the nepheloid layer relative to clear water. These differences are interpreted as being due to dilution of the coccoliths by other components (diatoms, clays, and mineral matter) which are readily resuspended into the nepheloid layer from the local surface sediments. For the western North Atlantic, the major compositional changes between clear water and the nepheloid layer include a decrease in small coccoliths and organic matter and an increase in mineral matter, clays, and aggregates. These differences are due to dissolution of the carbonate and decomposition and consumption of the organic matter on the seafloor with subsequent resuspension and advection of the refractory material into the near-bottom boundary layer.

## CHAPTER IV

### COMPARISON OF SEDIMENT TRAP SAMPLES AND THE SURFACE SEDIMENT: EVIDENCE FOR LOCAL RESUSPENSION

#### INTRODUCTION

There is ample geologic evidence that resuspension and redistribution of sediments by deep-sea currents has occurred over geologic time. The high frequency of hiatuses in DSDP and piston cores (Watkins and Kennett, 1971; Rona, 1973; Davies et al., 1975; Berggren and Hollister, 1977; Moore and Heath, 1977) is overwhelming evidence for periods of erosion and/or nondeposition. Terminating or outcropping reflectors in continuous seismic profiles corroborate erosion and nondeposition (Ewing et al., 1970; Tucholke, 1979). Coarse sediment lag deposits, interpreted as the material left behind in winnowing by currents, are also indications of erosion, at least of the fines (Huang and Watkins, 1977; Stow and Lovell, 1979).

Evidence for extensive redistribution and horizontal transport of deep-sea material is found in the size and structure of the sediment features in the ocean basins. If pelagic settling were the only factor in the distribution of sediments, the ocean floor would be uniformly blanketed with sediments. Instead, large (10's-100's km) bodies of sediment -- ridges, rises and drifts -- have been identified in many regions of the ocean basins (Jones et al., 1970; Tucholke et al., 1973; Hollister et al., 1978). Some of these features are associated with smaller scale (cm to 100's m)

bedforms -- ripples, furrows and mud waves (Hollister et al., 1974; Bouma and Treadwell, 1975; Jacobi et al., 1975; Lonsdale and Spiess, 1977; Flood, 1978). Formation of these sediment features may indicate sediment redistribution during the present day and up to millions of years ago.

Another probable indication of resuspension and transport of material by deep-sea currents comes from examining the components of the sediment. Distinctive tracers from a single source, e.g., Antarctic diatoms (Burckle and Biscaye, 1971; Johnson et al., 1977) and hemipelagic red clay (Ericson et al., 1961; Heezen et al., 1966; Hollister, 1967; Zimmerman, 1972) have been useful in inferring the paths of bottom currents. These tracers are transported and deposited by the currents, outlining the flow of Antarctic Bottom Water and the North Atlantic Western Boundary Undercurrent, respectively.

There is abundant geological evidence for resuspension and extensive transport of material having been important processes over time. A purpose of this chapter is to determine whether resuspension is occurring now or was restricted to phases of more vigorous bottom-water flow such as may have occurred during Pleistocene glacial epochs (e.g., Ledbetter and Johnson, 1976).

The approach used to test for present day resuspension in this chapter is to compare the material in the water column to that on the seafloor. Samples were obtained with sediment traps through the lower 500 m of the water column and from box core samples of the sediment surface layer.

## OBJECTIVES

The principal purpose of this work is to determine whether resuspension of deep-sea material is presently occurring on a time scale of days to weeks and to determine the influence of resuspension on suspended particulate matter. In carrying out this study, the focus is on the following objectives:

- (1) To examine samples of particulate matter from the water column and the seafloor below to assess and interpret the changes that occur to particles in transit through the water column and while residing on the seafloor.
- (2) To look for components of material in the water column which may be clearly identified as having previously resided on the seafloor, as evidence of resuspension.
- (3) To assess the vertical settling velocity versus horizontal current velocity scales involved to constrain the possible sources and distances of transport of the resuspended material.

## METHODS

### SUSPENDED PARTICULATE MATTER

Three moorings of sediment traps were deployed in the Iceland Rise region for periods from 4 to 13.5 days (Table 4.1). Two moorings were located along the northern transect at 1596 and 1971 m (Figure 4.1), with traps at 13, 103, 493 and 503 m above bottom (mab)(Figure 4.2). The third mooring was located in a turbidity-

Table 4.1

SEDIMENT TRAP MOORINGS

<u>Mooring No.</u>	<u>Station</u>	<u>Time Deployed</u>	<u>Time Recovered</u>	<u>Depth (m)</u>	<u>Location</u>	<u>Height of Traps Above Bottom (m)</u>
1	12	0200 June 27	1500 July 10	1971	62° 18.6'N 17° 26.2'W	13, 103, 503
2	14	0630 June 27	1500 July 3	1596	62° 28.5'N 17° 53.8'W	13, 103, 493
3	51	1153 July 5	1200 July 9	2146	61° 45.4'N 18° 39.2'W	13, 14, 54, 104, 494

Figure 4.1      Bathymetry of the study area with mooring locations and box cores identified. Three moorings and fourteen box cores were obtained from the study area. Samples were collected in the channel between the two ridges (Mooring 3, box cores 6, 7, 9, 10, 11 and 12) and along transects under the influence of the bottom current (Moorings 1 and 2, box cores 2, 3, 4, 5, 8, 13, 14, 15).



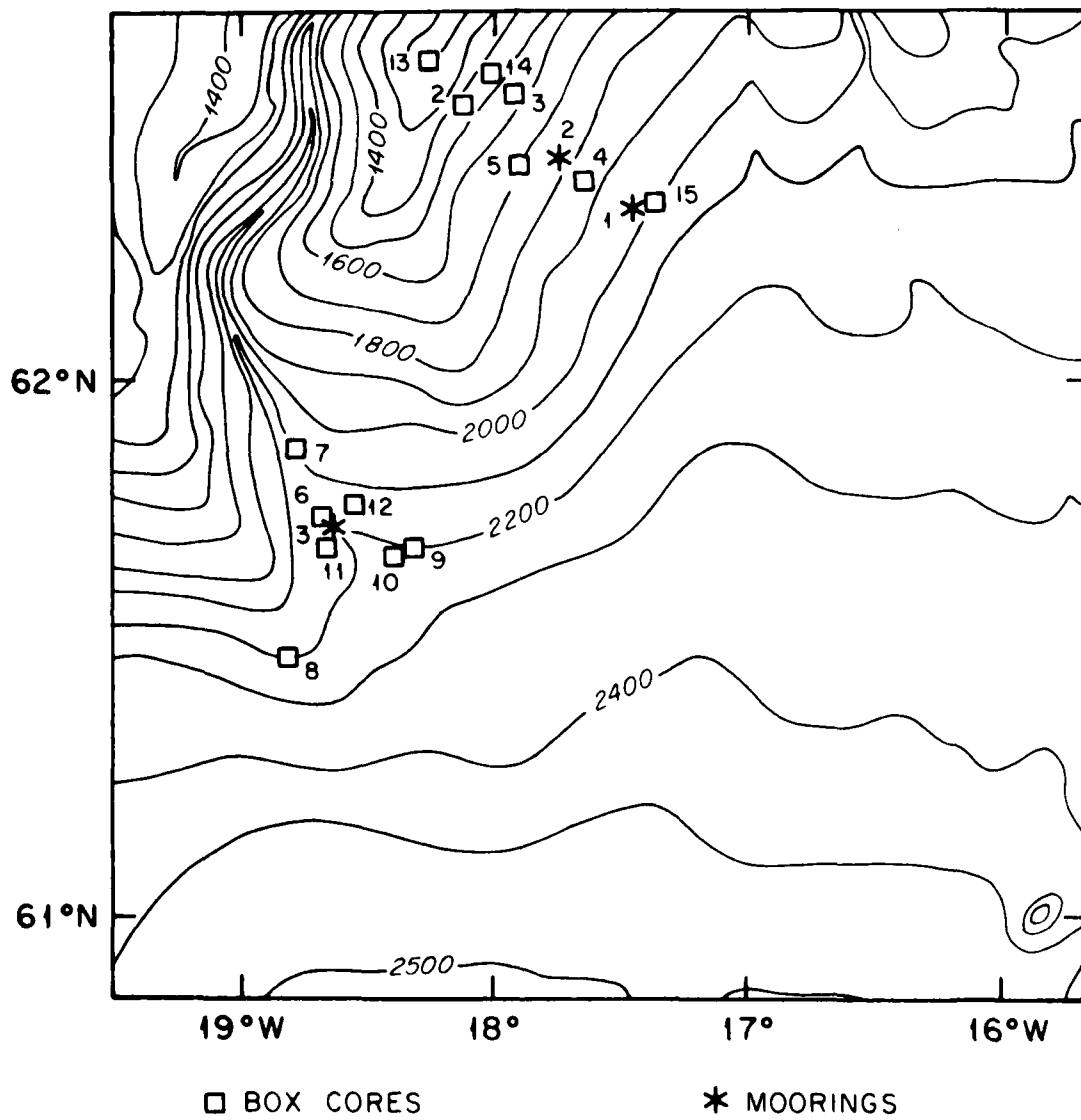
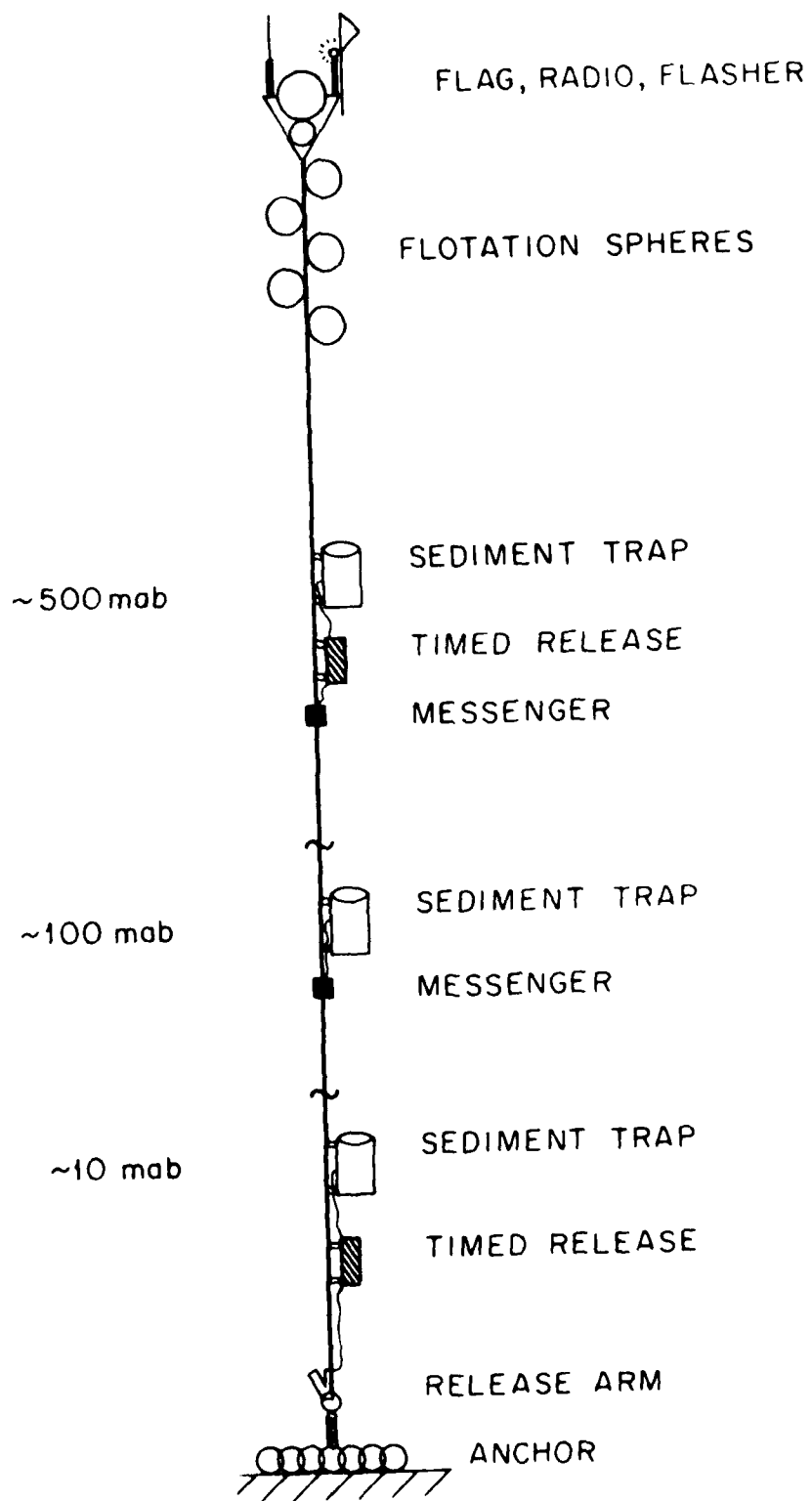


Figure 4.2      Diagram of sediment trap moorings from the northern transect. Traps were located at 503, 103 and 13 mab for Mooring 1 and 493, 103 and 13 mab for Mooring 2.



current canyon at 2146 m with additional traps at 53 and 13 mab (Figure 4.3). In the rest of this chapter the traps are referred to as being at 10, 50, 100 and 500 mab; these are their approximate heights above bottom and this description is used for convenience in comparison from one mooring to another. Water depths for the moorings are rounded to 2000, 1600, and 2150 m for moorings 1, 2, and 3, respectively.

The sediment traps used in this study were a modification of the type used by Gardner (1977a). The traps are PVC cylinders 25 cm in diameter and 62 cm in height (Figure 4.4). The lid of the trap is a butterfly valve recessed 30 cm from the top edge. The lid is held open by a spring-loaded PVC clamp. The valve is closed either by burning a nichrome wire attached to the spring mechanism or alternatively by dropping a messenger which releases a taut line to the spring mechanism. The burning of the wire or dropping of a messenger is actuated by a timed release.

#### SURFACE SEDIMENT SAMPLES

Sediment samples were obtained throughout the study area by piston coring and box coring. Box-core samples were used in this work since box corers more reliably recover the surface sediments. Fourteen box cores were obtained in the Iceland Rise region (Table 4.2, Figure 4.1). The box corer used is that described by Bouma (1969, p. 339-342). Surface scrapings from the top 1 cm were taken from the cores for comparison with the sediment-trap samples.

Figure 4.3      Diagram of sediment trap mooring from the channel station, Mooring 3. Traps were located at 494, 104, 54, 14 and 13 mab. The trap at 14 mab was a different design from the other traps and did not function properly.

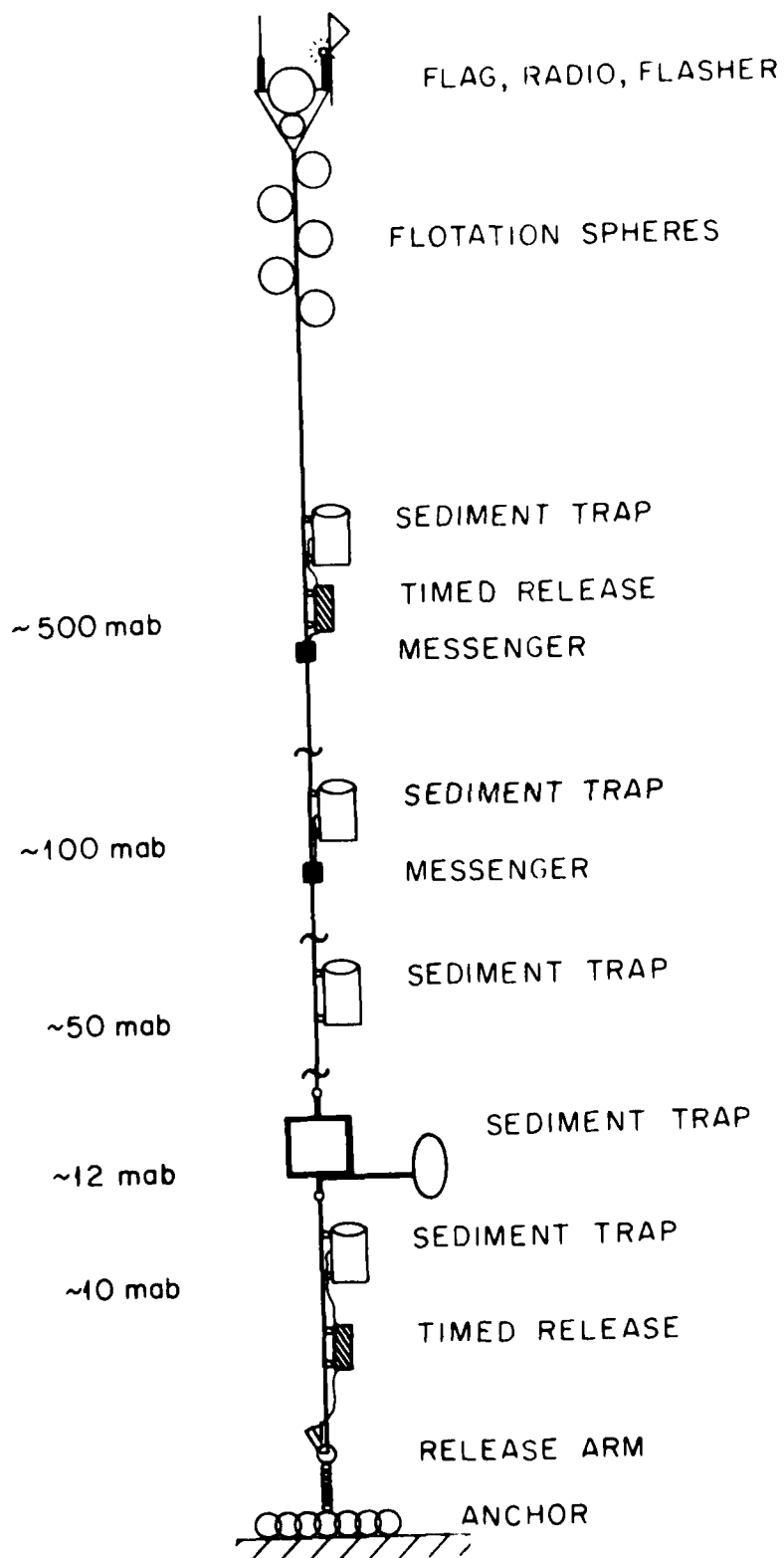


Figure 4.4      The sediment trap used in this study. The trap is a PVC cylinder with a height to width ratio of 2.5. The closing mechanism is a butterfly valve actuated by a timed release.

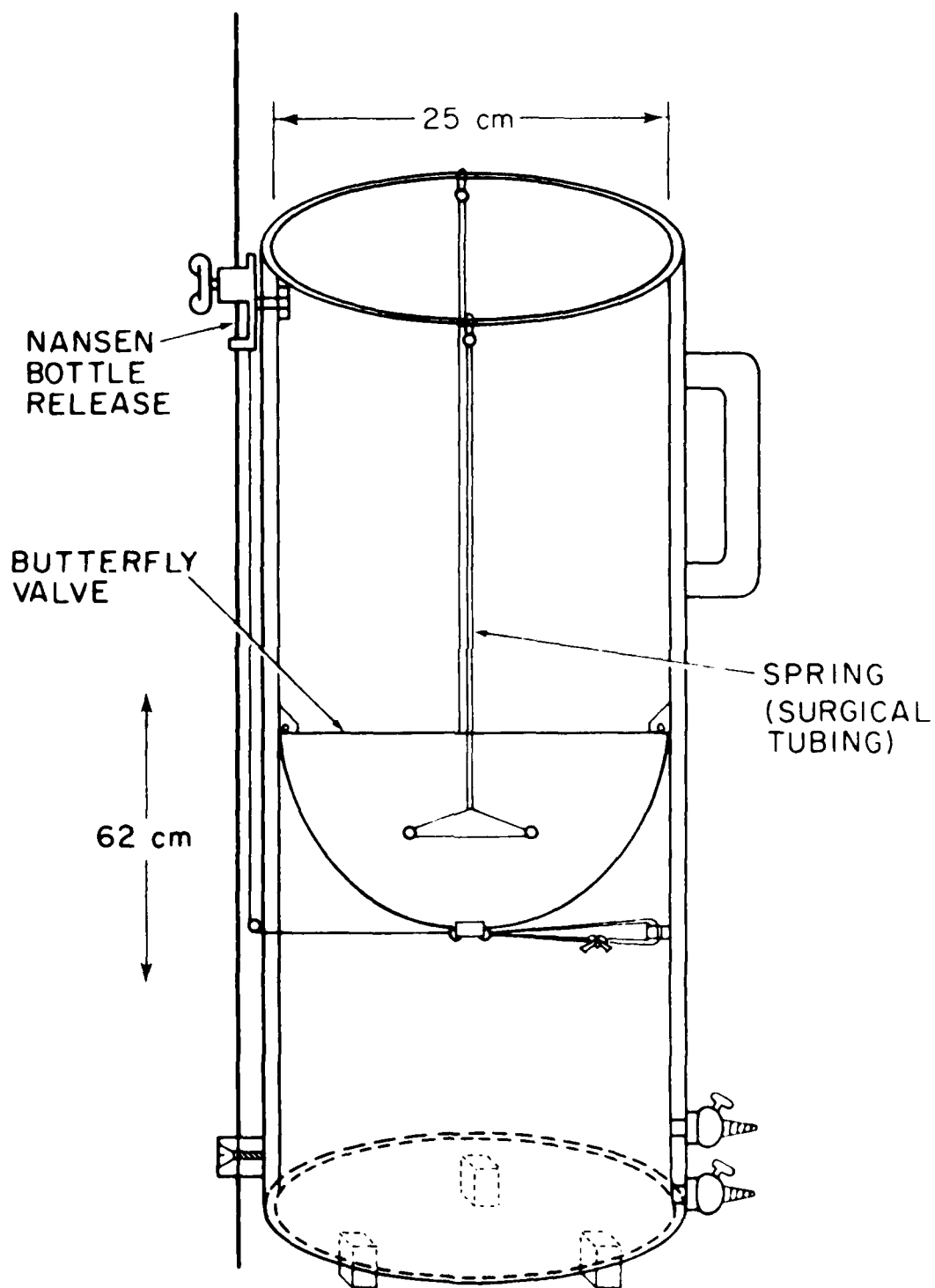




Table 4.2

BOX CORES

<u>Station</u>	<u>Core No.</u>	<u>Depth (m)</u>	<u>Latitude</u>	<u>Longitude</u>	<u>Remarks</u>
1	1-BC	4539	40°35.1'N	63°04.4'W	72 cm sample
21	2-BC	1391	62°30.4'N	18°06.4'W	1 kg sample
24	3-BC	1509	62°29.6'N	17°59.3'W	26 cm sample
43	4-BC	1839	62°22.5'N	17°35.8'W	
48	5-BC	1687	62°26.3'N	17°50.3'W	10 cm sample
56	6-BC	2175	61°44.0'N	18°39.0'W	
60	7-BC	2128	61°50.3'N	18°47.9'W	
73	8-BC	2203	61°31.0'N	18°46.5'W	
77	9-BC	2205	61°41.0'N	18°25.1'W	
78	10-BC	2248	61°40.5'N	18°27.2'W	
79	11-BC	2154	61°41.2'N	18°39.0'W	
80	12-BC	2133	61°45.6'N	18°37.0'W	
82	13-BC	1198	62°33.2'N	18°14.3'W	1/2 kg sample
83	14-BC	1409	62°31.8'N	18°02.0'W	1 kg sample
86	15-BC	1998	62°17.6'N	17°25.1'W	

#### SIZE DISTRIBUTION ANALYSES

Particle size analyses were performed on sediment trap material and surface sediments. Samples were wet sieved with gentle agitation at 250, 125, 63, and 20  $\mu\text{m}$ , yielding five size fractions per sample. Samples were sieved with seawater as distilled water might disperse the aggregates and loosely bound fecal pellets. Some particles smaller than the grid size remained on the sieves due to agglomeration with larger particles. Each size fraction was separately filtered onto 0.4  $\mu\text{m}$  Nuclepore filters or pre-combusted glass fiber filters (nominal pore size of 1  $\mu\text{m}$ ), for weight determination. Samples were rinsed ten times with 10 ml aliquots of filtered, buffered to pH 7, distilled water to remove residual salt.

#### OPTICAL IDENTIFICATION

Components of sediment trap samples and surface sediment samples were identified by optical microscopy and scanning electron microscopy. A binocular microscope was used to study the  $>63 \mu\text{m}$  fractions of the samples which comprised 37-70% of the total trap samples by weight. Counts were made of the major constituents of the samples. These include: foraminifera, radiolaria, pteropods, diatoms, dinoflagellates, fecal pellets, unidentified biogenic material, volcanic glass, mineral grains, and aggregates. Counts were made directly from filters obtained in the size-fraction analysis for the sediment-trap samples for all but the traps at 10 mab. The sieved fractions of the surface-sediment and

sediment-trap samples from 10 mab were later split into smaller, manageable fractions with a microsplitter before counting. Scanning electron microscopy was used to obtain photomicrographs of the various constituents in the samples.

#### MINERALOGY

X-ray diffraction was used to determine the mineralogy of surface-sediments and sediment-trap samples from 10 mab; trap samples above 10 mab had insufficient material for these analyses to be made. Bulk powder mounts were used to determine the overall composition of the samples, and oriented mounts of the  $< 2 \mu\text{m}$  fraction were used for clay mineralogy (Hathaway, 1972).

#### CARBONATE DETERMINATIONS

The calcium carbonate content of sediment-trap samples and surface-sediment samples was determined by acidification of a fraction of the samples. Sediment-trap samples were wet split with a plankton splitter into fractions small enough to be concentrated onto 25 mm diameter precombusted, preweighed glass-fiber filters. The samples were digested with 2N HCl and rinsed ten times with distilled water. Calcium carbonate content was calculated from weight loss.

#### ORGANIC CARBON AND NITROGEN ANALYSES

Organic carbon and nitrogen contents were determined for both the sediment-trap and surface-sediment samples. Samples obtained at

sea were fractionated by wet splitting and filtering these portions onto precombusted glass-fiber filters. These filters were frozen at sea to minimize organic decay. Subsequently, in the laboratory they were thawed, acidified to remove carbonate, and analyzed with a Perkin Elmer #240 elemental analyzer, to obtain organic carbon and nitrogen contents of the samples.

## RESULTS

All of the sediment trap moorings were successfully recovered, with almost complete success with the sediment traps. All traps were recovered with good samples except for the traps at 500 and 100 mab from Mooring 3. Material from these traps may have been partially washed out in the surface waters, because they remained open and subject to the pumping action of the swell before recovery.

### MASS COLLECTED BY THE SEDIMENT TRAPS

The quantity of material collected by the sediment traps increases substantially from 500 to 10 mab, particularly between 100 and 10 mab (Table 4.3). The greatest increase, more than two orders of magnitude, is for Mooring 2, located in the axis of the bottom current.

Apparent vertical fluxes of material can be calculated from the sediment-trap data (Figure 4.5; Gardner, 1977a). At 500 mab, apparent fluxes varied by a factor of 2, from  $1.8 \text{ mg/cm}^2/\text{yr}$  at Mooring 2 at 1600 m to  $3.6 \text{ mg/cm}^2/\text{yr}$  at Mooring 1 at 2000 m.

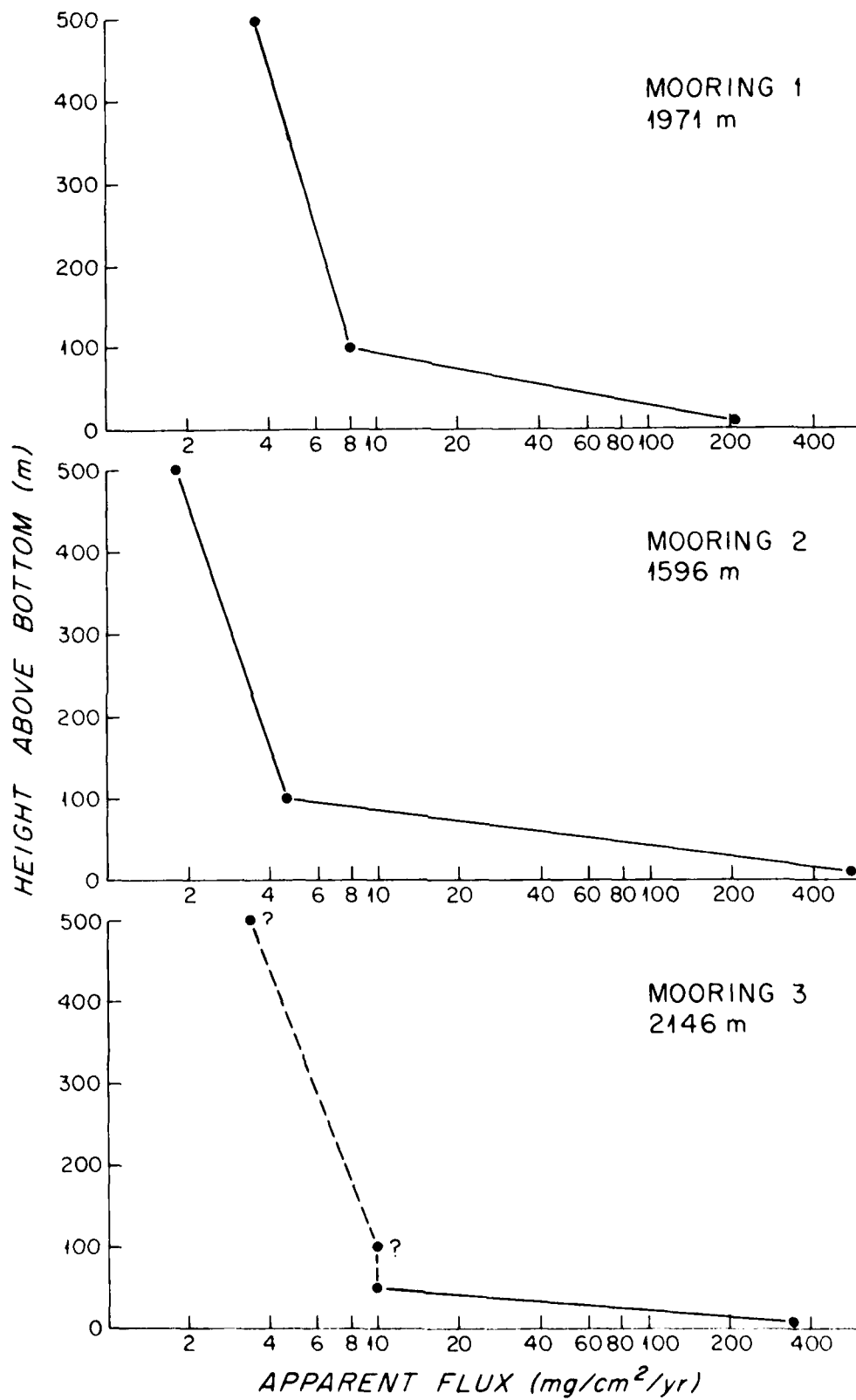
Table 4.3

MASS OF SEDIMENT TRAP SAMPLES

	MAB (m)	Mass Collected (mg)
Mooring 1	500	68.0
	100	147.6
	10	3867.
Mooring 2	500	15.9
	100	36.4
	10	4072.
Mooring 3	500	18.7*
	100	54.3*
	50	55.3
	10	1895.

\* traps returned open

Figure 4.5      Apparent vertical fluxes of material through the water column. Weight of material collected by the traps is divided by the area of the opening and duration of trapping. A dramatic increase in apparent flux is observed from 100 to 10 mab. The trap data from 500 mab and 100 mab from Mooring 3 are questionable since these traps were recovered open.



Traps were spaced up to 500 mab because it was thought that 500 m would be high enough to be above the nepheloid layer, and would catch only primary, surface-source material. However, from the light-scattering profiles discussed in Chapter III (Figure 3.8), the traps at 500 mab on Moorings 1 and 3 were still within the nepheloid layer; the 500 mab trap from Mooring 2 was above it. Apparent fluxes at 100 mab varied by a factor of 1.9, with the higher value at the deeper station, Mooring 1. At 10 mab, the fluxes vary by a factor of 2.3 with the highest flux,  $474 \text{ mg/cm}^2/\text{yr}$  at Mooring 2, in the axis of the bottom current.

#### PARTICLE SIZE DISTRIBUTIONS

Particle size distributions were examined for sediment-trap samples and nearby surface sediments to determine if grain size varies with water depth or between material in the water column and that on the underlying seafloor.

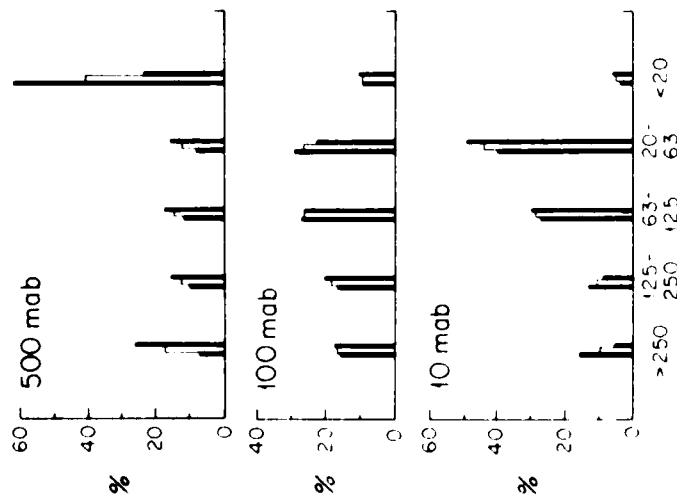
##### Sediment Traps

Particle size distributions vary considerably through the water column, but show the same general trends from mooring to mooring (Figure 4.6). Traps at 500 mab have roughly similar amounts in all size fractions  $>20 \mu\text{m}$ . The  $<20 \mu\text{m}$  fraction is a large percentage of the samples, 33 to 42%. This high proportion of small particles indicates that although large particles may theoretically compose a substantial portion of the vertical flux of material through the

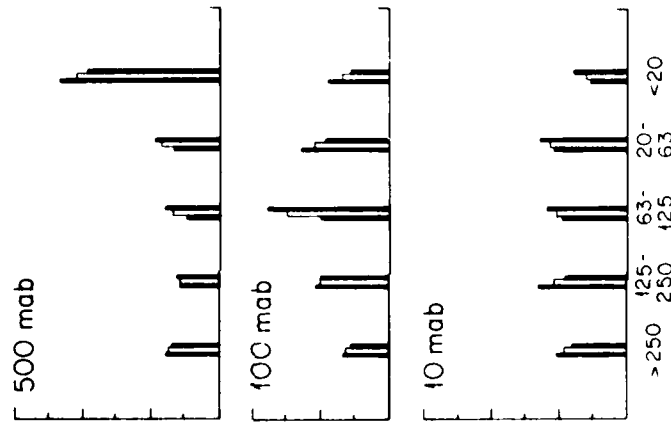


Figure 4.6 Particle size distributions for sediment trap samples by weight. Distributions were determined for two splits of the samples which are represented by the solid bars. The average size distribution of the combined splits is given as the open bars.

MOORING 1

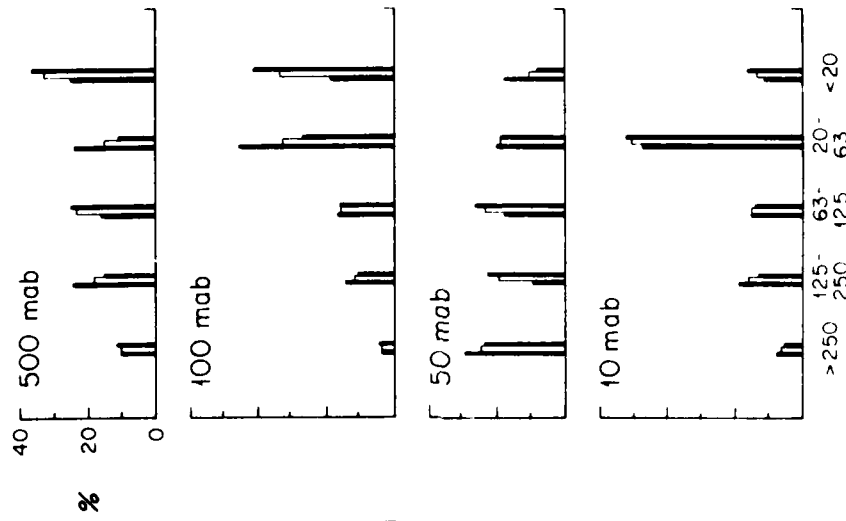


MOORING 2



SIZE FRACTION ( $\mu\text{m}$ )

MOORING 3



water column (McCave, 1975), small particles are equally important in this particular area.

The traps at 100 mab along the northern transect have a peak in the 63-125  $\mu\text{m}$  size fraction. The 50 mab trap from the channel mooring (the only trap at this height) has roughly equal amounts of material in the size fractions  $>20 \mu\text{m}$ , as do the traps at 500 mab, but has a decrease in material  $<20 \mu\text{m}$ .

The material from traps at 10 mab are more variable in their size distributions. A general trend among these three samples is low percentages of material  $<20 \mu\text{m}$ . This may be artificial. For these traps, up to one gram of material was sieved. The 20  $\mu\text{m}$  sieve would frequently clog, and sieving at this size fraction took several attempts to complete. Some material smaller than 20  $\mu\text{m}$  undoubtedly remained on the sieve due to the large amount of material processed. This could account for the strong decreases in the  $<20 \mu\text{m}$  size fraction for these samples.

A general trend observed among the trap samples is a decrease with depth in the percentage of material  $<20 \mu\text{m}$ .

#### Surface Sediments

Box cores were taken along the northern transect and in the channel. The samples recovered are somewhat biased, since some attempts made to recover box cores in the current axis along the northern line, were unsuccessful due to wash-out of the coarse sediments during recovery. Cores taken in the channel have fine

grained sediments, up to 96% <63  $\mu$ m (Figure 4.7). Cores along the northern transect tend to be composed of coarser material. Cores 3, 5, and 15 (Figure 4.7) and gravity cores 1, 5, and 11 (Shor, 1979) have surface sand layers from which the fines seem to have been winnowed.

#### OPTICAL IDENTIFICATION

The coarse material (>63  $\mu$ m) in flux at various depths in the water column was identified and counted to compare this material to that on the seafloor.

#### Sediment Traps

##### Foraminifera

Planktonic foraminifera comprise by number from 2 to 54% of the size fractions >63  $\mu$ m of the sediment-trap samples (Table 4.4). The >250  $\mu$ m size fraction had the largest percentage of planktonic forams; smaller size fractions had smaller percentages. The planktonic foraminifera >150  $\mu$ m in the sediment trap samples from 10 mab were identified to compare the trap species in the traps with those in the surface sediments. Forams <150  $\mu$ m were generally too small for reliable identification of species. Species identified and counted include Neogloboquadrina pachyderma (dextral and sinistral), Globigerinita glutinata, Globigerina bulloides, Globigerina quinqueloba and Globorotalia inflata (Plate 4.1, 3-8; Table 4.5). Some of the planktonic forams in the samples were coated with iron oxide (Plate 4.1,8; Table 4.5).

Figure 4.7      Particle size distributions for surface sediment samples. Samples were wet sieved and filtered on glass fiber filters for weight determination.

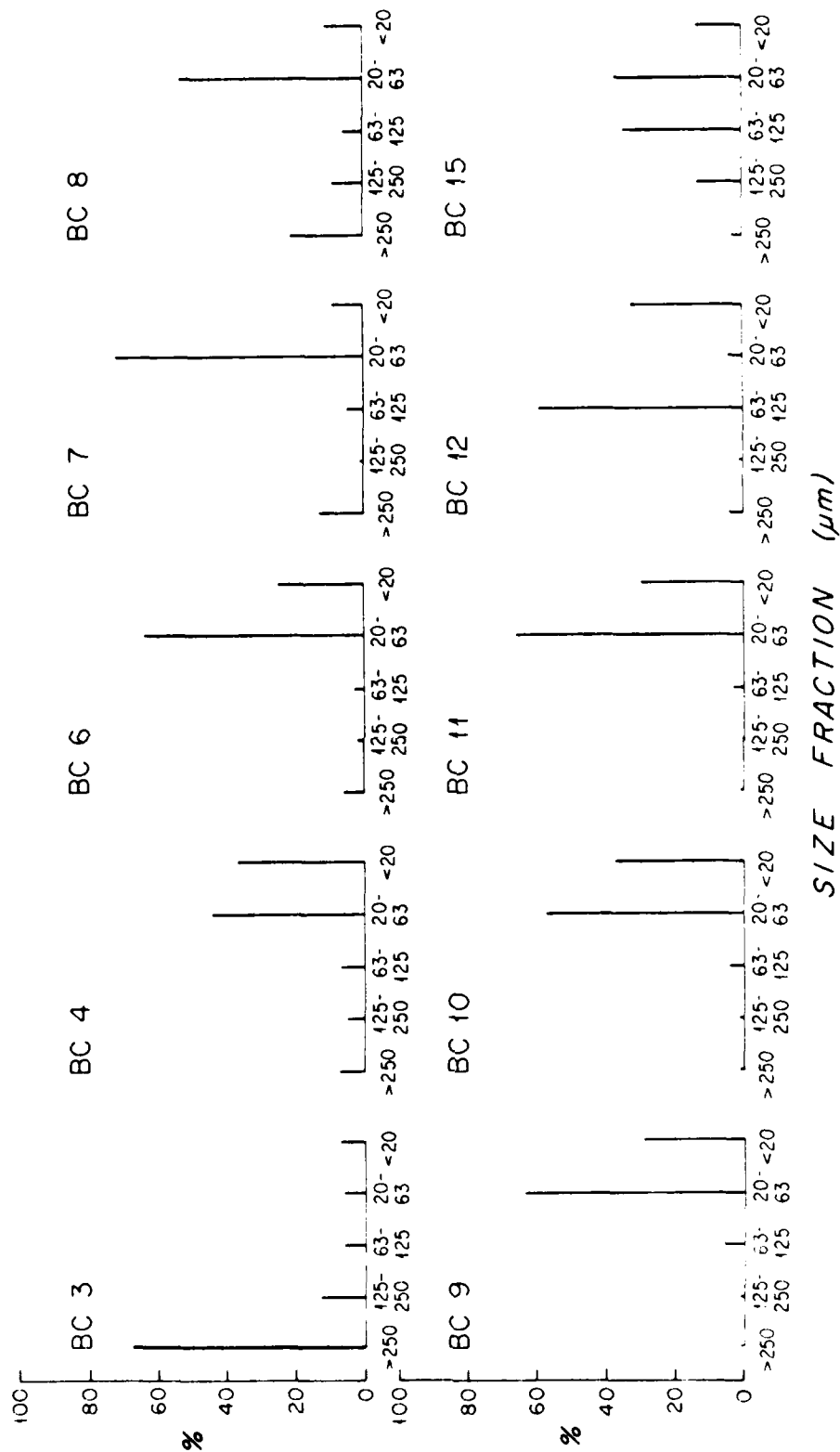




Plate 4.1 SEM photomicrographs of particles from the sediment traps.

- 1) Pteropod from Mooring 1, 10 mab, scale bar 200  $\mu$ m, X 65.
- 2) Pteropod from Mooring 1, 500 mab, scale bar 50  $\mu$ m, X 400.
- 3-8) Planktonic foraminifera from Mooring 2, 10 mab:
  3. Neogloboquadrina pachyderma (dextral), scale bar 50  $\mu$ m, X 250;
  4. Globigerina glutinata, scale bar 50  $\mu$ m, X 240;
  5. Globigerina bulloides, scale bar 50  $\mu$ m, X 200;
  6. Globigerinata quinqueloba, scale bar 50  $\mu$ m, X 380;
  7. Neogloboquadrina pachyderma (sinistral), scale bar 50  $\mu$ m, X 270;
  8. Globorotalia inflata, note the surface texture; this foram has an iron-oxide coating representative of residence at the seafloor, scale bar 50  $\mu$ m, X 260;
- 9-12) Benthic foraminifera from traps at 10, 100 and 500 mab:
  9. Parafissurina sp., from Mooring 2, 10 mab, scale bar 50  $\mu$ m, X 240;
  10. Uvigerina peregrina, from Mooring 2, 100 mab, scale bar 20  $\mu$ m, X 500;
  11. Cassidulina sp., from Mooring 2, 100 mab, scale bar 20  $\mu$ m, X 700;
  12. Astrononion sp., from Mooring 1, 500 mab, scale bar 50  $\mu$ m, X 380.
- 13-16) Radiolaria from the sediment traps:
  13. Phaeodarian, Protocystis xiphodon, from Mooring 2, 500 mab, scale bar 20  $\mu$ m, X 950;
  14. Nassellarian, Botryostrobus aquilonarias, from Mooring 1, 500 mab, scale bar 20  $\mu$ m, X 610;
  15. Smullerian, family Phacodiscidae, from Mooring 1, 10 mab, scale bar 50  $\mu$ m, X 270;
  16. Smullerian, family Lithelidae, from Mooring 1, 10 mab, scale bar 50  $\mu$ m, X 340.



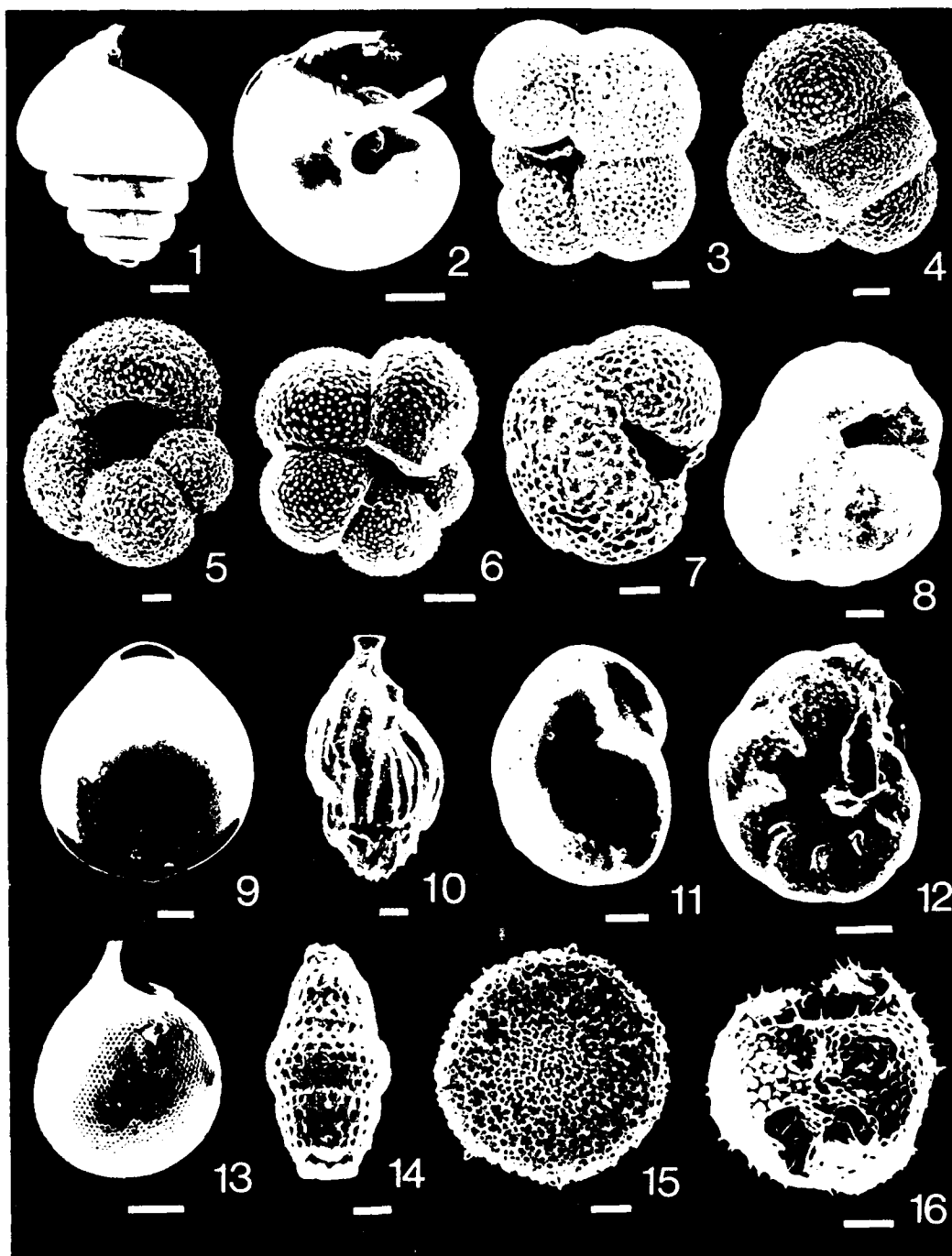


Table 4.1  
FORAMINIFERA IN THE SEDIMENT TRAP AND SURFACE SEDIMENT SAMPLES

core position (cm)	N. paucispina (Gibbula)	N. pachylina (Gibbula)	G. inflata	G. quadriloba	G. elunina	Bullidors	beudantic	fragments	others un? unknowns	iron- oxide coated	total planktonics	total forams
0-10	0	12	5	13	20	45	0	7	5	3	40	43
10-20	2	20	2	23	16	32	3	5	5	5	243	273
20-30	4	47	3	1	10	31	2	12	7	33	488	799
30-40	4	63	1	4	20	5	2	5	3	26	137	216
40-50	15	43	7	4	11	14	6	5	6	45	319	359
50-60	19	25	11	1	8	21	3	18	5	32	334	455
60-70	21	43	11	0	11	14	3	14	9	34	313	375
70-80	0	42	2	4	19	22	13	8	7	1	150	176
80-90	11	44	4	0	6	11	1	11	4	22	324	376
90-100	2	49	6	5	16	15	2	12	8	1	107	124
100-110	9	46	2	2	15	16	2	13	6	27	335	365

Benthic foraminifera were also found in the sediment-trap samples (Plate 4.1, 9-12). All traps at 10 mab and 100 mab contained at least a few benthic specimens. The trap at 500 mab from mooring 1, at 2000 m, contained 3 small ( $<100\text{ }\mu\text{m}$ ) benthic forams (Plate 4.1, 12). Some identified were Uvigerina sp., Parafissurina sp., and Cassidulina sp.

Due to the small size of the samples from the traps located at 500 and 100 mab, differentiating of the planktonics by species was not done, only the total number of individuals was counted. The presence or absence of benthic forams, the glacial assemblage foram, Neogloboquadrina pachyderma (sinistral), and iron-oxide staining in these samples was recorded since occurrences of these indicate resuspension of seafloor material.

#### Radiolaria

Radiolaria of the three major groups (spumellarians, nassellarians, and phaeodarians) were observed in the sediment trap samples (Plate 4.1, 13-16). They comprise  $<10\%$  by number of all the samples and are absent entirely from some of the  $>250\text{ }\mu\text{m}$  size fractions (Table 4.4). The percentage of nassellarians and phaeodarians generally decreases between 500 and 10 mab. This agrees with the observations by Takahashi and Honjo (1980) that spumellarians are less subject to dissolution than the nassellarians and phaeodarians.

### Pteropods

Pteropods were found in most of the sediment-trap samples (Table 4.4). Specimens were large, a millimeter or more in diameter, and have fragile transparent to translucent tests (Plate 4.1, 1-2). Pteropods comprise <7% by number of the total samples considering all size fractions. However, for the >250  $\mu$ m size fraction at the channel station, Mooring 3, they are the dominant component, forming 42% of the trap sample at 50 mab. In general, the percentage of pteropods in trap samples decreases toward the seafloor. At Mooring 2, at 1600 m, no pteropods were observed in the trap at 10 mab.

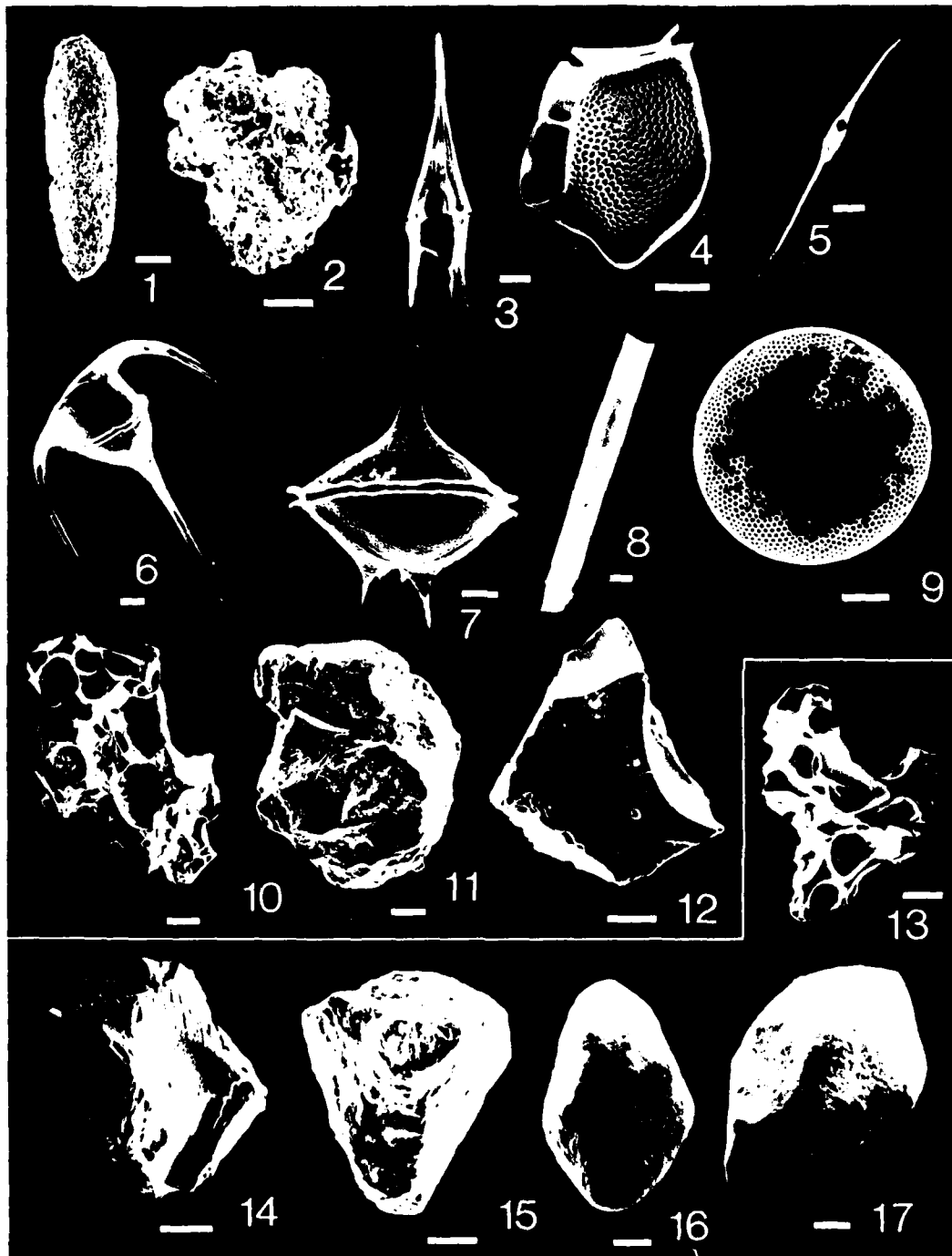
Pteropods are composed of aragonite, with which the bottom water may be undersaturated (Berner, 1977). The specimens observed in the traps probably fell rapidly through the water column from their surface source and have so far escaped dissolution. Some of the pteropods collected were so fragile that touching them with a wet fine-tipped brush caused them to break into several fragments.

### Diatoms

Both centric and pennate diatoms were found in the sediment-trap samples. Rhizosolenia was most prevalent (Plate 4.2, 8), but Coscinodiscus, 60-80  $\mu$ m in diameter, (Plate 4.2, 9) was also common. Diatoms comprise by number 11% or less of the bulk sediment-trap samples; individual size fractions have 1 to 15% diatoms. The two moorings along the northern transect show opposite trends with depth. For Mooring 1, 2000 m, diatoms increase in percentage from 500 to 10 mab, whereas for Mooring 2, 1600 m, a decrease is observed (Table 4.4).

Plate 4.2 SEM photomicrographs of particles from the sediment traps and surface sediments. 1-12 are trapped sediments; 13-17 are from the surface sediments.

- 1) Fecal pellet, Mooring 3, 50 mab, see Figure 4.8a for X-ray of elements present. Calcareous, siliceous, and clay material is seen at higher magnification. Scale bar 50  $\mu$ m, X 230.
- 2) Fecal pellet, Mooring 3, 50 mab, see Figure 4.8b for X-ray of elements present. Silica and calcium are the only elements detected. Scale bar 50  $\mu$ m, X 330.
- 3-7) Dinoflagellates from Mooring 2, 500 mab:
  3. Ceratium, scale bar 20  $\mu$ m, X 510;
  4. Dinophysis, scale bar 20  $\mu$ m, X 940;
  5. Ceratium, scale bar 50  $\mu$ m, X 220;
  6. Ceratium, scale bar 20  $\mu$ m, X 420;
  7. Peridinium, scale bar 20  $\mu$ m, X 610.
- 8) Diatom, perhaps part of Rhizosolenia, Mooring 2, 500 mab, scale bar 20  $\mu$ m, X 390.
- 9) Diatom, Coscinodiscus, Mooring 2, 500 mab, scale bar 20  $\mu$ m, X 800.
- 10-12) Volcanic shards and mineral grains from Mooring 2, 10 mab:
  10. Vesicular volcanic shard, see Figure 4.8c for X-ray of elements present, scale bar 50  $\mu$ m, X 230;
  11. Quartz grain with iron-oxide coating, see Figure 4.8d for X-ray of elements present, scale bar 50  $\mu$ m, X 230;
  12. Altered volcanic shard, see Figure 4.8e for X-ray of elements present, scale bar 50  $\mu$ m, X 330.
- 13-17) Volcanic shards and mineral grains from box core 5:
  13. Vesicular volcanic shard, see Figure 4.9a for X-ray of elements present, scale bar 50  $\mu$ m, X 270;
  14. Volcanic shard, see Figure 4.9b for X-ray of elements present, scale bar 50  $\mu$ m, X 360;
  15. Mineral grain, see Figure 4.9c for X-ray of elements present, scale bar 50  $\mu$ m, X 310;
  16. Mineral grain with iron-oxide coating, see Figure 4.9d for X-ray of elements present, scale bar 100  $\mu$ m, X 130;
  17. Quartz grain, see Figure 4.9e for X-ray of elements present, scale bar 50  $\mu$ m, X 250.



### Dinoflagellates

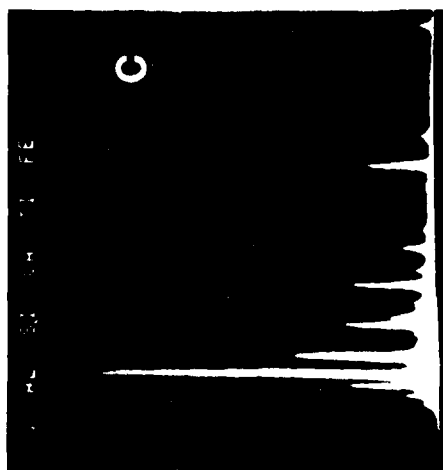
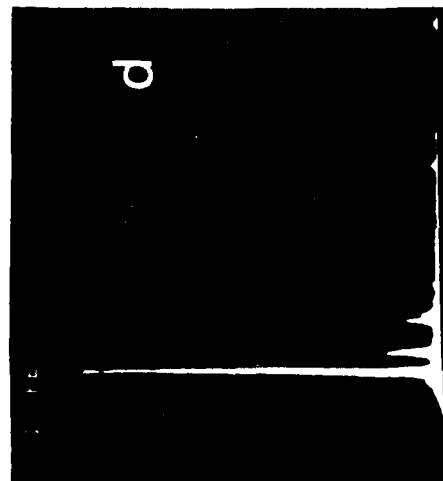
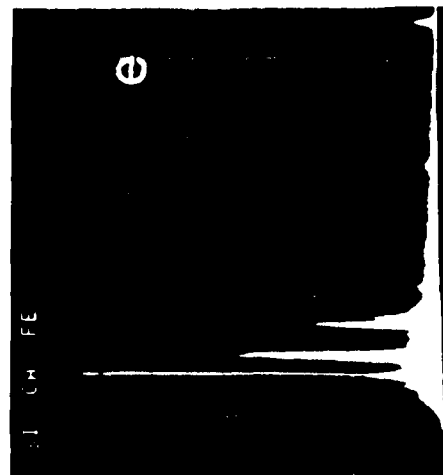
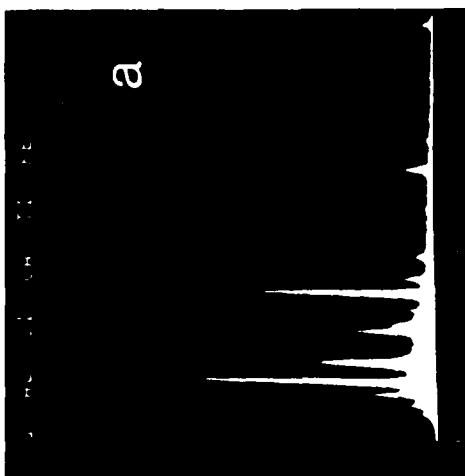
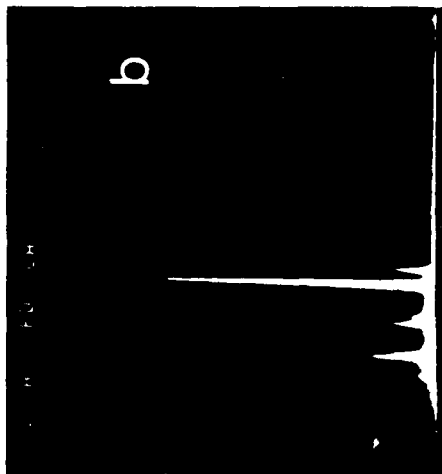
The principal genera of dinoflagellates observed in the sediment traps were Ceratium, Peridinium and Dinophysis (Plate 4.2, 3-7). They are found predominantly in the samples from 500 and 100 mab in the 63-125  $\mu$ m size fraction, usually comprising only a few percent by number of the samples. Few specimens were observed at 10 mab. These organisms have tests of organic material, which is highly susceptible to degradation in the water column and/or at the seafloor.

### Fecal Pellets

Fecal pellets of many shapes, colors, and sizes were found in the sediment traps (Plate 4.2, 1-2; Figure 4.8 a,b). Most were >125  $\mu$ m. The percentage, by number, of fecal pellets decreased toward the seafloor (Table 4.4). At 50 mab at Mooring 3 in the canyon, the sample is composed of 31% fecal pellets. This sample contains both well-formed tan to brownish fecal pellets and white fecal material as well. Traps at 100 mab at the other mooring sites have less than 5% of the sample composed of fecal pellets. Unfortunately, the traps at 500 and 100 mab from Mooring 3 did not function properly to determine if this high percentage of fecal material at 50 mab is regionally controlled. Counts of the samples from these two traps, which were open show ambiguous results. In the trap at 500 mab, 5% of the sample was fecal pellets, where in the trap at 100 mab, the figure was 68%.

Figure 4.8      Energy dispersive X-ray spectroscopy of sediment trap material; a) fecal pellet from Mooring 3, 50 mab, see Plate 4.2, 1 for photomicrograph; b) fecal pellet from Mooring 3, 50 mab, see Plate 4.2, 2 for photomicrograph; c) vesicular volcanic shard from Mooring 2, 10 mab, see Plate 4.2, 10 for photomicrograph; d) quartz grain with iron-oxide coating from Mooring 2, 10 mab, see Plate 4.2, 11 for photomicrograph; e) altered volcanic shard from Mooring 2, 10 mab, see Plate 4.2, 12 for photomicrograph.





#### Unidentified Biogenic Material

Unidentified biogenic material comprising <10% by number of the sample constituents was found in all size fractions of all the sediment traps. A general trend observed in the samples is a decrease in this group of particles toward the seafloor (Table 4.4). This category includes biogenic material too small to be definitively identified, biogenic aggregates, and unidentified test fragments.

#### Volcanic Glass

Two types of volcanic glass were observed in the trap samples; smooth glass shards and very vesicular fragments (Plate 4.2, 10,12; Figure 4.8, c, e). Both types were observed in all traps and in most size fractions. Volcanic glass was most prevalent in the small size fraction counted (63-125  $\mu\text{m}$ ), comprising up to 53% of this fraction. Some glass had smooth, shiny, sharp surfaces, while most volcanic shards showed alternation of its surface. A likely source of this component is Iceland.

#### Mineral Grains and Aggregates

Mineral grains and aggregates were combined in counting. Rounded particles and clay aggregates were the primary constituents in this category (Plate 4.2, 11; Figure 4.8 d). These components were found in all size fractions in most trap samples (Table 4.4). There is a dramatic increase in these components toward the

seafloor. For the traps at 10 mab, up to 60% of the trap sample >63  $\mu$ m is composed of mineral grains and aggregates. For the traps above, 13% or less of the sample is composed of these particles.

#### Surface Sediments

Surface sediments from box cores 3, 4, 5, 6, 8, 10 and 15 were sieved at 63  $\mu$ m to examine the coarse fraction of material and at 150  $\mu$ m to separate juvenile forams. Percentages of a particular component were determined as a fraction of the total number of particles counted.

#### Foraminifera

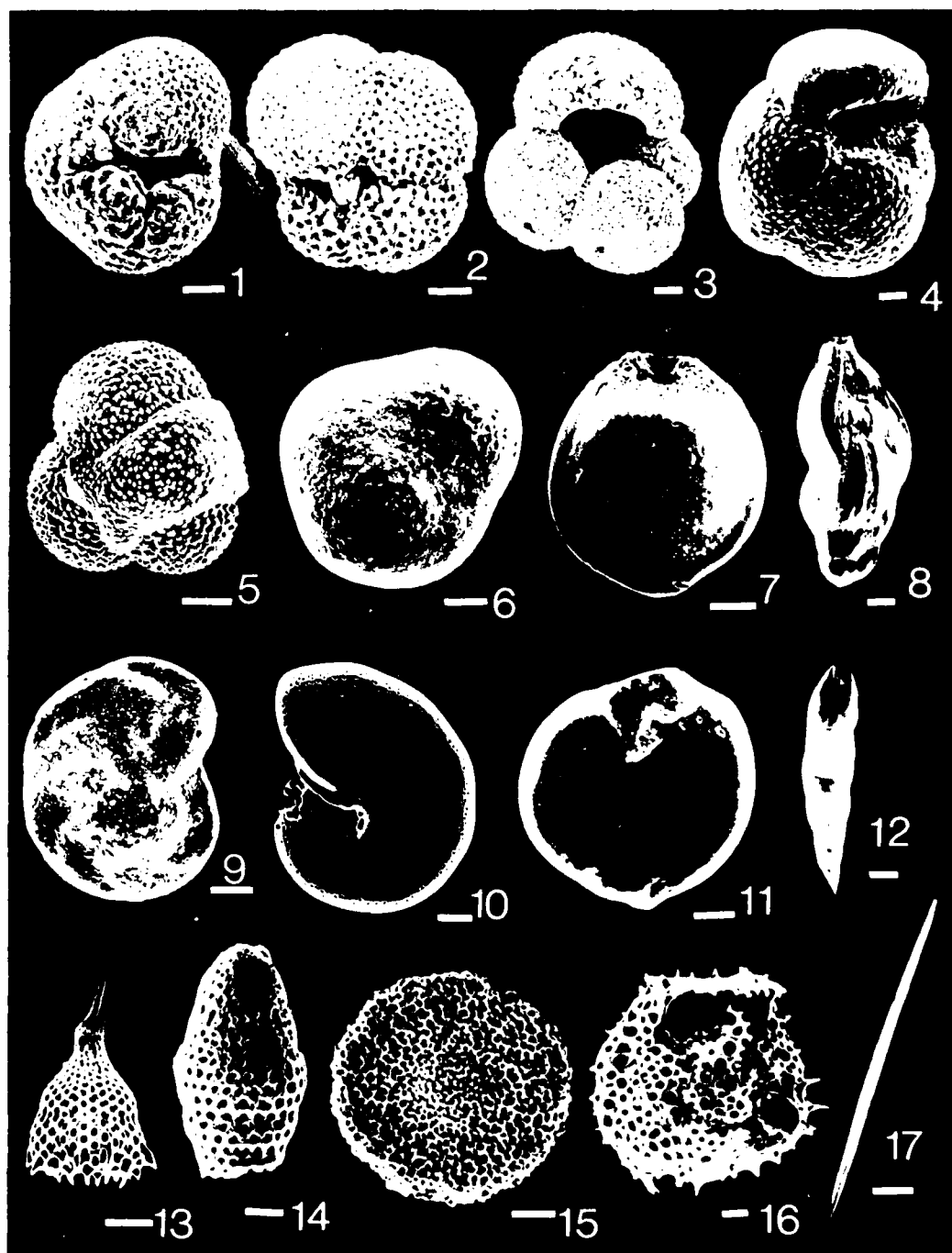
Planktonic foraminifera are one of the major components of material >150  $\mu$ m in the surface sediments (Table 4.6). Percentages of forams in this size fraction range from 12 to 65% and do not appear to be regionally controlled. The species of the forams do show some regional differences. N. pachyderma (dextral and sinistral), G. bulloides, G. glutinata, G. quinqueloba, and G. inflata (Plate 4.3, 1-6) were identified. N. pachyderma (sinistral) comprise 9-30% of the samples from box cores 3, 4, 5, 8 and 15, which all are located below the bottom current (Table 4.5). This same species comprises only 0-2% of the species from box cores 6 and 10 from the channel sites (Table 4.5). Other general trends are more N. pachyderma (dextral), G. bulloides, and G. quinqueloba in the box cores from the channel in comparison to the box cores

TABLE 10  
PERCENTAGE OF PARTICLES REMOVED BY PARTICLE TYPE

Particle Type	Size Range (microns)	Fungi	Bacteria	Protozoa	Diatoms	Flagellates	Other	Fecal Pellets	Unidentified biogenics	Volcanic Glass	Mineral Matter Aggregates	Total
1	0.5-1.0	100	100	100	100	100	100	100	9	33	40	182
2	1.0-2.0	100	100	100	100	100	100	100	7	44	42	193
3	2.0-4.0	100	100	100	100	100	100	100	5	36	26	267
4	4.0-8.0	100	100	100	100	100	100	100	2	21	25	907
5	8.0-16.0	100	100	100	100	100	100	100	5	27	49	1820
6	16.0-32.0	100	100	100	100	100	100	100	2	77	20	650
7	32.0-64.0	100	100	100	100	100	100	100	0	0	87	1493
8	64.0-128.0	100	100	100	100	100	100	100	5	45	30	943
9	128.0-256.0	100	100	100	100	100	100	100	3	7	44	596
10	256.0-512.0	100	100	100	100	100	100	100	5	58	19	473
11	512.0-1024.0	100	100	100	100	100	100	100	14	10	0	305
12	1024.0-2048.0	100	100	100	100	100	100	100	0	4	77	511
13	2048.0-4096.0	100	100	100	100	100	100	100	8	19	8	103
14	4096.0-8192.0	100	100	100	100	100	100	100	2	74	10	509

Plate 4.3 SEM photomicrographs of particles from the surface sediments.

- 1-6) Planktonic foraminifera:
1. Neogloboquadrina pachyderma (sinistral), scale bar 50  $\mu$ m, X 290;
  2. Neogloboquadrina pachyderma (dextral), scale bar 50  $\mu$ m, X 300;
  3. Globigerina bulloides, scale bar 50  $\mu$ m, X 190;
  4. Globorotalia inflata, scale bar 50  $\mu$ m, X 190;
  5. Globigerina glutinata, scale bar 50  $\mu$ m, X 340;
  6. Neogloboquadrina pachyderma (sinistral), same species as (1) but have an iron-oxide coating, scale bar 50  $\mu$ m, X 300.
- 7-12) Benthic foraminifera, 7-11 from box core 5; 12 from box core 6:
7. Parafissurina sp., scale bar 50  $\mu$ m, X 320;
  8. Trifarina sp., scale bar 50  $\mu$ m, X 190;
  9. Planulina wuellerstorfi, scale bar 50  $\mu$ m, X 290;
  10. Melonis barleenum, scale bar 50  $\mu$ m, X 230;
  11. A miliolid, Quinqueloculina or Triloculina, scale bar 50  $\mu$ m; X 280.
  12. Pleurostomella sp., scale bar 100  $\mu$ m, X 100.
- 13-16) Radiolaria from box cores 10 and 15:
13. Nasselarian, Anthocyrtidium ophirense, scale bar 50  $\mu$ m, X 330;
  14. Nasselarian, Botryostrobus aquilonaris, scale bar 20  $\mu$ m, X 630;
  15. Smullerian, family Phacodiscidae, scale bar 50  $\mu$ m, X 300;
  16. Smullerian, family Lithelidae, scale bar 20  $\mu$ m, X 430.
- 17) Diatom fragment, perhaps Rhizosolenia, from box core 15, scale bar 100  $\mu$ m, X 140.



beneath the bottom current. The distribution of iron-oxide coatings on the forams is similar to that of N. pachyderma (sinistral). Only 1% of the forams from the box cores in the channel are iron-oxide coated; 22-45% of the forams from the box cores beneath the bottom current have the coating. In the size fraction  $<150\text{ }\mu\text{m}$  forams compose a much smaller percentage of the sample (1-6%).

Benthic forams were found in all the sediment samples. Some observed were Parafissurina sp., Trifarina sp., Planulina wuellerstorfi, and Melonis barleeaanum (Plate 4.3, 7-12). Benthic forams constituted 1-13% of the total number of forams present. The benthic forams of a channel box core (core 6) were dominated by Pleurostomella sp. This same species was not observed in nearby box core 10.

#### Radiolaria

Radiolaria comprise only a few percent of the  $<150\text{ }\mu\text{m}$  and  $>150\text{ }\mu\text{m}$  size fractions for the box cores taken beneath the bottom current (Table 4.6). Within the canyon, radiolaria are relatively more abundant (Plate 4.3, 3-16). Spumellarians were the dominant group of radiolaria found in the sediments. Some nasselarians, but no phaeodarians, were present.

#### Pteropods

No pteropods were found in any of the surface sediment samples examined. However, layers of pteropods have been observed to be common down core in one piston core in the canyon (Sher, 1979).

#### Diatoms

Diatoms are generally absent from the  $>150\text{ }\mu\text{m}$  size fraction. However, 13% of the sample from box core 10 in the channel is composed of diatoms. Diatoms, mostly Rhizosolenia (Plate 4.3, 17), are a few percent of the  $<150\text{ }\mu\text{m}$  size fraction.

#### Dinoflagellates, Fecal Pellets and Unidentified Biogenic Material

Dinoflagellates and fecal pellets were absent from the sediment samples examined (Table 4.6). Unidentified biogenic material was found as only a very minor component of box core 15 (Table 4.6).

#### Volcanic Glass

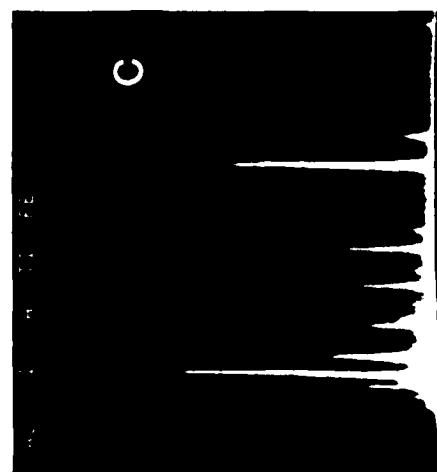
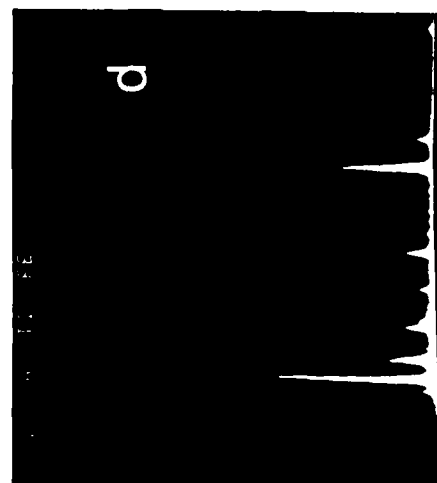
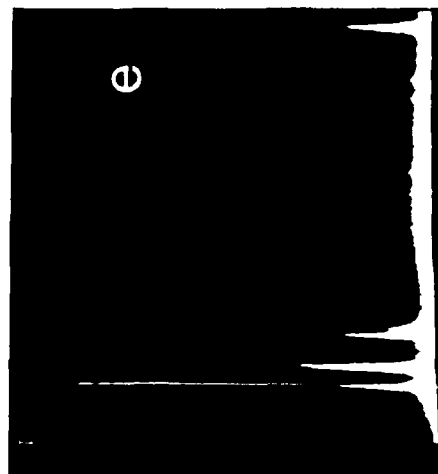
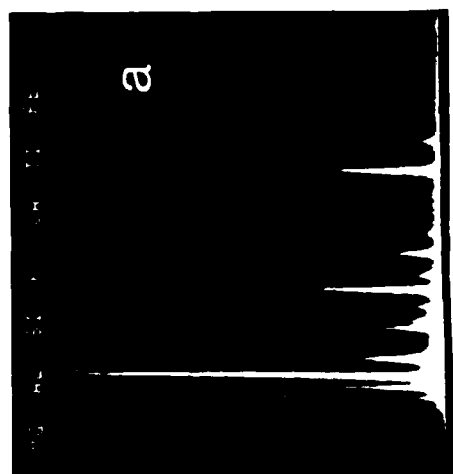
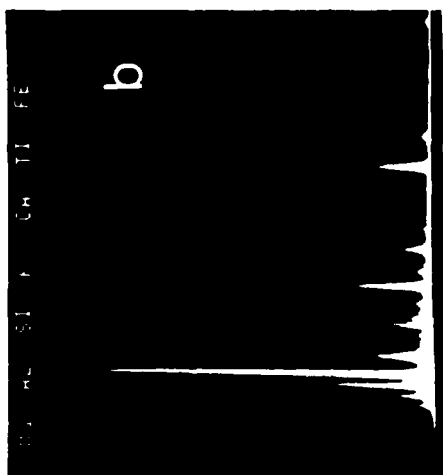
Volcanic glass is the most abundant component of the sediment samples (Plate 4.2, 13, 14; Figure 4.9a,b), comprising from 31-71% by number of the particles counted (Table 4.6). It is more common in the  $<150\text{ }\mu\text{m}$  fraction than the  $>150\text{ }\mu\text{m}$  fraction. Some of the glass shards show surface alteration.

#### Mineral Grains and Aggregates

Mineral grains and aggregates are another principal constituent of the sediment samples (Plate 4.2, 15-17; Figure 4.9c-e). They comprise 3-41% of the samples  $>63\text{ }\mu\text{m}$  (Table 4.6). Most particles counted were single grains. However, in box core 6 from the channel, the majority (87%) of the material  $>150\text{ }\mu\text{m}$  was composed of clay aggregates that were not disaggregated by sonification.



Figure 4.9      Energy dispersive X-ray spectroscopy of surface sediments from box core 5; a) vesicular volcanic shard, see Plate 4.2, 13 for photomicrograph; b) volcanic shard, see Plate 4.2, 14 for photomicrograph; c) mineral grain, see Plate 4.2, 15 for photomicrograph; d) mineral grain with iron-oxide coating, see Plate 4.2, 16 for photomicrograph; e) quartz grain, see Plate 4.2, 17 for photomicrograph.



Combining the categories of volcanic glass and mineral grains and aggregates demonstrates that the majority of the particles preserved at the seafloor are not biogenic. Together these categories comprise from 53 to 85% of the sediment samples.

### MINERALOGY

#### Sediment Traps

Due to the limited amount of material collected by the sediment traps, powder mounts for bulk composition by X-ray diffraction were made only for the surface sediment samples. However, enough material from sediment traps at 10 mab was available to make oriented mounts of the  $<2 \mu\text{m}$  fraction which was filtered onto silver filters. This procedure precludes semiquantitative analysis; only presence or absence of particular minerals can be determined. The principal minerals detected were quartz, feldspar, calcite, and some clays (Figure 4.10). The quartz and feldspar are from volcanic material and mineral grains; the calcite is biogenic. Clays were not well detected due to dilution by the other constituents. Those detected were chlorite, smectites, and illite. Illite was detected only at Mooring 2, in the axis of the bottom current.

#### Surface Sediments

Surface sediments from box cores have the same components as the sediment traps at 10 mab. Semiquantitative analysis was performed by using peak areas on the diffractograms of the minerals present

Figure 4.10 X-ray diffractogram for a sediment trap sample.  
Minerals detected are calcite, quartz, feldspar,  
montmorillonite, chlorite and illite.

X-RAY DIFFRACTOGRAM  
FROM MOORING 2, 1600 m  
TRAP AT 10 mab

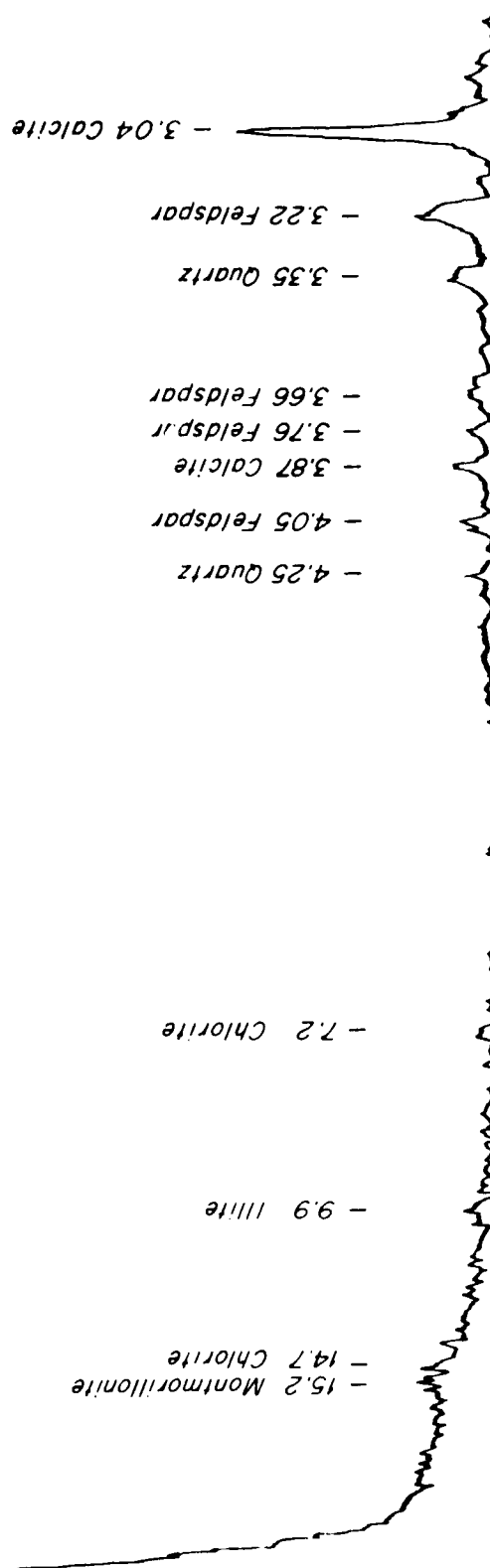


(Table 4.7). Quartz, feldspar, and calcite are the dominant minerals detected (Figure 4.11). Montmorillonite, chlorite, and illite are the clays present. Illite is absent from, or composes a smaller percentage than, montmorillonite or chlorite in the channel box cores (Table 4.7). For the box cores taken beneath the axis of the current, the percentage of illite is greater than or equal to the percentages of montmorillonite or chlorite. This suggests a differentiation of the clay minerals that may be controlled by the bottom current or channel.

#### CARBONATE CONTENT

The carbonate content of the sediment-trap samples decreases from 500 mab to 10 mab and then further to the surface sediments (Figure 4.12). From optical identification of the particles in the trap samples, both forams and pteropods comprise the coarse carbonate fraction. Acidification indicates that carbonate comprises up to 90% of the trap samples at 500 mab. Surface sediments at the mooring sites have values as low as 15%.

Carbonate percentages of the surface sediments vary regionally (Figure 4.13). Low values (9 to 21%) are found for the northern transect box cores and box core 8 atop the channel level, along the southern transect. The box cores within the channel have higher carbonate contents (21-30%). This indicates that the channel may be preferentially retaining or obtaining carbonate material, or the bottom current is preferentially removing it.

Table 4.7

SEMIQUANTITATIVE MINERALOGY OF SURFACE SEDIMENTS\*

Box Core	Calcite	Quartz	Feldspar	Montmor- illonite	Chlorite and Kaolinite	Illite
3	15	9	11	0.8	0.5	0.7
4	12	11	14	8	4	4
6	30	6	12	6	7	3
7	25	4	10	2	1	-
8	30	13	14	3	2	3
9	41	4	10	13	3	-
10	35	6	13	17	6	2
11	25	6	11	11	8	2
12	30	5	15	14	4	-
15	31	6	10	3	1	2

\*Values are recorded as the percentage of the samples composed of each mineral. Peak areas were compared to peak areas of standards to obtain relative percentages.

Figure 4.11 X-ray diffractogram for a box core sample. Minerals detected are quartz, feldspar, calcite, montmorillonite, chlorite and illite.



X-RAY DIFFRACTOGRAM  
BOX CORE 3

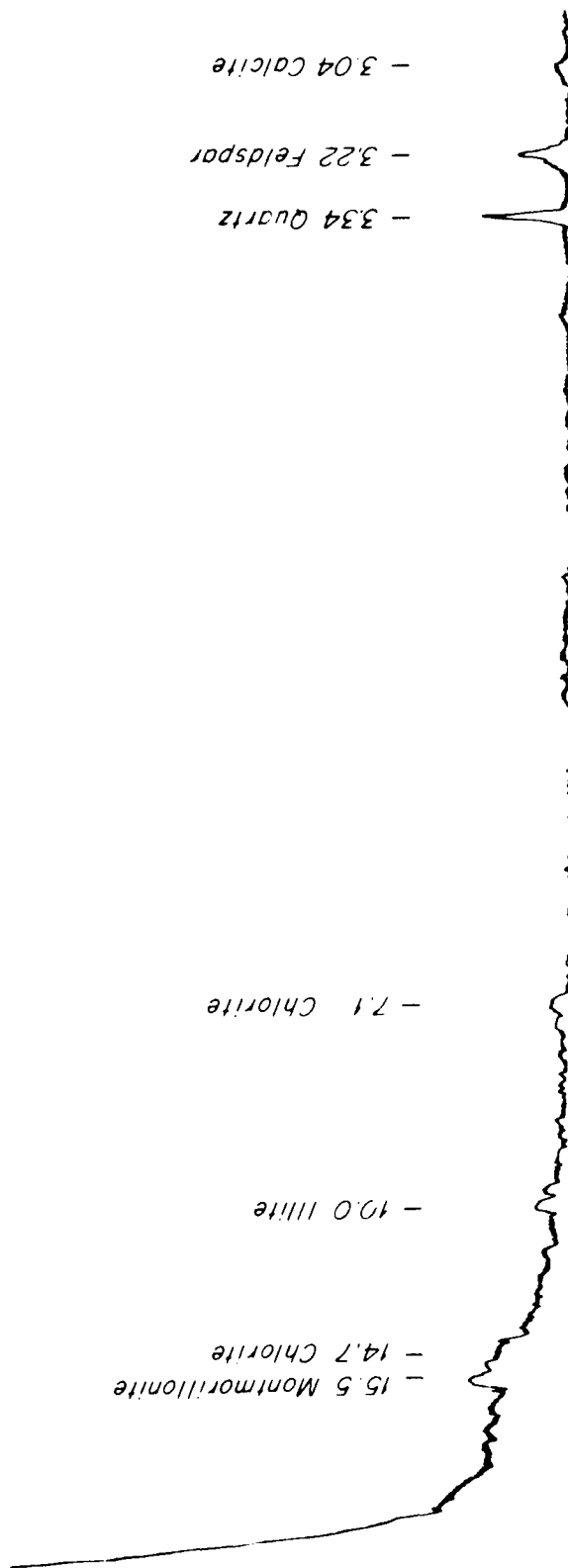


Figure 4.12 Carbonate percentage in sediment trap and box core samples. Percentage of carbonate decreases with depth through the water column to the surface sediments.

CARBONATE PERCENTAGE  
IN SEDIMENT TRAP AND  
BOX CORE SAMPLES

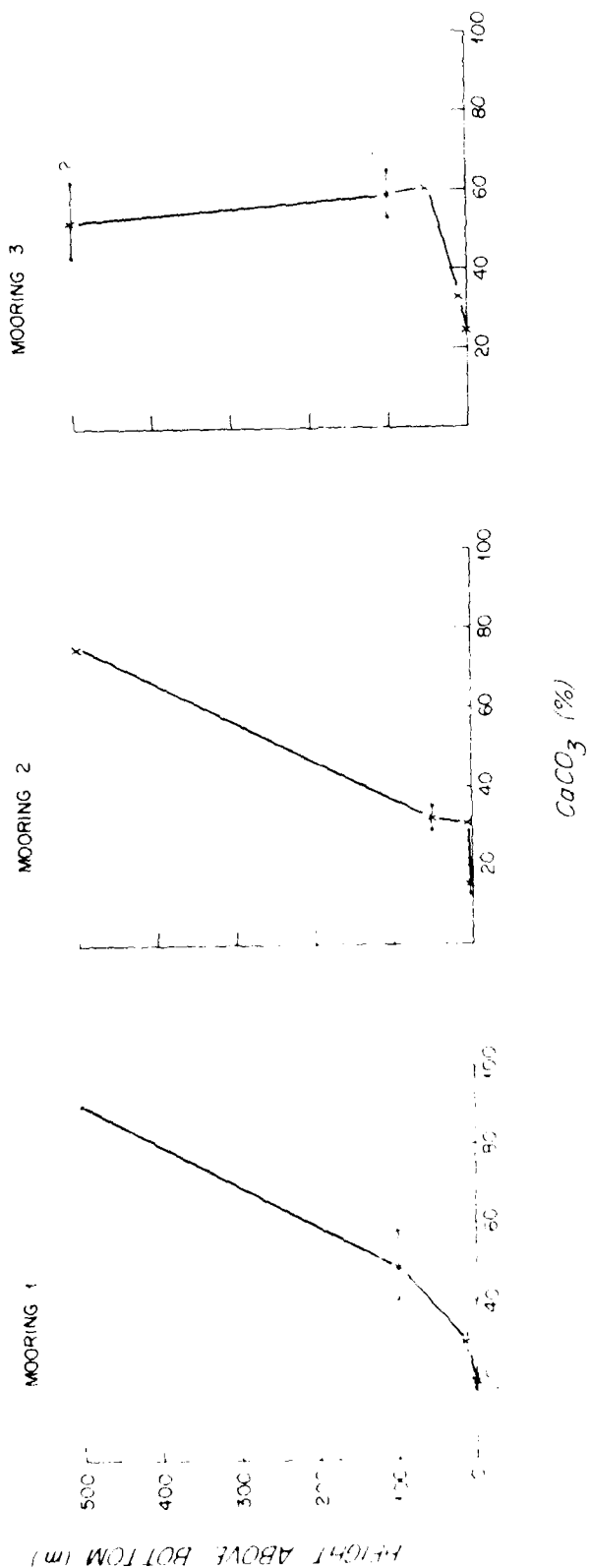


Figure 4.13 Calcium carbonate percentages for box core surface samples. The distribution of carbonate varies throughout the region with higher values in the channel stations.

AD-A092 231

WOODS HOLE OCEANOGRAPHIC INSTITUTION MASS

F/G 8/10

COMPOSITION AND CHARACTERISTICS OF PARTICLES IN THE OCEAN: EVID-ETC(U)

NOV 80 M J RICHARDSON

N00018-79-C-0071

NL

UNCLASSIFIED

WHOI-80-52

3 of 3

4-2

0-9

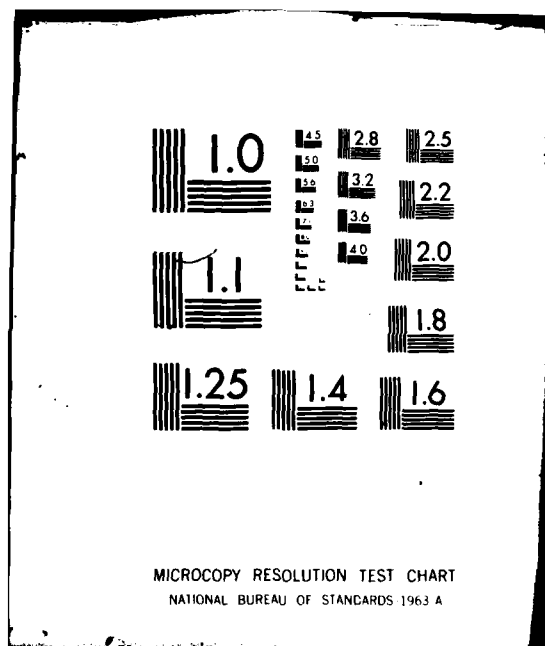
END

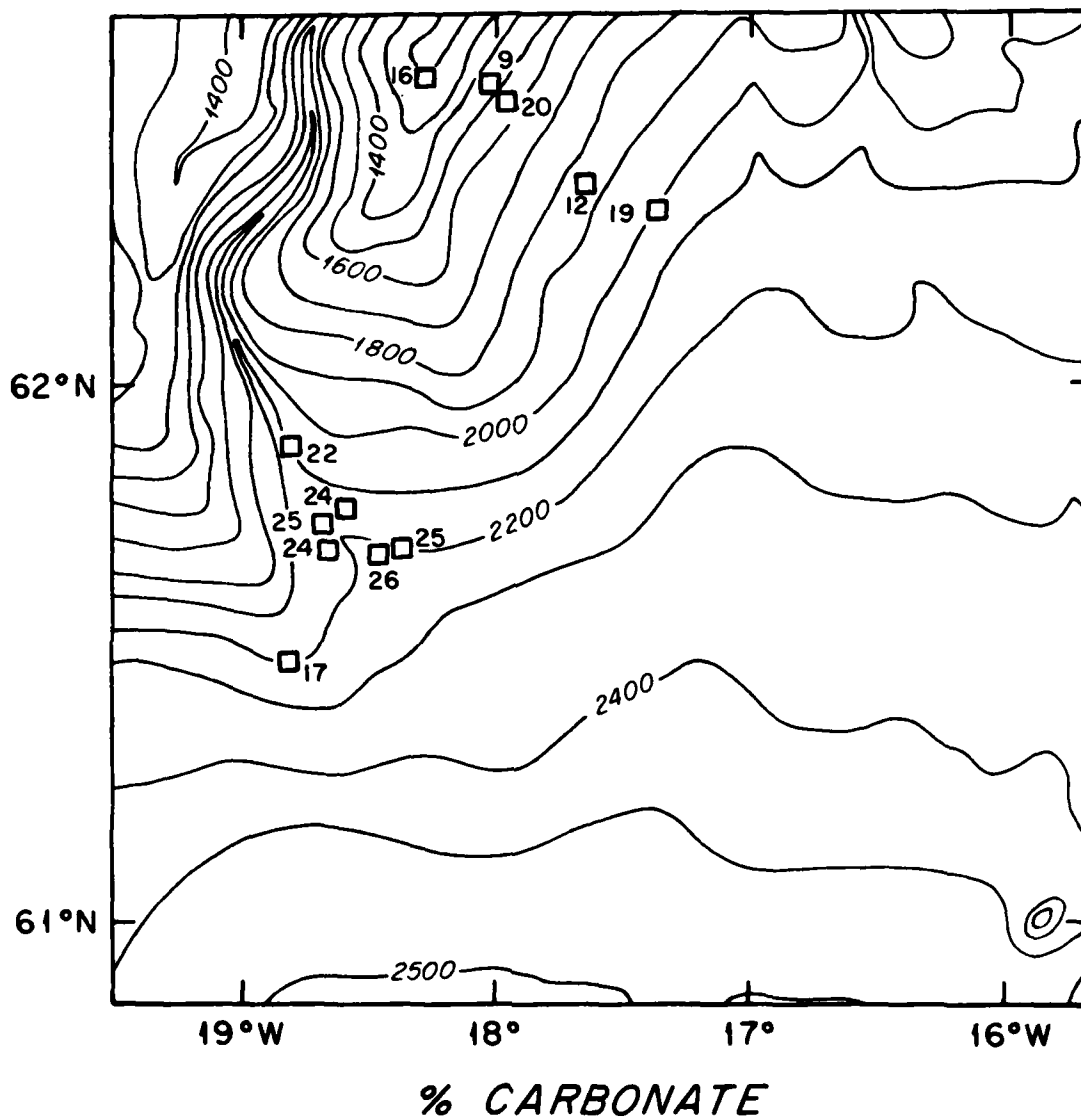
DATE

FILED

1-8

DTIC





#### ORGANIC CARBON AND NITROGEN CONTENTS

As with carbonate percentages, organic-carbon percentages in the sediment-trap samples show a decrease toward the seafloor (Figure 4.14). However, mooring 1, at 2000 m, shows a low organic carbon content at 500 mab, smaller than those values at 100 mab and 50 mab for the same mooring. This low value is anomalous, particularly since this sample has an overwhelming (90%) percentage of carbonate. In this case, organic carbon is unexpectedly not directly associated with biogenic calcium carbonate (Heath *et al.*, 1977). Organic-carbon contents decrease from  $>1.25\%$  for the trap samples at 10 mab to  $<1.25\%$  in the surface sediments.

The regional picture for the content of organic carbon in the surface sediments shows the same trends as for carbonate (Figure 4.15). Box cores from the channel have higher organic carbon content,  $\geq 0.80\%$ . Cores taken along the northern and southern transect strongly influenced by the bottom current, have lower organic carbon contents (0.16-0.50%).

Ratios of organic carbon to nitrogen also vary through the water column (Table 4.8). The moorings along the northern transect have high ratios ( $\geq 7.8$ ), but there are no consistent trends with depth. The sediments beneath these moorings also have high ratios (7.9-9.6). The channel mooring has lower ratios (8.4 and 7.0 at 50 and 10 mab, respectively), and ratios in box core surface sediments range from 6.9 to 7.6 (Table 4.9). These differences are not as distinct as those for the content of organic carbon.



Figure 4.14 Organic carbon percentages in sediment trap and box core samples. Values generally decrease through the water column to the surface sediments.

ORGANIC CARBON PERCENTAGE IN SEDIMENT  
TRAP AND BOX CORE SAMPLES

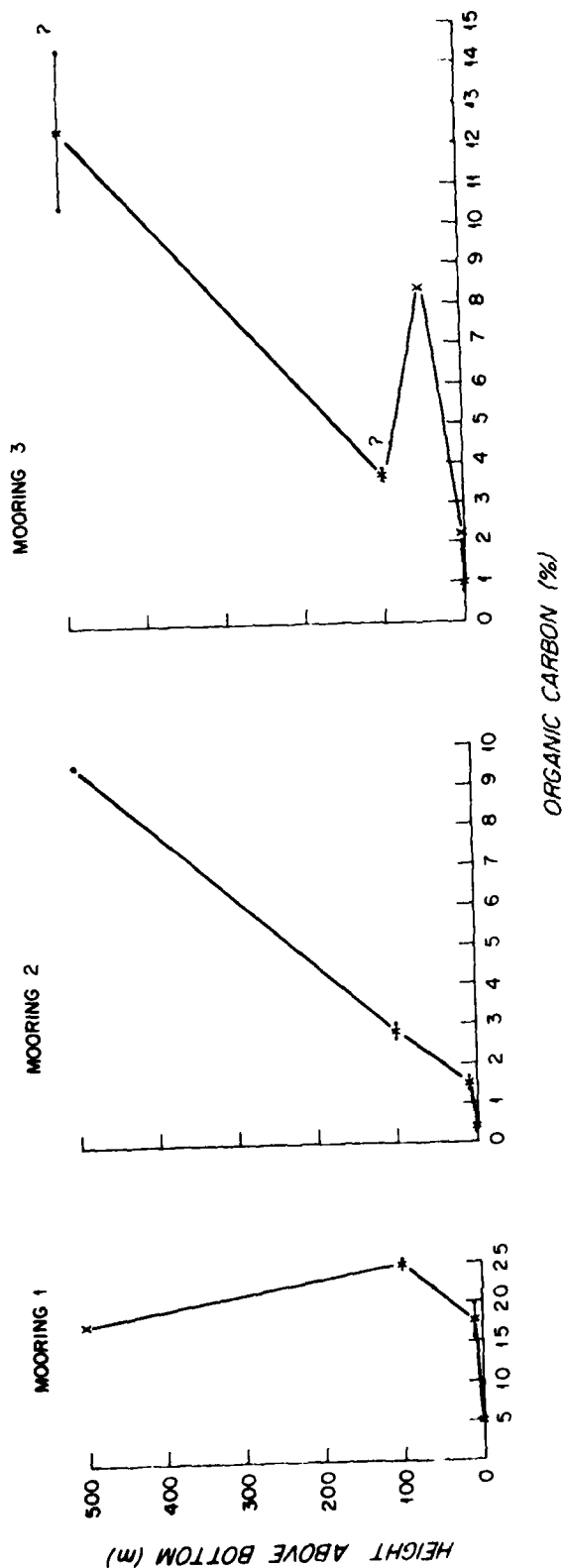
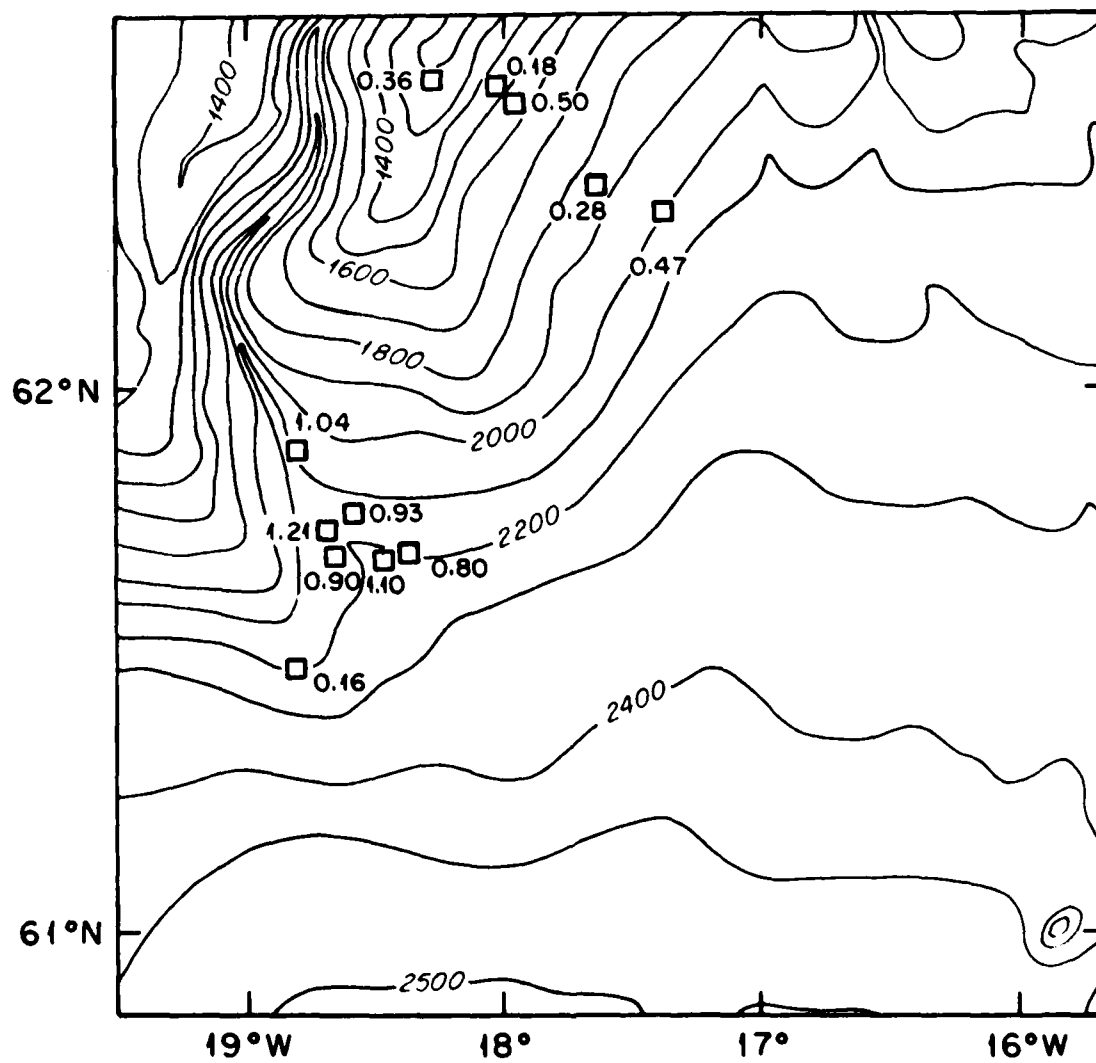


Figure 4.15 Organic carbon percentages for box core surface samples. The distribution of organic carbon varies throughout the region with higher values at the channel stations.



% ORGANIC CARBON

Table 4.8

## CARBONATE, ORGANIC CARBON AND NITROGEN FROM SEDIMENT TRAPS

Mooring	Mab	Split	Filter#	Total Weight (mg)	CaCO <sub>3</sub>	C (μg)	N (μg)	C/N	%CaCO <sub>3</sub>	%OC
1	500	1/128	587	2.83	2.55	49.7	5.5	9.0	90	1.76
1	100	1/64	585	3.25	1.89	78.7	10.0	7.9	58	2.42
1	100	1/64	586	3.50	1.41	87.7	9.0	9.7	40	2.51
1	10	1/256	583	26.03	8.07	532.	46.9	11.3	31	2.04
1	10	1/256	584	24.33	6.31	375.	47.9	7.8	26	1.54
2	500	15/128	552	1.76	1.33	168.	19.9	8.4	76	9.55
2	100	1/8	553	4.44	1.29	135.	14.2	9.5	29	3.04
2	100	15/128	554	4.67	1.63	129.	15.4	8.4	35	2.76
2	10	1/64	557	76.75	22.79	1192.	132.	9.0	29	1.55
2	10	1/64	558	78.42	25.25	1136.	146.	7.8	32	1.45
3	500	1/8	568	1.46	0.63	212.	19.6	10.8	43	14.52
3	500	15/128	569	1.04	0.64	109.	11.8	9.2	62	10.58
3	100	1/16	571	2.20	1.44	79.5	9.9	8.0	65	3.61
3	100	1/16	572	1.96	1.03	75.0	9.3	8.1	53	3.83
3	50	1/16	573	1.33	0.80	112.	13.3	8.4	60	8.42
3	10	1/64	582	25.71	8.43	570.	82.0	7.0	33	2.22

Table 4.9  
CARBONATE, ORGANIC CARBON AND NITROGEN FROM SURFACE SEDIMENTS

Box Core	Filter#	Total Weight (mg)	CaCO <sub>3</sub>	C(μg)	N(μg)	C/N	%CaCO <sub>3</sub>	%C
3	3213	71.79	14.0	360.	37.4	9.6	20	0.50
4	3214	44.03	5.35	125.	16.7	7.5	12	0.28
6	3216	57.82	14.27	697.	99.1	7.0	25	1.21
7	3217	43.19	9.68	449.	64.3	7.0	22	1.04
8	3218	65.64	11.30	108	25.8	4.2	17	0.16
9	3219	44.60	11.06	358.	47.4	7.6	25	0.80
10	3220	77.33	20.46	854.	123.	6.9	26	1.10
11	3221	44.33	10.57	401.	54.3	7.4	24	0.90
12	3222	43.57	10.5	410.	56.3	7.3	24	0.93
13	3223	60.90	9.52	218.	25.1	8.7	16	0.36
14	3224	97.27	8.52	179.	29.0	6.2	9	0.18
15	3226	46.05	8.77	217.	27.4	7.9	19	0.47

A parameter which shows a clear distinction between samples from the channel and those from beneath the bottom current is the ratio of the percentages of organic carbon to calcium carbonate. Cores from the channel have a ratio of  $0.041 \pm 0.006$ ; cores from beneath the bottom current,  $0.022 \pm 0.003$ . These ratios reflect that less organic carbon is found beneath the bottom current than in the channel cores with respect to calcium carbonate. This may be due to greater input or preservation of organic carbon in the channel, or alternatively, increased degradation beneath the bottom current. Another possibility would be that this ratio reflects differences in the sediment grain size or age. The material beneath the current is coarser and older than that in the channel.

#### DISCUSSION

The data obtained here are used to verify local resuspension and transport by the bottom current, assess changes that occur to particulate material in transit through the water column, and estimate the distance of transport of the material collected in the traps.

#### PRESENT-DAY RESUSPENSION OF SEDIMENTS

Four components of the size fraction greater than  $125 \mu\text{m}$ , for the traps at 10 mab, substantiate present-day local resuspension by the bottom current.

Benthic foraminifera (e.g., Parafissurina sp. and Uvigerina sp.) were collected in all the traps at 10 mab in the study area. These forams provide conclusive evidence of active, present-day resuspension. Benthic foraminifera reside on the seafloor, and therefore must have been resuspended from the seafloor into the traps. These forams are larger than 125  $\mu$ m and therefore have high settling velocities, (some >1 cm/sec), which would indicate that they are locally derived. Distance of transport of the trapped material is discussed in a later section.

Another component of the sediment-trap material indicative of active erosion is N. pachyderma (sinistral). The typical Recent subpolar assemblage in this area is composed of N. pachyderma (dextral), G. bulloides, and G. quinqueloba (Ruddiman and McIntyre, 1976). Indeed, these are the predominant foraminiferal species present in the trap samples. However, the single species which defines the polar water and Pleistocene glacial assemblage of this region, N. pachyderma (sinistral) (Ruddiman and McIntyre, 1976), is also present. This suggests that either glacial sediments are presently being eroded or N. pachyderma (sinistral) are being advected from polar regions. Surface sediments in the region contain N. pachyderma (sinistral), so extensive advection does not need to be invoked to explain the data.

A third line of evidence for present-day erosion of material lies in the condition of the planktonic foraminifera in the traps. Planktonic forams secrete their tests in surface waters. Forams



falling directly from the surface are translucent to white, and some still have spines (Bé, 1977). Some forams which have resided on the seafloor develop an iron-oxide staining to their tests and become orange in color. Numerous forams coated with iron oxide were observed in the surface sediments of the region (Table 4.5). Some iron-oxide-coated planktonic forams were observed in the sediment traps at 10 mab (Table 4.5), giving additional evidence of present-day resuspension.

Further evidence for resuspension is the increase in the percentage of volcanic glass and mineral matter collected in the sediment traps with depth (Table 4.4). Percentages of these components in the  $> 250 \mu\text{m}$  size fraction increase from  $< 1-7\%$  at 500 mab to  $15-67\%$  at 10 mab. Surface sediments near the moorings have  $27-87\%$  volcanic glass and mineral matter in the  $> 250 \mu\text{m}$  size fraction (Table 4.6). Dissolution and degradation of biogenic material at the seafloor probably accounts for the percentage differences seen from 500 mab to the surface sediments, while the increase from 500 mab to 10 mab (Table 4.4) is attributed to resuspension of the biogenic-poor surface sediments.

The size fraction of material from  $63-125 \mu\text{m}$  that is caught by the sediment traps is composed primarily of juvenile foraminifera, diatoms, fecal pellets, volcanic glass, and clay aggregates. A few tiny ( $< 125 \mu\text{m}$ ) benthonic forams were also found in this size fraction. These particles can be transported greater distances by the bottom current than those  $> 125 \mu\text{m}$  before they are deposited. In

the traps at 10 mab, the 63-125  $\mu$ m size fraction is dominated by volcanic glass and clay aggregates, but in the upper traps, forams and diatoms are also important.

Some benthic forams were found in the traps at 100 mab in the 63-125  $\mu$ m size fraction. In one case, three benthic forams were found in the trap at 500 mab from Mooring 1. These occurrences suggest that some small resuspended seafloor material is found up to 500 mab.

Resuspended material (benthic foraminifera, iron-oxide-coated planktonic foraminifera, and glacial-assemblage planktonic foraminifera, together with an increase in volcanic glass and mineral matter with depth) has been found in sediment traps located at 10 mab with some found up to 500 mab. These components of the sediment-trap material particularly at 500 mab, may conceivably have come from an upslope source and been transported downslope to the traps. However, the large size and fast settling velocities of the foraminifera and volcanic and mineral grains argues for a local source and local resuspension. An assessment of the distance of transport of the resuspended material is contained in a later section.

#### ADVECTIVE TRANSPORT BY THE BOTTOM CURRENT

The bottom current transports large quantities of material into and out of the study area. A relationship of the potential temperature to suspended particulate matter distributions, the quantity of material transported by the current and its variability

with time, and a comparison of horizontal and vertical fluxes are discussed in this section.

#### Relationship of the Bottom Water to Suspended Particulate Matter

The distribution of suspended particulate matter reflects the influence of the bottom current. A well developed near-bottom nepheloid layer is present throughout most of the region (Figure 3.8). An association between the bottom water and the nepheloid layer is brought out in a compilation of the data on potential temperature and light scattering from the hydrographic stations.

There is a sharp increase in light scattering in water colder than  $3.3^{\circ}\text{C}$  potential temperature (Figure 4.16). A diagram of potential temperature versus salinity shows that water colder than  $3.3^{\circ}\text{C}$  has a large component of Norwegian Sea Deep Water (Figure 4.17). Above  $3.3^{\circ}\text{C}$ , the salinity range increases dramatically due to the introduction of Labrador Sea Water. The  $3.3^{\circ}\text{C}$  boundary is below the reference level used by Shor (1979) in calculating volume transport through this region. His reference level was intended to be a level of no motion. The  $3.3^{\circ}\text{C}$  boundary separates water of Norwegian Sea origin from that having a strong component of Labrador Sea Water and may indicate the boundary of the strong flow of the bottom current. The association of the bottom water with the high light-scattering values suggests that the current carries large quantities of suspended sediment through the region and may locally resuspend material from the seafloor without significant mixing between the current and the surrounding water of the basin.

Figure 4.16 Potential temperature versus light scattering plot. A sharp increase in light scattering is seen below 3.3°C potential temperature indicating an association between high concentrations of suspended matter and the strong bottom current.

ICELAND RISE  
NORTHERN SECTION

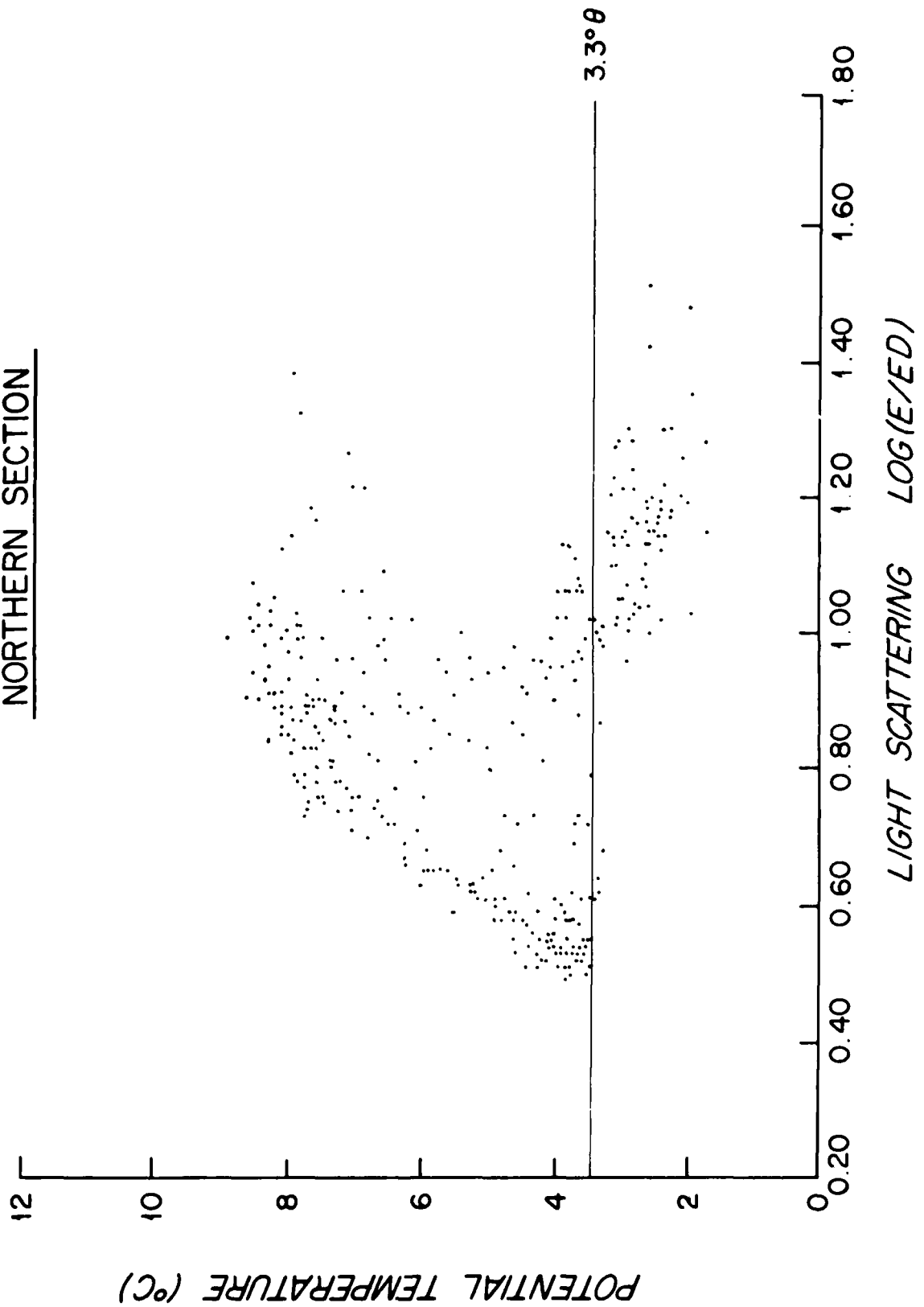
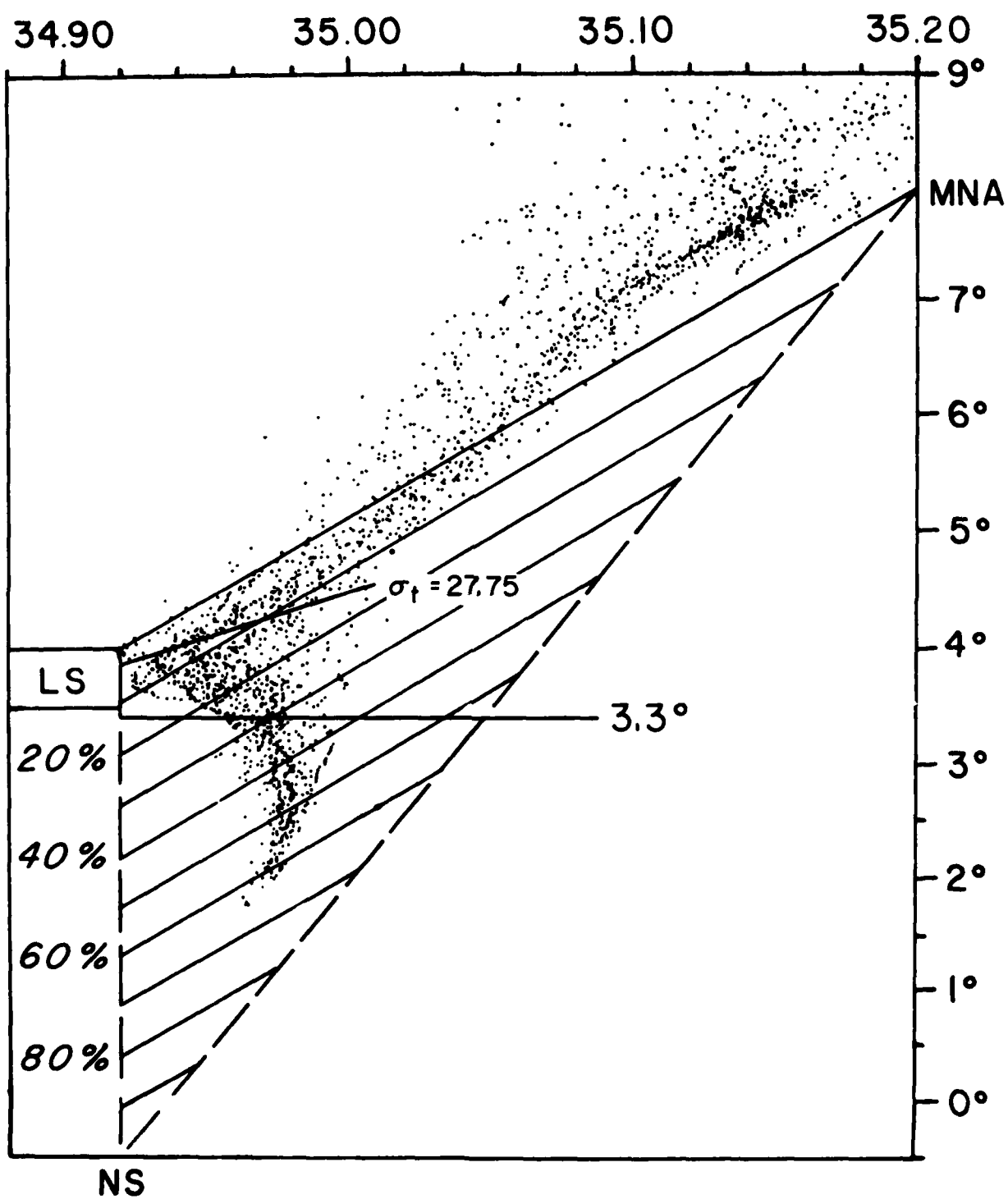


Figure 4.17 Potential temperature versus salinity plot showing the difference between the Shor (1979) reference level and the 3.3°C potential temperature boundary. The latter minimizes the Labrador Sea Water component.



### Quantity and Variability of Advective Transport

Rough estimates of horizontal fluxes of suspended particulate matter can be computed by multiplying current velocities by suspended-matter concentrations. Based on geostrophic calculations of water velocities (Shor, 1979) and suspended-particle concentrations from filtration of water samples, the amount of material advected through the northern transect of stations (Figure 2.2) is on the order of 50-200 kg/sec, using standard concentrations and corrected concentrations, respectively. Shor (1979) estimated the horizontal flux using light-scattering measurements converted to suspended-matter concentrations and obtained 100 kg/sec. These estimates of horizontal flux are subject to a large amount of temporal variability and measurement uncertainty.

A reoccupation of Station 28 at approximately 2000 m was made (Station 84), which provides one estimate of the variability in the geostrophic volume transport of water. Transport across the northern transect of stations using Station 28 yields a flow of  $5.6 \times 10^6 \text{ m}^3/\text{sec}$ ; substitution of Station 84 into the northern section results in transports of  $5.0 \times 10^6 \text{ m}^3/\text{sec}$  (Shor, 1979). The difference in the transport estimates between the nearest stations upslope and downslope of Stations 28 and 84 is  $2.5 \times 10^6$  and  $1.9 \times 10^6 \text{ m}^3/\text{sec}$ . Based on the hydrographic stations a temporal variability of at least 30% should be considered reasonable in estimates of water transport.



Current velocities measured by the current meters are uniform and steady in the axis of the bottom current (Figure 2.5). East of the axis of the current (at approximately 2000 m) flow speed varies by an order of magnitude, from current meter stall speeds  $< 2$  cm/sec to speeds in excess of 20 cm/sec. These measurements were taken on the boundary of the current and probably reflect spatial meandering of the current rather than temporal variability of the bottom current velocity.

Based on the nephelometer lowerings at Stations 28, 40, and 84, net particulate standing crops (Biscaye and Eittreim, 1977) were calculated to be 4075, 1834, and  $1775 \mu\text{g}/\text{cm}^2$  respectively. These values indicate temporal variation in suspended matter by at least a factor of two.

Combining the variations in water transport and in suspended-particle concentrations suggests that during this study, temporal variability of the horizontal flux of suspended particulate matter is approximately a factor of 2.5.

#### HORIZONTAL VERSUS VERTICAL FLUXES

Estimation of the apparent vertical flux of material to the bottom from the surface waters can be made with the sediment traps located at 500 mab. Apparent fluxes measured by the traps are  $\sim 2 \text{ mg}/\text{cm}^2/\text{yr}$ , which together with a density estimate of  $1.5 \text{ g}/\text{cm}^3$  implies a sedimentation rate of 3 cm/1000 yr. This rate is low in comparison to the long-term deposition rates for the

Recent measured in cores in the Iceland Basin,  $>30$  cm/1000 yr (Shor, 1979). The rate measured by traps compares most closely with the sedimentation rate observed beneath the current axis ( $<1-2$  cm/1000 yr), which certainly is not a situation of continuous deposition. Cores from beneath the current have coarse surface sediments, apparently winnowed of fines. If the traps collected an accurate vertical flux of material, as suggested by Gardner (1980), then, additional material must be introduced into the region other than directly from the surface waters, or alternatively, the fluxes were measured for an anomalous period of low surface input. This study was conducted over a short time scale of two weeks during the summer, a period of high biological productivity. Due to melting, the terrestrial input from Iceland would also be greatest during the spring and summer. Therefore, it seems likely that there is additional material input into the region from other than surface waters. The most likely sources for this additional material are turbidity currents or the bottom current. The horizontal flux of material into the region by the bottom current,  $\sim 100$  kg/sec or  $2 \times 10^4$  mg/cm<sup>2</sup>/yr, is three orders of magnitude greater than the sedimentation rate indicated for the Recent in cores, 30 cm/1000 yr or 20 mg/cm<sup>2</sup>/yr, indicating that the bottom current is a likely source of material transported into and deposited in the region, as well as further downstream south of the Iceland Rise. The large quantity of material carried by the current is sufficient to make up the deficit indicated by the sediment trap as well being a likely source of material for the Gardar sediment drift downstream.

#### ESTIMATES OF THE QUANTITY OF RESUSPENDED MATERIAL

Estimates can be made of the resuspended fraction in the trap samples based on the quantities and percentages of mass, calcium carbonate, and organic carbon. Gardner (1977a) estimated the resuspended component by assuming that the samples at 500 mab are composed entirely of primary material with no resuspended fraction. For the traps below 500 mab, the amount of resuspended material is the quantity of material greater than that collected at 500 mab, i.e.,

$$\% \text{ Resuspended} = \frac{M_{10} - M_{500}}{M_{10}}$$

where M = quantity of material collected by the traps and the subscripts represent heights above the seafloor. Using his method and assumptions, an average of 59%  $\pm$  6% of the material caught at 100 mab has a seafloor source (Table 4.10). At 10 mab 98-99% of the material is estimated to be resuspended (Table 4.10).

By assuming that the material in the traps at 100, 50, and 10 mab is a simple mixture of primary material of the composition caught at 500 mab and the surface sediments as obtained with box cores, calculations of the percentage of the resuspended component can be made, e.g.,

$$F \times \% \text{trap}_{500} + (1-F) \times \% \text{core} = \% \text{trap}_{10 \text{ or } 100}$$

where F = fraction of primary material and 1-F = fraction of resuspended material. Calculations are made only for Moorings 1 and 2, since the 500 mab sample at Mooring 3 returned open.

Table 4.10  
CALCULATED PERCENTAGE OF RESUSPENDED MATERIAL  
FROM MASS, CARBONATE AND ORGANIC CARBON

Mooring	Mass (mg)	% Resusp.	% CaCO <sub>3</sub>	% Resusp.	% OC	% Resusp.
1	500	68.0	90	0	1.51+0.36	0
1	100	147.6	49+13	54	2.47+0.06	0
1	10	3867.	28+4	98	1.79+0.35	0
Core 15			20+1		0.91+0.62	
2	500	15.9	56+28	0	9.55	0
2	100	36.4	32+4	56	2.93+0.23	72
2	10	4072.	30+2	99	1.50+0.07	87
Core 3			16+4		0.35+0.13	

These calculations lead to the estimate of 59% for the resuspended fraction at 100 mab. For 10 mab the value of the resuspended fraction is  $77\% \pm 17\%$ . Comparing these percentages with those from the mass-flux calculations shows that the estimates of the percentage of resuspended material at 10 mab based on %  $\text{CaCO}_3$  are low with respect to the estimates based on mass flux, that is, there is more carbonate at 10 mab than predicted from mass-flux calculations.

Similar calculations using organic carbon show that the percentage of resuspended material at 100 mab for organic carbon is  $74\% \pm 3\%$ . At 10 mab, the resuspended fraction is estimated to be  $88\% \pm 1\%$ . A comparison with the mass-flux calculations indicates that there is more resuspended material at 100 mab and less at 10 mab.

An explanation for the differences in the estimates of resuspended material using mass, calcium carbonate, and organic carbon may be due to the simplicity of the assumptions. Dissolution, degradation, and preferential resuspension have been ignored in the assumptions of the mixing scheme; however, these processes must be occurring or there would be no differences noted between the primary material and the surface sediments. Also, the material at 500 mab may not be all primary, but may contain some resuspended material as well.

From the calculations made, there is no significant difference in the calculated percentage of resuspended material at 100 mab

based on  $\text{CaCO}_3$  and mass (Table 4.1). However, there is more carbonate based on  $\text{CaCO}_3$  calculations than is predicted by mass calculations at 10 mab. The primary process that would affect the calcium carbonate content is dissolution. However, due to the shallow depths of the study region, the water column is saturated with respect to calcite (Takahashi, 1975; Broecker and Takahashi, 1978), so dissolution of forams and coccoliths is unlikely. However, in the sediments where organic carbon decomposes to liberate  $\text{CO}_2$ , local dissolution may occur. Pteropods are composed of aragonite. Individual specimens, but mostly fragments were found in the traps at 10 mab, and not in the sediments. Perhaps the greater quantity of carbonate at 10 mab is due to aragonite dissolution at the seafloor. An alternative and perhaps more plausible explanation is that carbonate may be preferentially resuspended into the sediment traps at 10 mab.

Differences in the percentage of resuspended material at 100 mab based on organic-carbon and mass-flux calculations indicate that there is less organic carbon in the trap than would be expected from the mass calculations. This phenomenon may be due to degradation and consumption of organic matter in the water column or trap, a factor ignored in the original assumptions. There is more organic carbon in the trap at 10 mab than is predicted by mass-flux calculations. This may be due to increased degradation and consumption between 10 mab and the seafloor, or preferential resuspension. The general trend of more carbonate and organic

carbon at 10 mab than predicted by mass-flux calculations suggests that carbonate and organic carbon being less dense components of the sediments, may be preferentially resuspended.

#### DISSOLUTION AND DEGRADATION AT THE SEAFLOOR

Profiles of the percentage of calcium carbonate and organic carbon from sediment-trap samples and box core surface sediments generally show a decrease in these components with increasing water depth (Figures 4.12, 4.14). From these figures, it is seen that the percentages of carbonate and organic carbon decrease downward through the water column, with the sharpest decrease from 10 mab to the seafloor. This decrease is on the order of 50% for carbonate and 70% for organic carbon. One possible explanation for this decrease in the lowermost 10 m is additional detrital material from the seafloor enters the system diluting the carbonate. A second hypothesis, and perhaps more plausible, is that present-day conditions are reflected in the water column, but the surface sediments are subject to dissolution and degradation for much longer periods of time than the material in transit through the water column, i.e., material in the water column does dissolve and decompose, but most of the loss occurs at the sediment-water interface. This latter concept is supported by the visual investigation of the trap and surface sediment samples and is in agreement with other investigators (Adelseck and Berger, 1975; Berner, 1977; Takahashi and Broecker, 1977; Honjo, 1977). For

example, aragonitic tests are absent from the surface sediments and organic material is not visually identifiable.

#### REGIONAL PATTERNS OF SURFACE SEDIMENTS

Distinct regional differences in the surface sediments are seen in the clay mineralogy and in the content of carbonate and organic carbon. Semi-quantitative X-ray diffraction shows that there are relatively higher proportions of illite in the clays present beneath the bottom current than in the channel (Table 4.7). Illite is formed from weathering of ancient continental rocks (Biscaye, 1965). The higher percentage of illite in the sediments beneath the bottom current may reflect extensive advection by the bottom current from weathered continental rocks, the nearest source being Rockall Plateau, ~500 km. Although Rockall Plateau is southeast of the study area, it is upstream along the current path.

Carbonate and organic carbon are both more abundant in the cores in the channel than in the cores beneath the bottom current (Figures 4.13 and 4.15). These components are also more abundant in the trap sample at 10 mab in the channel (Figures 4.12 and 4.14) than in the other traps. This may reflect a turbidity current component in the channel cores or the influence of the bottom current eroding and/or not depositing Recent sediments and exposing older glacial deposits. Glacial sediments have lower carbonate percentages, and probably less organic carbon (due to the longer period of time available for decomposition and consumption of the organic matter



present). In addition, the cores taken beneath the current have glacial-assemblage forams in the surface samples, suggesting that glacial sediments are exposed.

#### DISTANCE OF TRANSPORT

Specific components of the sediment trap samples are useful in estimating the distance of transport of the resuspended trapped material. Iron-oxide coated planktonic foraminifera, benthic foraminifera, the glacial assemblage foram N. pachyderma (sinistral), and some of the large (>250  $\mu\text{m}$ ) volcanic fragments and mineral grains found in the traps have a seafloor source. Eighteen particles from the trap at 10 mab at Mooring 2 were selected for a settling experiment to determine the particle fall velocities. Eight planktonic forams (four with iron-oxide coatings), three benthic forams, one pteropod and six volcanic shards and mineral grains, most specimens having a diameter of 300  $\mu\text{m}$ , were settled in filtered fresh water at 20°C in a one liter cylinder with a 6.2 cm diameter. A 20 cm vertical distance was used for determining fall velocities. Particles were submerged in water in a small flask, which was subsequently evacuated to remove any air contained in the specimens. The particles were transferred to the settling cylinder by means of a large pipette. Particles were settled three times to determine repeatability of the fall velocities as a means of determining whether air was successfully removed from the samples. A correction to take into account the difference in viscosity

between 20°C fresh water and 5°C seawater decreases the velocities to 63% of the measured values. The results of the experiment are given in Table 4.11.

Planktonic forams fell most slowly, averaging 0.65 cm/sec. Iron-oxide coated forams fell at 0.94 cm/sec and volcanic glass and mineral grains fall at 1.21 cm/sec. The orange iron-oxide coated forams fall from 1.06-1.76 times faster than the white forams. The maximum fall velocity was 1.75 cm/sec for a mineral grain with 185 and 300  $\mu$ m axes; the minimum was 0.52 cm/sec for a 1.5 mm long pteropod. From these results, it is found that resuspended material is likely to have a higher fall velocity than material settling from the surface waters. Another result of this study is that larger particles do not necessarily fall more rapidly than small ones. In particular, the smaller (250  $\mu$ m) N. pachyderma (dextral) fell 1.14 times more rapidly than a larger (300  $\mu$ m) foram of the same species and the largest specimen, the pteropod, had the slowest fall velocity. This may be due to both greater drag and lower density of the larger specimens.

A comparison of the experimentally determined fall velocities to Stokes law show deviations for these large particles. Stokes law applies only up to Reynolds numbers of 1. These particles settled have Reynolds numbers ranging from 3-6. Stokes law,

$$W = \frac{2\Delta\rho gr^2}{9\mu}$$

would predict a fall velocity of 7.3 cm/sec for a 300  $\mu$ m particle with a density difference of 1.5. With a  $\Delta\rho$  of 0.5, the fall

Table 4.11

PARTICLE FALL VELOCITIES FROM MOORING 2, TRAP 10 mab

Particle	Diameter ( m)		Settling Velocity* cm/sec
	Max.	Min.	
Pteropod	1500	750	0.52±0.03
<u>N. pachyderma</u> (dextral) - white	250	175	0.69±0.04
<u>N. pachyderma</u> (dextral) - white	300	200	0.60±0.01
<u>G. bulloides</u> - white	300	200	0.68±0.08
<u>N. pachyderma</u> (sinistral) - white	300	225	0.69±0.04
<u>N. pachyderma</u> (dextral) - orange**	300	188	0.69±0.06
<u>G. bulloides</u> - orange** (light iron-oxide coating)	300	200	0.72±0.03
<u>G. bulloides</u> - orange**	300	238	1.19±0.07
<u>N. pachyderma</u> (sinistral) - orange**	300	225	1.16±0.06
Benthic Foram	688	175	0.73±0.04
Benthic Foram	562	350	1.52±0.04
Benthic Foram	300	212	0.67±0.08
Mineral grain	300	188	1.75±0.05
Mineral grain	300	288	1.34±0.03
Mineral grain	500	362	1.68±0.03
Volcanic shard	300	188	0.97±0.01
Vesicular volcanic shard	300	162	1.17±0.01
Vesicular volcanic shard	300	88	0.84±0.04

\* Fall velocities were measured in 20°C fresh water. A viscosity correction was made to yield the fall velocity in 5°C seawater of 35%, given here.

\*\*iron-oxide coated.

velocity would be 2.4 cm/sec. These values are higher than those measured for particles with a 300  $\mu$ m diameter. Density differences of  $\sim$ 0.2, 0.3, 0.3 and 0.4 would be necessary for the white planktonic forams, iron-oxide coated forams, and volcanic shards and mineral grains respectively for Stokes law to apply. The deviations from Stokes law may be due to the use of a maximum diameter in the equation and to the non-spheroidal shapes of the particles. Using the smaller diameters, calculated density differences of  $\sim$ 0.5, 0.7, 0.8 and 1.5 for the same particles as above are found to be more reasonable.

By knowing the fall velocities of some of the material in the trap, the horizontal distance of transport can be estimated. Assuming that the particles are mixed vertically to the top of the isothermal mixed layer, how far could they travel horizontally in the bottom current and be caught in the traps at 10 mab? Mixed layers along the northern transect are 30-50 m thick. Fall velocities range from 0.60-1.75 cm/sec. Assuming particles are mixed no higher than the top of the mixed layer, particles would fall 40 m (from the top of the mixed layer to the traps at 10 mab) in  $2.3 \times 10^3 - 6.7 \times 10^3$  sec. Along the 1800 m isobath (the location of the mooring), in an average current of 20 cm/sec, the distance of transport would be 0.5-1.3 km.

This study was conducted along a ridge flank and in close proximity to Iceland and the Iceland-Faroe Ridge. Is it possible that the material caught in the traps is derived from these

topographic highs? Two hundred meters up the ridge flank is 13.2 km away. Particles would fall a 200 m vertical distance in  $1.1 \times 10^4$  to  $3.3 \times 10^4$  sec. The horizontal current required to transport the particles to the trap before falling to the seafloor is calculated to be 40-116 cm/sec. These velocities are in excess of those found even for the bottom current. Since the direction of transport from upslope is virtually orthogonal to the bottom current, this area as an immediate source is unlikely.

The crest of the East Katla Ridge is 32.4 km upslope. The vertical relief change is 600 m. By similar calculations to those above, the horizontal current velocities to transport the particles from the ridge crest to the traps in one resuspension-deposition cycle, would be 32-94 cm/sec, which as a cross-current is also unlikely.

The shelf of Iceland is 110 km north of the sediment trap mooring. Calculations reveal that a horizontal velocity averaging 40-120 cm/sec would be needed to resuspend material on the shelf and transport it to the traps in one resuspension-deposition cycle. These high currents are also unlikely.

The Iceland-Faroe Ridge is 250 km upstream from the traps. Velocities of 100-292 cm/sec would be required to transport the resuspended material from the ridge to the traps. Although high velocities of the overflow water may occur at other times, the measurements taken during this study do not even approach that range. The largest size particles that could be transported from

the Iceland-Faroe Ridge assuming a constant horizontal velocity of 20 cm/sec (comparable to that measured during this study) are ones with maximum diameters of 100  $\mu\text{m}$  for mineral grains and 140  $\mu\text{m}$  for planktonic forams.

Particles smaller than 100  $\mu\text{m}$  may be transported from the topographic highs as well as being resuspended locally. The high concentrations of SPM and high light-scattering values in mid-water suggest that for the small particles (< 20  $\mu\text{m}$ ) are carried quasi-conservatively by the water masses.

The above calculations indicate that virtually all the trapped coarse material > 125  $\mu\text{m}$  which comprises 21-34% of the trap samples is locally (few kilometers) derived resuspended sediment.

#### CONCLUSIONS

- 1) Bottom currents cause local resuspension of material in the region south of Iceland.
- 2) Resuspension is shown by the presence of benthic, glacial assemblage, and iron-oxide coated forams caught at 10 mab and in some cases 100 and 500 mab in the sediment traps.
- 3) The maximum primary flux of material from the surface was measured to be far less than the Recent sedimentation rate, indicating substantial transport of material into the region by the bottom current.
- 4) The observed axis of the deep current system off Iceland (1400-1800 m) overlies coarse sediments, suggesting that the current

has been causing preferential erosion, and/or winnowing, of fine material and removal from the region.

5) The large flux of suspended material in the bottom current (approximately 100 kg/sec) may be responsible for the formation of the Gardar sediment drift to the southwest of the region.

6) Regional differences of clay mineralogy in the surface sediments suggest that the bottom current transports material from continental source rocks which are at least 500 km away, up current.

7) Regional differences in contents of organic carbon and carbonate in the box cores reflect preferential preservation in the cores from the channel versus those beneath the bottom current, or alternatively, preferential decomposition, dissolution, and/or erosion in the cores beneath the bottom current.

8) Presence of aragonitic tests and fragments in the traps at 10 mab but not in the surface sediments, is evidence of dissolution or mechanical destruction of this material at the seafloor and not in the water column.

9) Calculations for determining the distance of transport of the coarse, trapped material indicate that the greater than 125  $\mu\text{m}$  size fraction, which comprises 21-34% of the trap samples, is locally (few kilometers) derived resuspended sediment.

## CHAPTER V

### SUMMARY AND CONCLUSIONS

Strong evidence for the transport and redistribution of large volumes of deep-sea sediment over geologic time is the presence of massive sediment drifts in the northern North Atlantic. As demonstrated in this thesis, resuspension and redistribution of deep-sea sediments also occurs in the present day on time scales of days to weeks. Two approaches were used to investigate present-day resuspension: 1) clear-water and nepheloid-layer suspended particulate matter was examined to determine the differences between the particles, and to determine the possible influence of resuspended material, and 2) the composition of particles obtained with sediment traps located from 500 mab to 10 mab was compared with the surface sediments below.

The conclusions of the SPM clear-water and nepheloid-layer studies are:

- 1) A correlation between light scattering and concentration of suspended particulate matter in the Iceland Rise area using the L-DGO nephelometer, demonstrates that there are differences between particles in clear water and the nepheloid layer. Clear-water samples show larger variations in concentration for a given change in light scattering when compared with nepheloid-layer samples. When the Iceland Rise regression equations for light scattering versus concentration of suspended particulate matter are compared to



those of Biscaye and Eitrem (1974; 1977) on the Blake-Bahama Outer Ridge, Hattaras Abyssal Plain and Lower Continental Rise, distinct differences are observed. These studies indicate that correlations of light scattering to concentration of suspended matter vary both regionally and between clear water and the nepheloid layer.

However, in predicting concentrations from light scattering, the correlations determined here are indistinguishable from those of Biscaye and Eitrem. The 95% confidence limits for prediction of a future observation in the Iceland Rise area encompasses the Biscaye and Eitrem curves for  $\log E/E_D$  values in excess of 0.5.

2) Particle size distributions of suspended particulate matter show differences between clear-water and nepheloid-layer samples. Clear-water samples have roughly equal volumes of material in logarithmically increasing size grades between 1 and 20  $\mu\text{m}$ . Nepheloid-layer samples have lower variance distributions. These differences are also reflected in the normalized differential volume curves which show two-slope distributions being characteristic of nepheloid layer samples, a feature previously observed only in surface waters. The two-slope distribution is interpreted in this study as being due to resuspension of material from the seafloor.

3) Differences in apparent density between suspended matter from clear-water and nepheloid-layer samples are noted in the western North Atlantic, but not in the Iceland Rise area. Compositional differences between clear-water and nepheloid-layer particles in the western North Atlantic are more extreme than in the Iceland Rise

area, and are regarded as a probable explanation of the differences in apparent density. Apparent densities of nepheloid-layer samples in the western North Atlantic study are greater than for clear-water samples. The greater apparent densities correspond with large increases in clays and mineral matter and a decrease in organic matter between clear-water and nepheloid-layer samples.

4) Differences in the principal components of the suspended particulate matter between clear-water and nepheloid-layer samples are primarily an increase in clays and mineral matter and a decrease in coccoliths. For the Iceland Rise study, this is interpreted as being due to resuspension of material from the seafloor. In the western North Atlantic, the decrease in coccoliths is due to dissolution of carbonate at the seafloor and subsequent resuspension of carbonate-poor sediments.

An examination and comparison of the sediment trap and surface sediment samples support resuspension and redistribution of material continuing in the present day. Conclusions are:

1) Coarse sediments underlie the bottom current axis from 1400 to 1800 m along the northern transect of stations with more fine-grained sediment on either side of the axis suggesting winnowing and preferential erosion in the current axis.

2) Surface sediments beneath the current axis contain an assemblage of planktonic foraminifera representative of glacial subpolar, or present-day polar conditions. The presence of these forams is indicative of erosion or extensive advective transport.

3) Regional variations in clay mineralogy, organic carbon and carbonate contents indicate preferential preservation in cores from the channel or preferential decomposition, dissolution and/or erosion of the surface sediments beneath the bottom current.

4) A large horizontal flux of suspended material ( $\sim 100$  kg/sec) is transported across the northern transect of stations. The vertical flux of sediment calculated from sediment traps located at 500 mab was an order of magnitude less than Recent sediment accumulation rates. This suggests that a large fraction of the sediments in the region are brought into the area via the bottom current or turbidity currents from Iceland. The large horizontal flux of sediment may also contribute to the formation of Gardar sediment drift to the southwest.

5) An increase of greater than two orders of magnitude in material collected between 500 mab and 10 mab is indicative of present day resuspension and advection by the bottom current.

6) Resuspension of sediments is substantiated by the collection of particles whose source is clearly the seafloor in sediment traps located at 10, 100 and 500 mab. These resuspended components include benthic foraminifera, iron-oxide coated planktonic foraminifera, and the glacial, subpolar assemblage planktonic foraminifera (N. pachyderma (sinistral)).

7) The rapid settling velocity of the coarse ( $>125\ \mu\text{m}$ ), resuspended components indicate that they are locally derived (few kilometers) rather than horizontally advected from topographic highs. However, the smaller size fractions ( $<125\ \mu\text{m}$ ) may be transported from topographic highs as well as being locally resuspended.

# REFERENCES

- Adelseck, C.G. and W.H. Berger (1975). On the dissolution of planktonic foraminifera and associated microfossils during settling and on the sea floor. In: W.V. Sliter, A.W.H. Be and W.H. Berger (eds.), Dissolution of Deep-Sea Carbonates. Cushman Foundation Foram. Research Special Publication No. 13, pp. 70-81.
- Armi, L. (1978). Some evidence for boundary mixing in the deep ocean. Journal of Geophysical Research 83: 1971-1979.
- Bader, H. (1970). The hyperbolic distribution of particle sizes. Journal of Geophysical Research 75: 2822-2830.
- Baker, E.T., R.A. Feely and K. Takahashi (1979). Chemical composition, size distribution and particle morphology of suspended particulate matter at DOMES sites A, B, and C: Relationships with local sediment composition. In: J.L. Bischoff and D.Z. Piper (eds.), Marine Geology and Oceanography of the Pacific Manganese Nodule Province. Plenum, New York, pp. 163-201.
- Baker, E.T., R.W. Sternberg and D.A. McManus (1974). Continuous light-scattering profiles and suspended matter over Nitinat deep sea fan. In: R.J. Gibbs (ed.), Suspended Solids in Water. Plenum, New York, pp. 155-172.
- Bartz, R., J.R.V. Zaneveld and H. Pak (1978). A transmissometer for profiling and moored observations in water. SPIE Vol. 160, Ocean Optics V: 102-108.
- Bé, A.W.H. (1977). An ecological, zoogeographic and taxonomic review of Recent planktonic foraminifera. In: A.T.S. Ramsay (ed.), Oceanic Micropaleontology. Academic Press, London, vol. 1, pp. 1-100.
- Beardsley, G.F., H. Pak, K. Carder and B. Lundgren (1970). Light scattering and suspended particles in the eastern Equatorial Pacific Ocean. Journal of Geophysical Research 75: 2837-2845.
- Berggren, W.A. and C.D. Hollister (1977). Plate tectonics and paleocirculation - commotion in the ocean. Tectonophysics 38: 11-48.
- Berner, R.A. (1977). Sedimentation and dissolution of pteropods in the ocean. In: N.R. Anderson and A. Malahoff (eds.), The Fate of Fossil Fuel CO<sub>2</sub> in the Oceans. Plenum, New York, pp. 243-260.

- Betzer, P.R. and M.E.Q. Pilson (1971). Particulate iron and the nepheloid layer in the western North Atlantic, Caribbean and Gulf of Mexico. Deep-Sea Research 18: 753-761.
- Biscaye, P.E. (1965). Mineralogy and sedimentation of Recent deep-sea clay in the Atlantic Ocean and adjacent seas and oceans. Geological Society of America Bulletin 76: 803-832.
- Biscaye, P.E. and S.L. Eittreim (1974). Variations in benthic boundary layer phenomena; nepheloid layers in the North American Basin. In: R. Gibbs (ed.), Suspended Solids in Water. Plenum, New York, pp. 227-260.
- Biscaye, P.E. and S.L. Eittreim (1977). Suspended particulate loads and transports in the nepheloid layer of the abyssal Atlantic Ocean. Marine Geology 23: 155-172.
- Bishop, J.K.B. (1977). The chemistry, biology and vertical flux of oceanic particulate matter. Ph.D. Thesis, M.I.T./W.H.O.I. Joint Program in Oceanography, 292 pp. (unpublished manuscript).
- Bishop, J.K.B., J.M. Edmond, D.R. Ketten, M.P. Bacon and W.B. Silker (1977). The chemistry, biology, and vertical flux of particulate matter from the upper 400 m of the equatorial Atlantic Ocean. Deep-Sea Research 24: 511-548.
- Bouma, A.H. (1969). Methods for the Study of Sedimentary Structures. John Wiley and Sons, New York, 458 pp.
- Bouma, A.H. and T.K. Treadwell (1975). Deep-sea dune-like features. Marine Geology 19: M53-M59.
- Brewer, P.G., D.W. Spencer, P.E. Biscaye, A. Hanley, P.L. Sachs, C.L. Smith, S. Kadar and J. Fredericks (1976). The distribution of particulate matter in the Atlantic Ocean. Earth and Planetary Science Letters 32: 393-403.
- Broecker, W.S. and T. Takahashi (1978). The relationship between lysodine depth and in situ carbonate ion concentration. Deep-Sea Research 25: 65-95.
- Brun-Cottan, J.-C. (1971). Étude de la granulometrie des particules marines mesures effectuees avec un compteur Coulter. Cahiers Oceanographiques 23: 193-205.
- Brun-Cottan, J.-C. (1976). Stokes settling and dissolution role model for marine particles as a function of size distribution. Journal of Geophysical Research 81: 1601-1606.

- Burckle, L.H. and P.E. Biscaye (1971). Sediment transport by Antarctic Bottom Water through the eastern Rio Grande Rise. Geological Society of America Abstracts with Programs 3: 518-519.
- Carder, K.L., G.F. Beardsley, Jr. and H. Pak (1971). Particle size distributions in the Eastern Equatorial Pacific. Journal of Geophysical Research 76: 5070-5077.
- Carder, K.L., P.R. Betzer and D.W. Eggimann (1974). Physical, chemical and optical measures of suspended particulate concentrations: their intercomparison and application to the West African shelf. In: R.J. Gibbs (ed.), Suspended Solids in Water. Plenum, New York, pp. 173-193.
- Crease, J. (1965). The flow of Norwegian Sea water through the Faroe Bank Channel. Deep-Sea Research 12: 143-150.
- Crow, E.L., F.A. Davis and M.W. Maxfield (1960). Statistics Manual - with examples taken from ordnance development. Dover Publications, Inc., New York, 288 pp.
- Davies, T.A. and A.S. Laughton (1972). Sedimentary processes in the North Atlantic Ocean. In: A.S. Laughton, W. Berggren et al. Initial Reports of the Deep Sea Drilling Project, XII. U.S. Government Printing Office, Washington, D.C., pp. 905-934.
- Davies, T.A., O.E. Weser, B.P. Luyendyk and R.B. Kidd (1975). Unconformities in the sediments of the Indian Ocean. Nature 253: 15-19.
- Dietrich, G. (1967). The International "Overflow" Expedition (ICES) of the Iceland-Faroe Ridge, May-June 1960, A review. Rapports et Procès-verbaux des Réunions Conseil Permanent International pour l'Exploration de la Mer 157: 268-274.
- Drake, D.E., R.L. Kolpak and P.J. Fischer (1972). Sediment transport on the Santa Barbara-Oxnard Shelf, Santa Barbara Channel, California. In: D.J.P. Swift, D.B. Duane and O.H. Pilkey (eds.), Shelf Sediment Transport. Dowden, Hutchinson and Ross, Stroudsburg, Pa., pp. 307-331.
- Einstein, H.A. and R.B. Krone (1962). Experiments to determine modes of cohesive sediment transport in salt and water. Journal of Geophysical Research 67: 1451-1461.
- Eittrheim, S.L. and M. Ewing (1972). Suspended particulate matter in the deep waters of the North American Basin. In: A.L. Gordon (ed.), Studies in Physical Oceanography. Gordon and Breach, London, pp. 123-167.

- Eittreim, S.L. and M. Ewing (1974). Turbidity distribution in the deep waters of the western Atlantic trough. In: R. Gibbs (ed.), Suspended Solids in Water. Plenum, New York, pp. 213-225.
- Eittreim, S., A.L. Gordon, M. Ewing, E.M. Thorndike and P. Bruchhausen (1972). The nepheloid layer and observed bottom currents in the Indian-Pacific Antarctic Sea. In: A.L. Gordon (ed.), Studies in Physical Oceanography. Gordon and Breach, London, pp. 19-35.
- Ellett, D.J. and D.G. Roberts (1973). The overflow of Norwegian Sea deep water across the Wyville-Thompson Ridge. Deep-Sea Research 20: 819-835.
- Ericson, D.B., M. Ewing, G. Wollin and B.C. Heezen (1961). Atlantic deep-sea sediment cores. Geological Society of America Bulletin 72: 193-286.
- Ewing, J.I. and C.D. Hollister (1972). Regional aspects of deep sea drilling in the western North Atlantic. In: C.D. Hollister, J.I. Ewing et al., Initial Reports of the Deep Sea Drilling Project, Volume XI. U.S. Government Printing Office, Washington, D.C., pp. 951-973.
- Ewing, J., C. Windisch and M. Ewing (1970). Correlation of Horizon A with JOIDES bore-hole results. Journal of Geophysical Research 75: 5645-5653.
- Ewing, M. and E.M. Thorndike (1965). Suspended matter in deep ocean water. Science 147: 1291-1294.
- Feely, R.A. (1975). Major-element composition of the particulate matter in the near-bottom nepheloid layer of the Gulf of Mexico. Marine Chemistry 3: 121-156.
- Feely, R.A. (1976). Evidence for aggregate formation in a nepheloid layer and its possible role in the sedimentation of particulate matter. Marine Geology 20: M7-M13.
- Field, M.E. and O.H. Pilkey (1971). Deposition of deep-sea sands: comparison of two areas of the Carolina continental rise. Journal of Sedimentary Petrology 41: 526-536.
- Flood, R.D. (1978). Studies of deep-sea sedimentary microtopography in the North Atlantic Ocean. Ph.D. Thesis, M.I.T./W.H.O.I. Joint Program in Oceanography, 395 pp. (unpublished manuscript).



- Gardner, W.D. (1977a). Fluxes, dynamics and chemistry of particulates in the ocean. Ph.D. Thesis, M.I.T./W.H.O.I. Joint Program in Oceanography, 405 pp. (unpublished manuscript).
- Gardner, W.D. (1977b). Incomplete extraction of rapidly settling particles from water samplers. Limnology and Oceanography 22: 764-768.
- Gardner, W.D. (1980). Field assessment of sediment traps. Journal of Marine Research 38: 41-52.
- Garner, D.M. (1972). Flow through the Charlie-Gibbs Fracture Zone, Mid-Atlantic Ridge. Canadian Journal of Earth Science 9: 116-121.
- Hathaway, J.C. (1972). Regional clay mineral facies in estuaries and continental margin of the United States East Coast. Geological Society of America Memoirs 133: 293-315.
- Heath, G.R., T.C. Moore and J.P. Dauphin (1977). Organic carbon in deep-sea sediments. In: N.R. Anderson and A. Malahoff (eds.), The Fate of Fossil Fuel CO<sub>2</sub> in the Oceans. Plenum, New York, pp. 605-626.
- Heezen, B.C., C.D. Hollister and W.F. Ruddiman (1966). Shaping of the continental rise by deep geostrophic contour currents. Science 152: 502-508.
- Hollister, C.D. (1967). Sediment distribution and deep circulation in the western North Atlantic. Ph.D. Thesis, Columbia University, New York, 471 pp. (Unpublished manuscript).
- Hollister, C.D., R.D. Flood, D.A. Johnson, P.E. Lonsdale and J.B. Southard (1974). Abyssal furrows and hyperbolic echo traces on the Bahama Outer Ridge. Geology 2: 395-400.
- Hollister, C.D., R. D. Flood and I.N. McCave (1978). Plastering and decorating in the North Atlantic. Oceanus 21: 5-13.
- Hollister, C.D. and B.C. Heezen (1972). Geologic effects of ocean bottom currents, western North Atlantic. In: A.L. Gordon (ed.), Studies in Physical Oceanography. Gordon and Breach, London, pp. 37-66.
- Honjo, S. (1976). Coccoliths: production, transportation and sedimentation. Marine Micropaleontology 1: 65-79.
- Honjo, S. (1977). Biogenic carbonate particles in the ocean; Do they dissolve in the water column? In: N.R. Anderson and A. Malahoff (eds.), The Fate of Fossil Fuel CO<sub>2</sub> in the Oceans. Plenum, New York, pp. 269-294.

- Honjo, S. (1978). Sedimentation of materials in the Sargasso Sea at a 5,367 m deep station. Journal of Marine Research 36: 469-492.
- Honjo, S., K.O. Emery and S. Yamamoto (1974). Non-combustible suspended matter in surface waters off eastern Asia. Sedimentology 21: 555-575.
- Huang, T.C. and N.D. Watkins (1977). Contrasts between the Brunhes and Matuyama sedimentary records of bottom water activity in the South Pacific. Marine Geology 23: 113-132.
- Jacobi, R.D., P.D. Rabinowitz and R.W. Embley (1975). Sediment waves on the Moroccan Continental Rise. Marine Geology 19: M61-M67.
- Jerlov, N.G. (1968). Optical Oceanography. Elsevier Publ. Co., Amsterdam, 194 pp.
- Johnson, D.A., M. Ledbetter and L.H. Burckle (1977). Vema channel paleo-oceanography: Pleistocene dissolution cycles and episodic bottom water flow. Marine Geology 23: 1-33.
- Johnson, D.A. and A.N. Shor (1977). Initial cruise report ATLANTIS II-94, Leg I. W.H.O.I. Technical Report #77-70 (unpublished manuscript).
- Johnson, G.L. and E.D. Schneider (1969). Depositional ridges in the North Atlantic. Earth and Planetary Science Letters 6: 416-422.
- Jones, E.J.W., M. Ewing, J.I. Ewing and S.L. Eittreim (1970). Influence of Norwegian Sea overflow water on sedimentation in the northern North Atlantic and Labrador Sea. Journal of Geophysical Research 74: 1655-1680.
- Kolla, V.R., L. Sullivan, S. Streeter and M. Langseth (1976). Spreading effects of Antarctic bottom water on the floor of the Indian Ocean inferred from bottom water potential temperature, turbidity, and sea-floor photography. Marine Geology 21: 171-189.
- Krishnaswami, S. and M.M. Sarin (1976). Atlantic surface particulates: composition, settling rates and dissolution in the deep sea. Earth and Planetary Science Letters 32: 430-440.
- Laine, E.P. and C.D. Hollister (1980). Geological effects of the Gulf Stream System on the Northern Bermuda Rise. Marine Geology (in press).
- Ledbetter, M. and D.A. Johnson (1976). Increased transport of Antarctic Bottom Water in the Vema Channel during the last Ice Age. Science 194: 837-839.

- Lee, A. and D. Ellett (1965). On the contribution of overflow water from the Norwegian Sea to the hydrographic structure of the North Atlantic Ocean. Deep-Sea Research 12: 129-142.
- Lonsdale, P. and C.D. Hollister (1979). A near-bottom traverse of Rockall Trough: hydrographic and geologic inferences. Oceanologica Acta 2: 91-105.
- Lonsdale, P. and J.B. Southard (1974). Experimental erosion of North Pacific red clay. Marine Geology 17: M51-M60.
- Lonsdale, P. and F.N. Spiess (1977). Abyssal bedforms explored with a deeply towed instrument package. Marine Geology 23: 57-75.
- Luyten, J.R. (1977). Scales of motion in the deep Gulf Stream and across the continental rise. Journal of Marine Research 35: 49-74.
- Malmberg, S.-A. (1974). A note on the deep water south of Iceland -- "Overflow '73." ICES Reference C.M. 1974/C:32 (unpublished manuscript).
- McCave, I.N. (1975). Vertical flux of particles in the ocean. Deep-Sea Research 22: 491-502.
- McCave, I.N., P.F. Lonsdale, C.D. Hollister and W.D. Gardner (1980). Sediment transport over the Hatton and Gardar contourite drifts. Journal of Sedimentary Petrology (in press).
- Meade, R.H. (1972). Transport and deposition of sediments in estuaries. Geological Society of America Memoirs 133: 91-120.
- Moore, T.C. Jr. and G.R. Heath (1977). Survival of deep-sea sedimentary sections. Earth and Planetary Science Letters 37: 71-80.
- Pak, H. and J.R.V. Zaneveld (1977). Bottom nepheloid layers and bottom mixed layers observed on the continental shelf off Oregon. Journal of Geophysical Research 82: 3921-3931.
- Peterson, W.H. and G.G.H. Rooth (1976). Formation and exchange of deep water in the Greenland and Norwegian Seas. Deep-Sea Research 23: 273-283.
- Pierce, J.W. (1976). Suspended sediment transport at the shelf break and over the outer margin. In: D.J. Stanley and D.J.P. Swift (eds.), Marine Sediment Transport and Environmental Management. John Wiley and Sons, New York, pp. 437-458.

- Plank, W.S., H. Pak, and J.R.V. Zaneveld (1972). Light scattering and suspended matter in nepheloid layers. Journal of Geophysical Research 77: 1689-1694.
- Richardson, P.L. (1977). On the crossover between the Gulf Stream and the Western Boundary Undercurrent. Deep-Sea Research 24: 139-159.
- Rona, P.A. (1973). Worldwide unconformities in marine sediments related to eustatic changes of sea level. Nature Physical Science 244: 25-26.
- Rowe, G.T. and W.D. Gardner (1979). Sedimentation rates in the slope water of the northwest Atlantic Ocean measured directly with sediment traps. Journal of Marine Research 37: 581-600.
- Ruddiman, W.F. and A. McIntyre (1976). Northeast Atlantic Paleoclimatic changes over the past 600,000 years. Geological Society of America Memoirs 145: 111-146.
- Schmitz, W.J., Jr. and N.G. Hogg (1978). Observations of energetic low frequency current fluctuations in the Charlie-Gibbs Fracture Zone. Journal of Marine Research 36: 725-734.
- Sheldon, R.W. and T.R. Parson (1967). A practical manual on the use of the Coulter Counter in marine science. Coulter Electronics, Toronto, 66 pp.
- Sheldon, R.W., A. Prakash and W.H. Sutcliffe, Jr. (1972). The size distribution of particles in the ocean. Limnology and Oceanography 17: 327-340.
- Shor, A.N. (1978). Bottom currents on East Katla Ridge, NW Iceland Basin. ICES Reference C.M. 1978/C:60 (unpublished manuscript).
- Shor, A.N. (1979). Bottom currents and abyssal sedimentation processes south of Iceland. Ph.D. Thesis, M.I.T./W.H.O.I. Joint Program in Oceanography, 246 pp. (unpublished manuscript).
- Shor, A., P. Lonsdale, C.D. Hollister and D. Spencer (1980). Charlie-Gibbs Fracture Zone: bottom-water transport and its geological effects. Deep-Sea Research (in press).
- Shor, A.N., D. Muller and D.A. Johnson (1977). Transport of Norwegian Sea Overflow -- preliminary results of ATLANTIS II cruise 94, June - July, 1977. ICES - CM 1977/C:44 Hydro. Comm. (unpublished manuscript).

- Southard, J.B., R.A. Young and C.D. Hollister (1971). Experimental erosion of calcareous ooze. Journal of Geophysical Research 76: 5903-5909.
- Spencer, D.W., P.G. Brewer, A. Fleer, S. Honjo, S. Krishnaswami and Y. Nozaki (1978). Chemical fluxes from a sediment trap experiment in the deep Sargasso Sea. Journal of Marine Research 36: 493-523.
- Spencer, D.W., P.G. Brewer and P.L. Sachs (1972). Aspects of the distribution and trace element composition of suspended matter in the Black Sea. Geochimica et Cosmochimica Acta 36: 76-86.
- Steele, J.H., J.R. Barrett and L.V. Worthington (1962). Deep currents south of Iceland. Deep-Sea Research 9: 465-474.
- Sternberg, R.W., E.T. Baker, D.A. McManus, S. Smith and D.R. Morrison (1974). An integrating nephelometer for measuring suspended sediment concentrations in the deep sea. Deep-Sea Research 21: 887-892.
- Stow, D.A.V. and J.P.B. Lovell (1979). Contourites: their recognition in modern and ancient sediments. Earth Science Reviews 14: 251-291.
- Swift, J.H., K. Aagaard and S.-A. Malmberg (1980). The contribution of the Denmark Strait overflow to the deep North Atlantic. Deep-Sea Research 27: 29-42.
- Takahashi, K. and S. Honjo (1980). Vertical flux of radiolaria: a taxon-quantitative sediment trap study from the western tropical Atlantic. Micropaleontology (in press).
- Takahashi, T. (1975). Carbonate chemistry of sea water and the calcite compensation depth in the oceans. In: W.V. Sliter, A.W.H. Bé and W.H. Berger (eds.), Dissolution of Deep-Sea Carbonates. Cushman Foundation Foram. Research Special Publication No. 13, pp. 11-26.
- Takahashi, T. and W.S. Broecker (1977). Mechanisms for calcite dissolution on the seafloor. In: N.R. Anderson and A. Malahoff (eds.), The Fate of Fossil Fuel CO<sub>2</sub> in the Oceans. Plenum, New York, pp. 455-478.
- Thorndike, E.M. (1975). A deep-sea photographic nephelometer. Ocean Engineering 3: 1-15.

- Tucholke, B.E. (1979). Relationships between acoustic stratigraphy and lithostratigraphy in the western North Atlantic Basin. In: B.E. Tucholke, P.R. Vogt et al. (eds.), Initial Reports of the Deep Sea Drilling Project Vol. XLIII. U.S. Government Printing Office, Washington, D.C., pp. 827-846.
- Tucholke, B.E., W.R. Wright and C.D. Hollister (1973). Abyssal circulation over the Greater Antilles Outer Ridge. Deep-Sea Research 20: 973-995.
- Watkins, N.P. and J.P. Kennett (1971). Antarctic Bottom Water: major change in velocity during the Late Cenozoic between Australia and Antarctica. Science 173: 813-818.
- Worthington, L.V. (1969). An attempt to measure the volume transport of Norwegian Sea overflow water through the Denmark Strait. Deep-Sea Research 16: 421-432.
- Worthington, L.V. (1970). The Norwegian Sea as a Mediterranean Basin. Deep-Sea Research 17: 77-84.
- Worthington, L.V. (1976). On the North Atlantic circulation. The Johns Hopkins University Press, Baltimore, 110 pp.
- Worthington, L.V. and G.H. Volkmann (1965). The volume transport of the Norwegian Sea overflow water in the North Atlantic. Deep-Sea Research 12: 667-676.
- Young, R.N. and J.B. Southard (1978). Erosion of fine-grained marine sediments: sea-floor and laboratory experiments. Geological Society of America Bulletin 89: 663-672.
- Zimmerman, H.B. (1971). Bottom currents on the New England continental rise. Journal of Geophysical Research 76: 5865-5876.
- Zimmerman, H.B. (1972). Sediments of the New England Continental Rise. Geological Society of America Bulletin 83: 3709-3724.

BIOGRAPHICAL NOTE:

I, Mary Jo Richardson, was born on March 17, 1954, in Lynn, Massachusetts. I received my primary and secondary school education there and in nearby Salem. As an undergraduate I attended Smith College and Wesleyan University, graduating magna cum laude and phi beta kappa from the former with a bachelor's degree in geology in June, 1975. I began my graduate student career during the summer of 1975 when I entered the WHOI/MIT Joint Program in Oceanography. Research interests throughout these past five years have centered around suspended particulate matter studies in regions of dynamic current systems. I plan to continue doing research in this and related fields as a postdoctoral investigator at Lamont-Doherty Geological Observatory of Columbia University.

MANDATORY DISTRIBUTION LIST

FOR UNCLASSIFIED TECHNICAL REPORTS, REPRINTS, AND FINAL REPORTS  
PUBLISHED BY OCEANOGRAPHIC CONTRACTORS  
OF THE OCEAN SCIENCE AND TECHNOLOGY DIVISION  
OF THE OFFICE OF NAVAL RESEARCH

(REVISED NOVEMBER 1978)

- |   |   |    |  |
|---|---|----|--|
| 1 | Deputy Under Secretary of Defense<br>(Research and Advanced Technology)<br>Military Assistant for Environmental Science<br>Room 3D129<br>Washington, D.C. 20301 | 12 | Defense Documentation Center<br>Cameron Station<br>Alexandria, VA 22314<br>ATTN: DCA |
|   | Office of Naval Research<br>800 North Quincy Street<br>Arlington, VA 22217  |    | Commander<br>Naval Oceanographic Office<br>NSTL Station<br>Bay St. Louis, MS 39522   |
| 3 | ATTN: Code 483  | 1  | ATTN: Code 8100  |
| 1 | ATTN: Code 460  | 1  | ATTN: Code 6000  |
| 2 | ATTN: 102B  | 1  | ATTN: Code 3300  |
| 1 | CDR J. C. Harlett, (USN)<br>ONR Representative<br>Woods Hole Oceanographic Inst.<br>Woods Hole, MA 02543  | 1  | NODC/NOAA<br>Code D781<br>Wisconsin Avenue, N.W.<br>Washington, D.C. 20235           |
|   | Commanding Officer<br>Naval Research Laboratory<br>Washington, D.C. 20375   |    |  |
| 6 | ATTN: Library, Code 2627  |    |  |



<p>Woods Hole Oceanographic Institution WHOI-80-52</p> <p>COMPOSITION AND CHARACTERISTICS OF PARTICLES IN THE OCEAN: EVIDENCE FOR PRESENT DAY RESUSPENSION, by Mary Josephine Richardson, 238 pages, November 1980. Prepared for the Office of Naval Research under Contracts N00014-79-C-0071; NR 083-004, N00014-74-C-0262; NR 083-004, N00014-75-C-0291 and Sandia Laboratories through Contracts 13-7923 and 13-2559.</p> <p>For abstract refer to pages 2 and 3 of thesis.</p>	<p>1. Suspended sediment WHOI-80-52</p> <p>2. Resuspension processes</p> <p>3. Abyssal sedimentation</p> <p>I. Richardson, Mary J. II. N00014-79-C-0071; NR 083-004 III. N00014-74-C-0262; NR 083-004 IV. N00014-75-C-0291 V. 13-7923 VI. 13-2559</p> <p>This card is UNCLASSIFIED</p>	<p>Woods Hole Oceanographic Institution WHOI-80-52</p> <p>COMPOSITION AND CHARACTERISTICS OF PARTICLES IN THE OCEAN: EVIDENCE FOR PRESENT DAY RESUSPENSION, by Mary Josephine Richardson, 238 pages, November 1980. Prepared for the Office of Naval Research under Contracts N00014-79-C-0071; NR 083-004, N00014-74-C-0262; NR 083-004, N00014-75-C-0291 and Sandia Laboratories through Contracts 13-7923 and 13-2559.</p> <p>For abstract refer to pages 2 and 3 of thesis.</p>	<p>1. Suspended sediment WHOI-80-52</p> <p>2. Resuspension processes</p> <p>3. Abyssal sedimentation</p> <p>I. Richardson, Mary J. II. N00014-79-C-0071; NR 083-004 III. N00014-74-C-0262; NR 083-004 IV. N00014-75-C-0291 V. 13-7923 VI. 13-2559</p> <p>This card is UNCLASSIFIED</p>
<p>Woods Hole Oceanographic Institution WHOI-80-52</p> <p>COMPOSITION AND CHARACTERISTICS OF PARTICLES IN THE OCEAN: EVIDENCE FOR PRESENT DAY RESUSPENSION, by Mary Josephine Richardson, 238 pages, November 1980. Prepared for the Office of Naval Research under Contracts N00014-79-C-0071; NR 083-004, N00014-74-C-0262; NR 083-004, N00014-75-C-0291 and Sandia Laboratories through Contracts 13-7923 and 13-2559.</p> <p>For abstract refer to pages 2 and 3 of thesis.</p>	<p>1. Suspended sediment WHOI-80-52</p> <p>2. Resuspension processes</p> <p>3. Abyssal sedimentation</p> <p>I. Richardson, Mary J. II. N00014-79-C-0071; NR 083-004 III. N00014-74-C-0262; NR 083-004 IV. N00014-75-C-0291 V. 13-7923 VI. 13-2559</p> <p>This card is UNCLASSIFIED</p>	<p>Woods Hole Oceanographic Institution WHOI-80-52</p> <p>COMPOSITION AND CHARACTERISTICS OF PARTICLES IN THE OCEAN: EVIDENCE FOR PRESENT DAY RESUSPENSION, by Mary Josephine Richardson, 238 pages, November 1980. Prepared for the Office of Naval Research under Contracts N00014-79-C-0071; NR 083-004, N00014-74-C-0262; NR 083-004, N00014-75-C-0291 and Sandia Laboratories through Contracts 13-7923 and 13-2559.</p> <p>For abstract refer to pages 2 and 3 of thesis.</p>	<p>1. Suspended sediment WHOI-80-52</p> <p>2. Resuspension processes</p> <p>3. Abyssal sedimentation</p> <p>I. Richardson, Mary J. II. N00014-79-C-0071; NR 083-004 III. N00014-74-C-0262; NR 083-004 IV. N00014-75-C-0291 V. 13-7923 VI. 13-2559</p> <p>This card is UNCLASSIFIED</p>